Copper recovery from fine particle grain size fraction of bottom ash from Waste to Energy plants

Von der Fakultät für Ingenieurwissenschaften,
Abteilung Maschinenbau und Verfahrenstechnik
der
Universität Duisburg-Essen

zur Erlangung des akademischen Grades

eines

Doktors der Ingenieurwissenschaften

Dr.-Ing.

genehmigte Dissertation

von

Reza Miftahul Ulum
aus
Jakarta (Indonesien)

Gutachter: Univ.-Prof. Dr.-Ing. Rüdiger Deike
Univ.-Prof. Dr.-Ing. Karl-Heinz Spitzer

Tag der mündlichen Prüfung: 25.09.2017

Table of content

Table of figures

List of tables

Preface

At the accomplishment of this study, the author would like to express his gratitude to the staff member in the ITM Laboratory at the University of Duisburg-Essen for their cooperation ever since the beginning of this research, including the financing of all experiments. My highest appreciation and gratitude I would like to extend to my supervisor, Prof. Dr.-Ing. Rüdiger Deike for his support, motivation, and careful supervision during my study. It is a blessing for me to have had the opportunity to meet and work with him. Secondly, I wish to thank to my colleagues in the ITM lab, especially Daniel Schubert, Aron Brümmer, Dominik Ebert, Bartoz Smaha, Carsten Reschke, Manuel Foppe, Andreas Kahrl, Ralph Pollmann, Herr Perry, and others who participated and collaborated with me during my research.

Special gratitude to my beloved family in Indonesia: my father and mother, Mr. Ajun Junaedi and Mrs. Ida Ruvaida; my brothers and sisters; my colleagues and friends from Indonesia who gave me their full support: Dr.-Ing. Alfian Ferdiansyah, Dr.rer.pol. Romadhani Ardi, Dr.-Ing. Asep Ridwan, Dr. Muhammad Ibadurrohman, Dr. Zulkarnain, Dr. Marta Indriyati, Arif Rahman, Suryadi N., Dr.-Ing Budi Sudiarto, Aji Nur W, Noverli, Widodo D. P., Irawan Nurhas, and Nurbiah Nurdin; as well as master students who participated in this research, including Almira Larasati, Abi Putra Prayogi, and Anindya Aulia Pratiwi.

The latter was the author's scholarship sponsor, as well as DIKTI Directorate General of Higher Education of Indonesia for four years, on scholarship from the University of Duisburg Essen in the last year of the author's study. I praise Allah, the most beneficent and the most merciful. I do believe that in every difficulty there will be ease.

"The biography is not included in the online version for reasons of data protection".

Duisburg, 2017

Abstract

Waste generation worldwide is increasing drastically every year, due to a growing global population and growing income per capita. Waste management in an environmentally and economically sustainable way is needed. In the context of waste management, waste-to-energy plants (WtE) are categorized as waste treatment, which nowadays is preferred due to its ability to reduce mass and volume of the waste and produce energy (heat and electricity) in the process.

Solid residues, called bottom ash, produced from WtE plants have been increasing every year. Whether bottom ash can be used for public road construction, or exclusively for road construction in landfill areas, depends on the composition of the bottom ash in question and different legislation in the different Federal States of Germany. There is a danger that heavy metals could leach out into the soil over time, polluting ground water and damaging the environment in general. Because of increasing metal prices over the last 15 years, the fact that bottom ash contains valuable metals will become increasingly important in the future.

The contribution of this study is in the treatment of fine-particle, grain-size bottom ash (< 2mm) in such a way as to entirely recover the metals from the ash and to produce a clean mineral fraction that can be used in the cement industry as raw material. Because metal particles are glued together with the slag, in this approach principles of ore processing are used. The bottom ash is milled and classified by sieving technology. Because knowledge about the structure of metal particles in bottom ash is limited, particles are characterized by optical microscope and by scanning electron microscope together with energy dispersive spectroscopy.

In the further course of the study, a semi-continuous wet magnetic separation technology has been developed on the basis of a modified sluice-box process. The strong magnetic effect is thought to be produced by the iron oxide magnetite (Fe_3O_4). It has been shown that elements like chromium, nickel, and

cobalt can be separated from bottom ash because magnetite acts as a collector for these elements. A process has also been developed to flatten the non-ferrous metal particles with an optimized milling process, after which it is possible to separate the metal particles easily by a sieving process. The residual mixture of heavy non-magnetic and light non-magnetic fractions is separated via density separation. With washing of bottom ash by sluice-box and gold-pan processes, it was possible to drastically reduce the sulphur and chlorine contents in the residual mineral fraction of the bottom ash.

The combination of wet magnetic separation during the sluice-box process and the density separation during the gold-pan and vacuum processes shows clearly a promising result for waste treatment of bottom ash in the context of metallic fraction recovery. After the liberation of metal particles from bottom ash, it is necessary that the residual mineral fraction be so clean that it can be used as raw material in the cement industry. Improvements in the quality of the mineral fraction have been achieved, but the cleaning process needs further optimization.

The results of this study show clearly that copper in bottom ash exists mainly as metal. The results of this study also show that it is not impossible to get the copper out of the bottom ash, and by a cheap and easy process. Further work is needed for optimization, but the effort makes a great deal of sense, because the copper content in the bottom ash is as high as in the poor natural copper ores that are mined today. But copper in bottom ash does have the advantage, shown in this study, that it is already a metal, so that additional metallurgical work to separate copper from oxygen and sulphur (a necessary step in the processing of natural ores) is not necessary when processing copper form bottom ash.

Zusammenfassung

Von Jahr zu Jahr entsteht mehr Müll durch eine weltweit wachsende Bevölkerung und durch einen zunehmenden Wohlstand. Müll muss in umweltfreundlichen und nachhaltigen technischen Prozessen entsorgt werden. In diesem Zusammenhang spielen Müllverbrennungsanlagen eine große Rolle, da einerseits die Müllmengen und das Müllvolumen reduziert und andererseits Strom und Wärme produziert werden.

Durch den Verbrennungsprozess selbst entsteht mengenmäßig als größte Abfallmengen die Müllverbrennungsschlacke (MV-Schlacke). In den Bundesländern kann in Deutschland die MV-Schlacke unter Umständen zum öffentlichen Straßenbau oder nur zum Deponiebau verwendet werden, wobei es dafür im Moment keine einheitliche Regelung gibt. Dadurch dass Schwermetalle und andere Metalle aus der MV-Schlacke möglicherweise ausgelaugt werden können, kann unter Umständen eine Verunreinigung des Grundwassers verursacht werden.

Im Rahmen dieser Arbeit wurde untersucht, ob die feine Fraktion der MV-Schlacke (< 2mm) von Metallen und Schwermetallen befreit und dabei die restliche mineralische Fraktion so sauber dargestellt werden kann, dass sie als Rohstoff in der Zementindustrie zu verwenden ist. Dadurch dass die Metallpartikel mit den Schlackenpartikeln während des Verbrennungsprozesses und der Schlackenaufbereitung miteinander verwachsen, wurden im Rahmen dieser Arbeit Methoden aus der Erzaufbereitung angewandt, um diese Verbindungen zu trennen. Die MV-Schlacke wurde gebrochen, gemahlen und durch Sieben klassifiziert. Da bisher nahezu keine Kenntnisse über Strukturen und chemische Zusammensetzungen der Partikel in den feinen Fraktionen der MV-Schlacke vorliegen, wurden Partikel mittels optischer Mikroskopie, Rasterelektronenmikroskopie in Kombination mit EDX (Energiedispersive Röntgenspektroskopie) charakterisiert.

Im Rahmen dieser Arbeit wurde ein semikontinuierliches nassmagnetisches Separationsverfahren auf der Basis einer Goldwaschrinne

entwickelt. Bei der nassmagnetischen Trennung wird aus den feinen Fraktionen Magnetit (Fe_3O_4) abgetrennt, da in diesen Fraktionen kein reines Eisen mehr vorliegt. Da der Magnetit aufgrund seiner Spinellstruktur ein größere Löslichkeit für Elemente wir Chrom, Nickel und Cobalt hat, kann er hier als Sammler für genutzt werden, so dass diese Elemente über den Magnetit relativ leicht aus der MV-Schlacke entfernt werden können. Im weiteren wurde ein optimierter Mahlprozess entwickelt mit dem Drähte und runde Partikel zu flachen Partikeln verformt werden, die im Anschluss daran durch einen relativ einfachen Siebprozess abgetrennt und dadurch aufkonzentriert werden können. Die verbleibende Mischung aus einer schwermetallhaltigen nicht-magnetischen Fraktion und aus einer leichten nicht-magnetischen Fraktion wird über eine Dichtetrennung (Goldwaschpfanne und Vakuumsaugverfahren) voneinander getrennt. Durch den Waschprozess in der Goldwaschrinne und der Goldwaschpfanne können die Gehalte an Schwefel und Chlor in der MV-Schlacke deutlich abgesenkt werden.

Die Ergebnisse der hier durchgeführten Versuche zeigen, dass vielversprechende Ergebnisse hinsichtlich der Metallabtrennung aus den feinen Fraktionen der MV-Schlacke erreicht wurden. Nach der Entfernung der Metalle hängt die Wirtschaftlichkeit des gesamten Prozesses aber davon ab, ob die Verwendung der restlichen mineralischen Fraktion in anderen Industrien, wie z.B. der Zementindustrie möglich ist. Die Ergebnisse zeigen, dass deutliche Verbesserungen, was die Reinheit der mineralischen Fraktion angeht, erzielt werden konnten, dass aber noch weitere Optimierungen notwendig sind. Hier hat sich gezeigt, dass die Art und Weise der Analytik eine große Rolle spielt, da die konventionelle Röntgen-Fluoreszenz-Analyse (RFA) in vielen Fällen keine ausreichend genauen Ergebnisse liefert. Hier müssen zukünftig andere analytische Wege ausprobiert werden.

Die Ergebnisse dieser Arbeit zeigen eindeutig, dass Kupfer in den feinen Fraktionen der MV-Schlacke im Wesentlichen als Metall vorliegt und dass es nicht unmöglich ist, Kupfer aus diesen Fraktionen der MV-Schlacke auf eine wirtschaftliche Art und Weise zurückzugewinnen. Es sind weitere

Optimierungsarbeiten notwendig, die aber sinnvoll sind, da in einer feinen Fraktion der MV-Schlacke so viel Kupfer enthalten ist, wie in einem armen Kupfererz, das heute auf der Welt abgebaut wird. Dabei hat das Kupfer aus der MV-Schlacke den Vorteil, dass es schon als Metall vorliegt und nicht wie bei den natürlichen Erzen aus Kupferoxiden oder -sulfiden raffiniert werden muss.

1. Introduction

1.1 Background of the resarch

In waste treatment or waste management, incineration is practiced in many countries because of its effect of reducing waste volume by 80%–90% [Chimenos **1999**] and because of the additional heat and electricity generated by the incineration process. The production of waste in Europe and Central Asia combined is predicted to increase from 254 ton/day in 2010 to 355 ton/day in 2025; (the complete data is described in chapter 2 in **Table 2.1**) [Goorhuis **2014** from World bank **2012**]. According to the German Federal Environmental Agency [Umweltbundesamt **2017**], Germany incinerated about 19.6 million tonnes of municipal waste in about 68 waste-to-energy (WtE) plants in 2010. These plants are producing about 5 million tonnes per year of a solid residue called bottom ash. In Germany, depending on different legislation in different federal states, the bottom ash can be used either in public road construction after processing or only in construction activities in landfill areas. The different limitations, for the most part, are due to the possible leaching effects of heavy metals and subsequent possible contamination of ground water and long-lasting soil pollution.

Bottom ash contains certain amounts of ferrous and non-ferrous metals that are recoverable today by state-of-the-art techniques [Deike **2012**], but metals still remain, especially in the fine fraction, in which form they are liable to leach heavy metals into the soil during construction activities. In general, in the fine fraction the copper content is 0.3–0.4 wt%, as high as in natural ores. That is why bottom ash being produced in WtE plants in Germany could be useful for recycling purposes, because it contains valuable metallic fractions. If these metals could be recycled by an environmentally friendly and economical process, resource efficiency could be improved and, in addition, possible environmental problems caused by heavy metal leaching could be prevented.

That is why a great deal of research is done on the recovery of metals from bottom ash, because it contains heavy metals and salts such as Cu, Mo, Sb,

sulphates, and chlorides [Tang **2014** and Tang **2015**]. Lenka Muchová et al. [Muchová **2009**], for example, point out that precious metals (100 ppm of gold, 1500–4000 ppm of silver, copper, zinc, lead, iron, and/or tin) in bottom ash at the Amsterdam WtE-plant, are contained mainly in a particle size of $\leq$ 6 mm, which probably came from waste electronic and electrical equipment (WEEE).

Some methods used in mineral processing could also be used in recycling processes to recover metals [Shen **2003**]. Low-cost processes are needed and, if the metals are separated, it is necessary that the remaining minerallic fraction can be used in other industrial areas, so as to complete the total process in an economical way. As reported by Deike et al. [Deike **2015**], the potential of an economical bottom ash recycling is only realizable if it is not needed to landfill the remaining minerallic fraction. Thus, it is necessary to look for opportunities to use the minerallic fraction. Because bottom ash contains major compounds (CaO, SiO_2, Al_2O_3, Fe_2O_3 and MgO) that are generally needed in the cement industry [Pan **2008**], the use of bottom ash in that sector might be one avenue for future research. This kind of research is needed, because raw materials that will be used for cement production in Germany must comply with very low limit values for different trace elements.

Water washing and metal separation of the ash, as used in this study, may be a useful pretreatment method, as it can reduce most of the chloride salt (from approximately 15% to less than 1%), which holds out the possibility of overcoming chloride-related problems during kiln operation, as well as during the ultimate application of the produced cement clinkers. The use of inorganic wastes in cement production is only feasible if precise chemical analysis is provided and guaranteed [Pan **2008**].

In this study, bottom ash samples from three different incineration plants located in Germany were used to develop a low-cost process for recovering metals, mainly copper, from the fine fraction (on the one hand) and (on the other) for preparing the remaining minerallic fraction in such a way that it can be used as raw material in the cement industry. According to the results

and parameters developed in this study, an optimal recovery of metallic copper from bottom ash is possible with an appropriate particle size fraction.

1.2 Research objective

This study focusses on processing fine-particle grain-size bottom ash to recover metallic particles (especially copper) via a cheap separation process and by environmentally friendly methods. The objective was achieved by physical separation methods. The use of chemical reactions (e.g., leaching process) may induce the dissolution of some heavy metals, resulting in the production of yet more waste. This is the basic consideration in choosing a physical separation method as the methodology of this study. Detailed research objectives are described below:

1. There are some physical separation methods available for concentrating valuable materials contained in bottom ash; thus, to find a suitable method with suitable parameters for metallic particle recovery in bottom ash, some physical separation has been applied to find the optimal result.
2. Each incineration plant has a typical and different composition of bottom ash their produced. This bottom ash certainly has different recycling potential from one incineration plant to others which mainly depends on its material (initial waste) input. Therefore, it is important to observe the characterization of the bottom ash to observe the recycling potential of each incineration plant.
3. After the preferable methods, the parameter was choosen and the characterization of bottom ash was done, then the recovery of metallic particles could be achived by modifying the separation method and process to produce the optimal result.

1.3 The thesis manuscript organization

This thesis is organized as follows: Chapter 2 consists of a literature review relevant to the topic of waste management, the worldwide production of waste (especially in Europe and Germany), and the treatment of bottom ash for specifically recycling purposes. Chapter 3 describes the research methodology followed to recover the metallic fraction contained in fine-particle grain-size bottom ash. Chapter 4 deals with the characteristics of bottom ash after processing by the methods set forth in chapter 3. In chapter 5, the results are discussed and a process for improve the recovery of metallic fractions is proposed. Chapter 6 summarizes the significant results of this study.

2 Waste management, waste production overview, WtE technology, and bottom ash recycling

2.1 Waste management

A hierarchy of waste management was formally adopted in the EU in 1989, consisting of five important steps: prevention, preparing for reuse, recycling, other recovery (notably, energy recovery), and disposal [Sabbas **2003**]. To overcome the waste-generation increment, an integrated system of environmentally and economically sustainable waste management is needed. Sabbas et al. [Sabbas **2003**] have investigated such a system, as described in **Figure 2.1**.

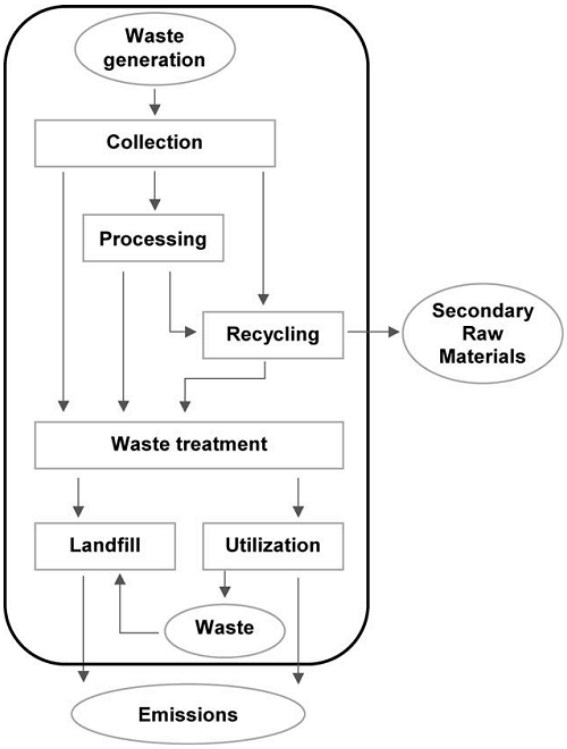

Figure 2.1: An integrated waste management system as reported by Sabbas et. al. [Sabbas **2003**].

The waste management system described in **Figure 2.1** includes all processing steps, starting with the generation of the waste to the landfilling process. The important steps of waste management, as shown in **Figure 2.1,** are:

- **Waste generation** is an all-encompassing process, a precursor to waste production, and comes from both the industrial and the commercial sectors as well as from households.
- **Waste collection** comprises those processes that initially separate the waste at its source into different material streams.
- **Waste processing** includes the steps of sorting and dismantling waste products and preparing the waste for reuse.
- **Recycling** is the production of secondary raw materials from waste, for example, steel from ferrous scrap, paper production from waste paper, etc.
- The **waste treatment** process includes every technology that treats the waste by various methods, for example, thermal treatment (including incineration), chemical treatment (of hazardous waste), etc.
- **Waste utilization** is the productive use of treated waste, for example, the use of bottom ash for road construction.
- **Landfilling,** or disposal of waste by burial, is a step that is currently avoided in many EU-27countries.

In waste management, the waste-to-energy (WtE) plant is the site of waste treatment shown in **Figure 2.1**. There are many forms of waste treatment with different purposes, depending on the part of the world in which it occurs. Incineration, for instance, aims to reduce the mass and volume of waste, to produce heat and electricity, and to recover valuable metals contained in the waste [Sabbas **2003**].

In the context of EU waste management strategy, waste treatment via thermal processes is favored in most western EU countries. The development of waste management in EU countries from 1990 to 2020 (projection) via incineration and recycling-composting (**Figure 2.2**) will affect the continuous percent reduction of landfilling over the years.

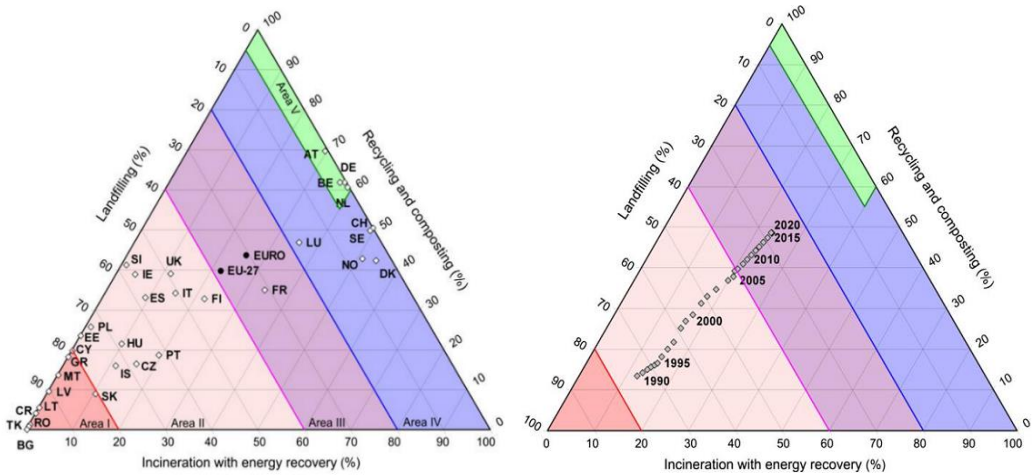

Figure 2.2: The waste management among EU countries in the period 2012 (left) and the projection of waste management in EU countries from 1990 – 2020 (right) [Goorhuis **2014** and Bartl **2012**].

Marrten Goorhuis [Goorhuis **2014**] and Bartl [Bartl **2012**] have discussed waste management in Europe for 2012, as shown in **Figure 2.2**. The treatment of bottom ash is basically categorized into classes such as disposal (landfill), combustion processes/incineration (thermal recovery), and recycling (composting). Based on the kind of waste treatment, waste management in EU countries is classified into five categories, as shown in **Figure 2.2 (left)**:

- In class I are countries that still are landfilling > 80% of their waste and treating < 20% of their waste in WtE-plants.
- In classes II to IV, the percentage of landfilling is reduced and the percentage of incineration treatment is increased.
- In class V are those countries with very low landfill rates, such as Germany, Netherlands, Belgium, and Austria.

The forecast for waste management of EU countries in the next five years is shown in **Figure 2.2 (right),** with a total European average falling into class III.

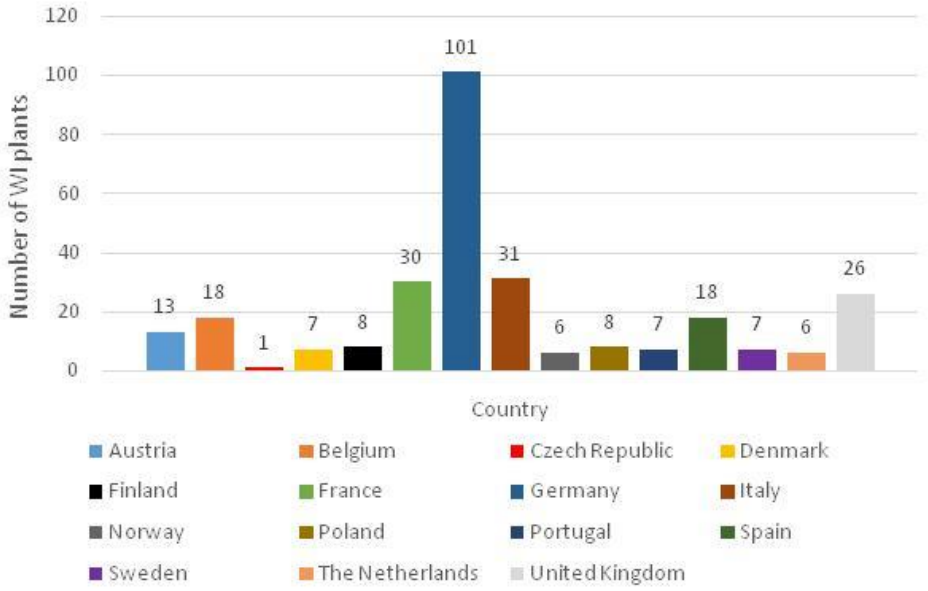

Figure 2.3: The distribution of WtE-plants in different EU countries [Gleis **2016**].

Apart from Germany, the number of WtE-plants in different EU countries is less than 20, and in three countries it is near 30 plants. As reported by Chandler et al. [Chandler **1997**], incineration technology has increased dramatically. This development was influenced by the introduction of various modified combustion processes and the development of highly sophisticated filter systems to improve air pollution control (APC).

Today, waste incineration is the most efficient method of waste management, because it is possible thereby to reduce mass and volume of solid waste while producing heat and electricity [Wiles **1996**]. In the process, it is also possible to separate ferrous and non-ferrous metals of different sizes contained in the waste [Cimpan **2013**].

2.2 An overview of waste generation, waste management in EU, and WtE plants technology

Municipal solid waste generation on a global scale, as discussed by Marrten Goorhuis [Goorhuis **2014**] on the basis of World Bank data [World Bank **2012**], is depicted in **Table 2.1**. The production of waste is always related to economic development and income per capita in each region. The World Bank

research shows that the predicted growth from 2010 to 2025 in both Europe and Central Asia together will be from 254,389 ton/day in 2010 up to 354,810 ton/day in 2025. The general composition of waste is mainly as follows:

- 46%, organic waste
- 17% paper
- 10% plastic
- 5% glass
- 4% metals
- 18% others (include textiles, leather, rubber, electronic waste, appliances, other inert materials, etc.)

  [World Bank **2012**]

Table 2.1: The waste generation worldwide [World bank **2012** and Goorhuis **2014**].

	Current Available Data (2010 Estimation)			Projection for 2025			
		Urban Waste Generation		Projected Population		Projected Urban Waste	
Region	Urban population (millions)	Per capita (kg/capita/day)	Total (t/day)	Total population (millions)	Urban population (millions)	Per capita (kg/capita/day)	Total (t/day)
Sub Saharan Africa	260	0.65	69,119	1152	518	0.85	441,840
East Asia and Pacific	777	0.95	738,958	2124	1229	1.5	1,865,379
Europe and Central Asia	227	1.1	254,389	339	239	1.5	354,810
Latin America and Caribbean	399	1.1	437,545	681	466	1.6	728,392
Middle East and North Africa	162	1.1	173,545	379	257	1.43	369,320
OECD	729	2.2	1,566,286	1031	842	2.1	1,742,417
South Asia	426	0.45	192,410	1938	734	0.77	567,545
Total	2980	1.2	3,532,252	7644	4285	1.4	6,069,703

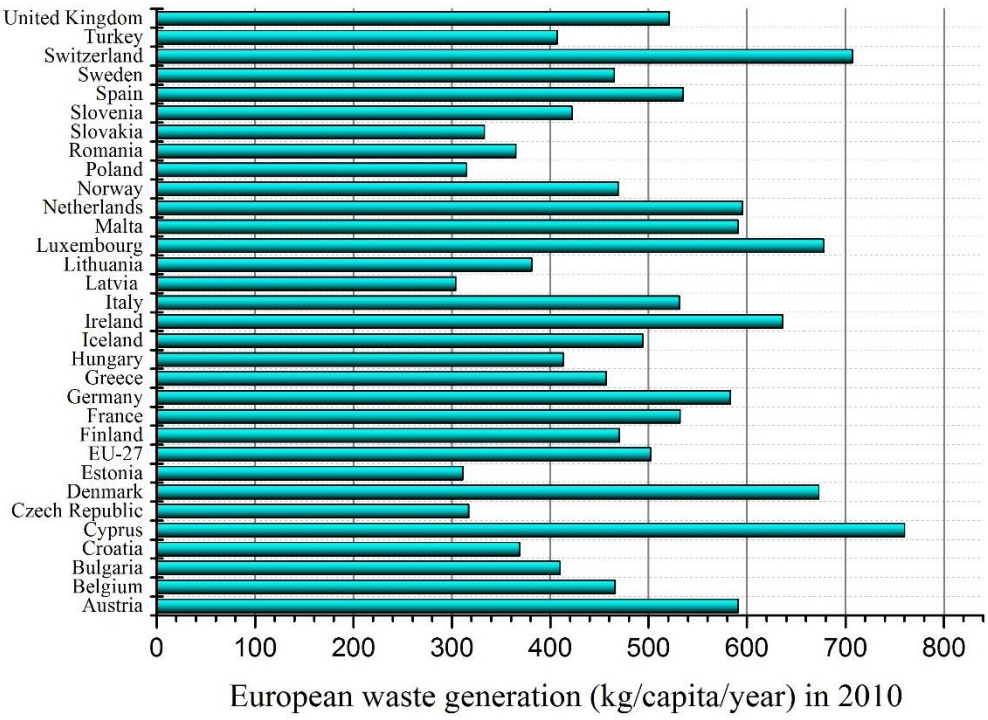

Figure 2.4: The European waste generation in 2010 as reported by European Environment Agency [EEA **2013**]**.**

European waste generation in 2010 is shown in **Figure 2.4**. The growth of waste generation in the future will endanger both human life and the environment if there is no waste strategy or management to prevent it. That is the reason why a reduction of waste quantity together with a system for global waste treatment in an environmentally and economically sustainable way is necessary.

Amongst EU countries, in 2013, Germany, Sweden, Belgium, Netherlands, Denmark, and Austria have treated their waste with very low percentage of waste being landfilled (1%–4%) [CEWEP **2013**]. In the same year, in Germany, 64% of the waste was recycled and composted and the rest was incinerated. By comparison (again, in 2013), in 28 EU countries, an average of 43% of waste was recycled and composted, 26% was incinerated, and 31% was landfilled. As reported by the Waste-to-Energy Research and Technology Council (WtERT) GmbH [WtERT **2015**], in Germany, in 2015, about 46% and 18% of waste, respectively, was recycled and composted, 35% of waste was incinerated, and <1% of waste was landfilled. Today, in European countries, it is in general forbidden by law to landfill non-treated waste. Because of very different

economic conditions in western and eastern European countries, in the western countries it is strictly forbidden while in the eastern countries there are certain ”grace periods” for complying with this law. In the future, however, landfilling of non-treated waste will be prohibited throughout Europe.

Landfilling of waste, if not done properly, can contaminate the soil and water and endanger both human life and the enviroment for generations to come. Landfilling also requires large spaces to dispose of the waste, and its maintenance incurs a high cost. As an alternative to landfilling, WtE-technology is the most widely used method for waste treatment. The growing trend of waste treatment in WtE-plants in Germany is shown in **Figure 2.5** [Thomé-Kozmiensky **2014**]. The total quantity of burned waste in 2010 was about 20 million tonnes per year among 74 WtE-plants.

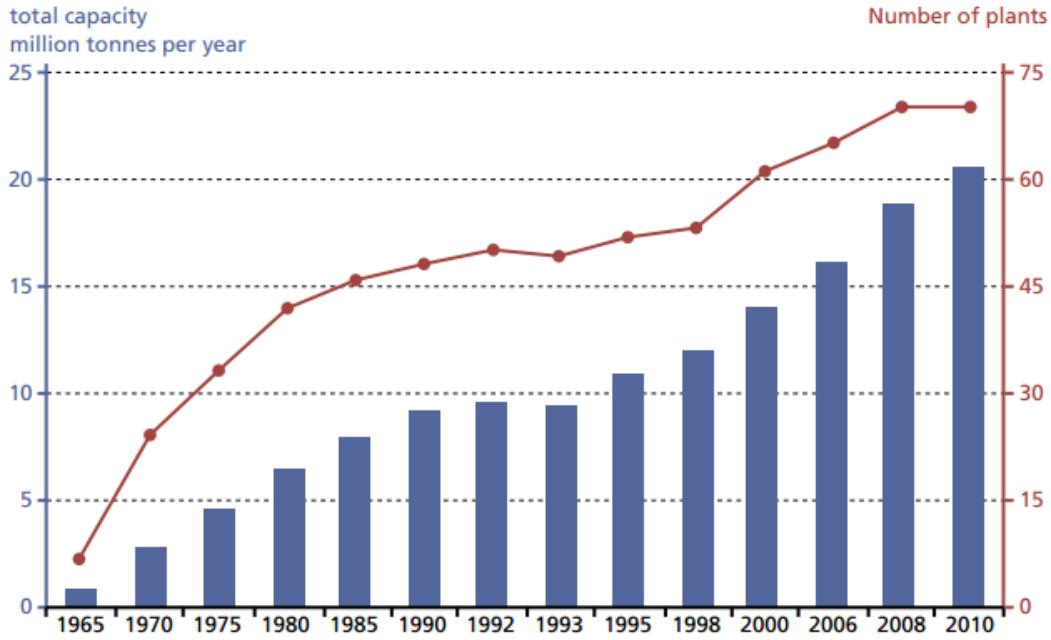

Figure 2.5: The growth of incineration plants in Germany [Thomé-Kozmienszky **2014**].

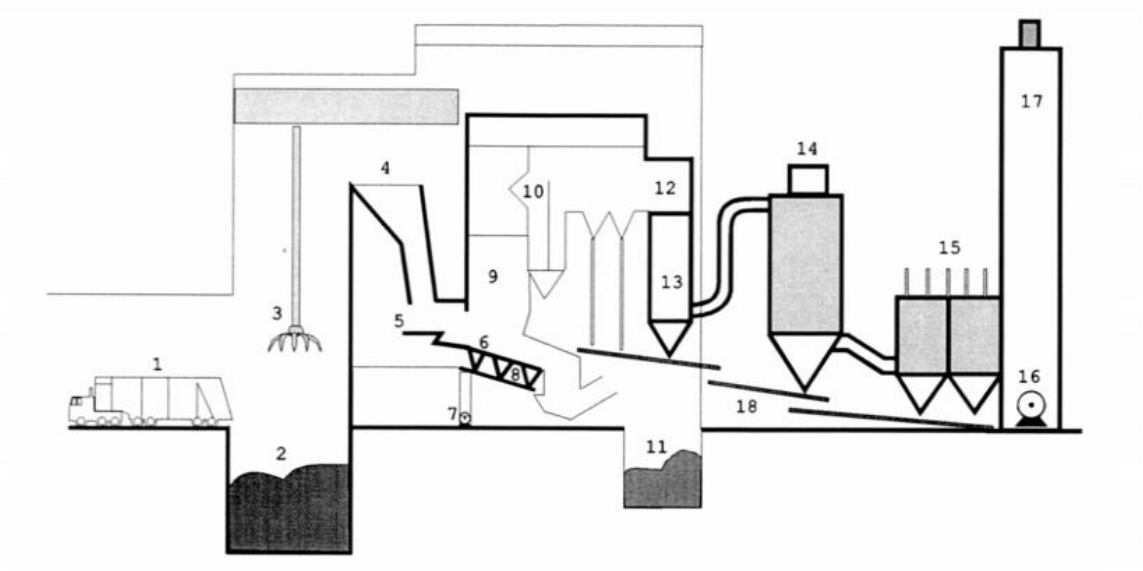

1. Refuse collection vehicle
2. Refuse storage pit
3. Refuse handling crane
4. Feed hopper
5. Feeder
6. Grate
7. Forced-draft fan
8. Under-grate air zones
9. Furnace
10. Boiler
11. Ash bunker
12. Super-heater
13. Economiser
14. Dry scrubber
15. Fabric filter baghouse
16. Induced-draft fan
17. Stack
18. Fly ash conveyor

Figure 2.6: The schematic of processes in incinerator plant, courtesy of Martin GmbH as reported by Chandler et. al. [Chandler **1997**].

A principal sketch of a WtE-plant is shown in **Figure 2.6,** with different general process steps:

1. Sections 1–3: waste transporting, storage and handling process
2. Sections 3–5: area of the waste inlet into combustion process
3. Section 9: combustion process in the furnace
4. Sections 10, 12: heat recovery system
5. Section 11: bottom ash collection and bottom ash discharge
6. Sections 12-18: filter system for flue gas cleaning

The heat produced from the combustion process is transferred and converted into steam in the heat-recovery system and the steam is subsequently conducted into a turbine to produce electricity. In the context of electricity generation, the value of energy recovery is mainly dependent on plant size. For large plant sizes, where advanced technical solutions can be applied and

sustained from an economic point of view, net electric efficiency may reach values of up to 30%–31%.

In small-to-medium plants, net electric efficiency is constrained by scale effect to around 20%–24% [Lombardi **2015**]. There are two different types of combustion systems in operation, mass burning and refuse derived fuel (RDF). Mass burning is a combustion process whereby the waste, as received, is directly fed into a furnace without any pretreatment; whereas, in the RDF process some preparation of the waste or separation of certain materials is done prior to burning. Mass burning, via incinerators, has been evolved favorably in European countries over the past fourty years [Chandler **1997**]. During combustion, the waste is fed into the furnace at temperatures around 900 ^{o}C. The combustion processes are optimized to avoid the formation of dioxins, and sufficient air supply is used to reduce the formation of CO [Lam **2010**].

I n Germany, 30 to 40 years ago, there was much public discussion of WtE plants because harmful gases, mainly dioxins, were being emitted from such plants into the environment. That is why modern WtE-plants are equipped with highly sophisticated and very effective gas cleaning systems at different steps in the process, to ensure that no air pollution is caused by these plants. Fine atomized lime powder is sprayed into the exhaust gas to neutralize any escaping sulfur oxide and hydrogen chloride. Moreover, heavy metals, mercury, organic pollutants, and very fine dust particles are captured via bag filter systems and activated carbon. Finally, selective non-catalytic reduction systems reduce nitrogen-oxide pollution by using ammonia to decompose these gas into nitrogen, carbon-dioxide, and water [Lam **2010**].

It has been reported that in WtE-plants, different amounts of residues like bottom ash, grate siftings, fly ashes, boiler and economizer ash, and APC residues are generated by the incineration process [Chimenos **1999**]. In general, bottom ash is the largest portion of solid residue being produced by the incineration process, compared to other ashes. The actual composition of bottom ash varies and different compositions from one incinerator to another and from one country to another country are typical. The composition of bottom

ash depends on factors such as the main composition of the waste, the volatility of elements contained in the waste, and differing combustion system parameters [Hjelmar **2009**]. Thus, bottom ash contains a heterogeneous mixture of oxides, silicates, carbonates, sulfides, sulfates, and salts [Klein **2002**].

2.3 The comparison of reusing materials from bottom ash to primary resources

The competitive advantage of using raw materials from secondary resources rather than from primary resources depends on the energy required in the recycling process. Most metals are extracted from ores as primary raw material. In these ores, most of the metals are highly dissipative and distributed in compounds mainly as oxides or sulphides. That is why the distribution of most of the metals in ores is characterized by a high degree of entropy.

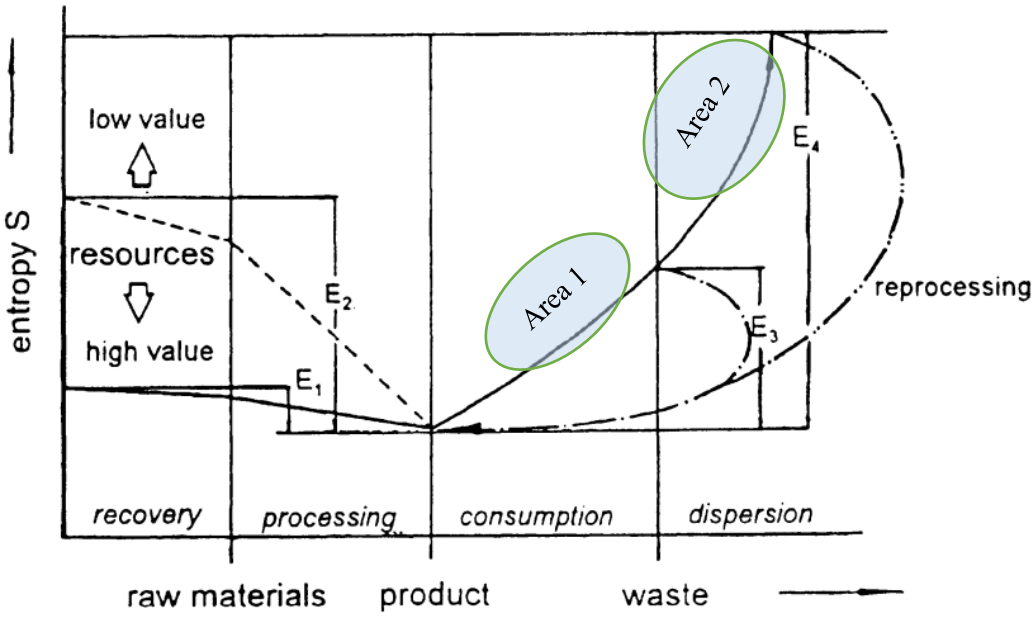

Figure 2.7: The material conversion process [Esser **1992**].

As shown in **Figure 2.7**, the higher the entropy, the higher the energy needed to extract the metals from the ore matrices. If the metals are used in products during consumption, they are very often highly concentrated and

accordingly the entropy is lower. After consumption, when the products are at the end of their life, they become waste and, accordingly, the entropy starts to increase again, depending on how dissipative is the distribution of metals in the waste. The greater the entropy, the greater the energy needed to recycle and to recover the desired elements. Thus, the recycling of elements or compounds from Area 1 is easier, with less energy consumption and lower costs, than the recycling of elements or compounds from Area 2, due to their higher degree of entropy. Whether a recycling process under these circumstances is economical or not greatly depends on metal prices, in addition to the concentrations of the target substances in the matrix or samples. It also depends on whether one or more products can be obtained from the recycling process [Deike **2012**].

So, if the waste has a high concentration of metals, it has a high potential to be raw material for metal recovery, just as much potential as primary resources. In terms of fine fraction of bottom ash with a conservative estimate of 0.3% – 0.4% copper [Deike **2012**], the copper content in bottom ash is as high as that in the poor copper ores that are mined today. That is why copper contained in bottom ash (or other valuable materials) should be considered as valuable secondary raw material. Considering the production of bottom ash nowadays, it is estimated that 800 WtE units are in production worldwide, and most of them are in Europe [Bunge **2015**]. In Germany, about five million tonnes of bottom ash are produced per year and from this quantity of bottom ash it is possible to retrieve 400,000 tonnes of scrap iron and 37,000 tonnes of non-ferrous scrap by common separation techniques [Deike **2015**]. In addition, after this kind of bottom ash processing, metals are still contained in the fine fraction of bottom ash, which are only separated in small quantities today. That is why bottom ash still has a high potential for recovery of metals.

Whether the recycling of metals from bottom ash is economically feasible depends greatly on the metal prices. The fluctuations in metal prices for the copper, nickel, zinc, and aluminium commonly contained in bottom ash are described in **Figure 2.8**. These very strong fluctuations are why the recovery of

metals from bottom ash could only be realized with cheap and easy processes, which can be operated in an environmentally friendly manner.

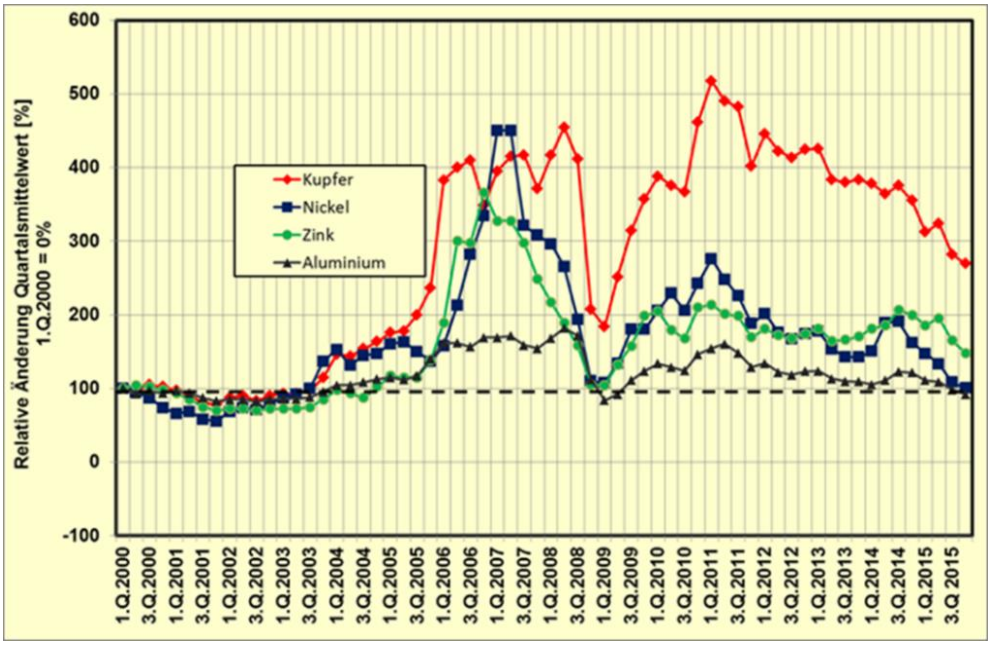

Figure 2.8: The fluctuation of copper, nickel, zinc, and aluminium prices for the last 15 years [Deike **2016**].

Copper, nickel, zinc, and aluminium prices depend on supply and demand of these metals. Beginning in 2003–2004, the prices started to increase and kept rising from 2005 to 2008 before dropping drastically in 2008-2009. The drop in prices was mainly caused by the global crises at that time. After 2009, metal prices started to rise again, but, with the exception of copper, the prices never reached the same level as before the economic crisis. Regardless of this, since 2011 a more or less continuous trend of decreasing metal prices can be seen. This development is mainly caused by lower economic growth rates in China. Because China is the most important nation in global raw material consumption today, therefore economic changes in China have a direct effect on the global raw materials business.

Incinerator bottom ash is a solid waste residue deposited at the bottom of the stoker grate in the combustion/incineration process. The composition of bottom ash is heterogenous and may differ from one incinerator to another and from one region to another. The main factor in bottom ash composition is the composition of the material input before the combustion

process. Generally, the major constituents of bottom ash are aggregates such as stone, ceramic, and glass, which have similar components as primary building materials such as gravel and sand [Muchová **2010**]. There is no exact composition in bottom ash. As discussed above, it contains a heterogeneous mixture of oxides from silicon, calcium, iron, and aluminium. Other compounds may also contain alkali—alkali earth compounds, salts, sulfates, ferrous and non-ferrous compounds, etc. Generally, bottom ash is classified into several different particle sizes. Usually, it has 80 wt.% particles less than 10 mm and the finest particle size (less than 2 mm) is up to 40 wt.% [Hjelmar **2009**].

The production of bottom ash in EU countries [CEWEP **2016**] reached approximately 18 million tonnes in 2014. This amount of bottom ash contains about 85% mineral fraction, steel and ferrous metals up to 12%, and non-ferrous metals 2%–5% (including aluminium in proportions of 60%). Metals are separated, in general, using state-of-the-art techniques as shown in **Figure 2.9**. After sieving in different steps, two fractions of bottom ash are produced. They are a coarse fraction which has a particle grain size of >50 mm, and a fine fraction particle grain size of < 50 mm. Magnetic components in the > 50-mm coarse fraction are separated by magnets, while non-ferrous components are seperated by sensor-sorting techniques, by eddy-current separators, and manually, particularly heavy parts like old electric motors and stainless steel implements. After separation, the metals are mainly traded via scrap companies in ferrous and non-ferrous industries. The < 50-mm fine fraction is further classified by sieving for smaller grain sizes, while the metals separation starts in all grain size classes with a magnetic separation, followed by eddy-current separation processes, and sometimes also by sensor-sorting techniques. These metals are also traded out to the ferrous and non-ferrous industries.

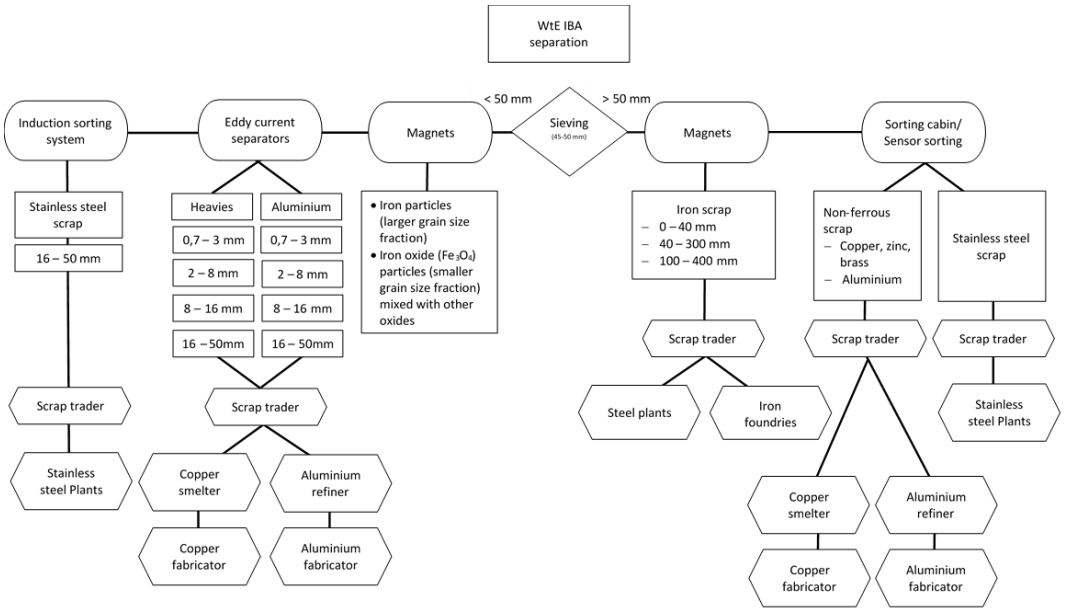

Figure 2.9: Bottom ash treatment and recycling distinguished by its particle grain size [Deike **2014**].

Ferrous materials comprise, on average, up to 10% and non-ferrous up to 2% of bottom ash [CEWEP **2016**]. The current processing of bottom ash is distinguished by particle size. Ferrous metals contained in bottom ash are mainly concentrated in coarse fractions [Deike **2014**]. As shown in **Figure 2.9,** the existence of metallurgical plants is mandatory for developing successful recycling strategies, because they are needed to close the material cycle. Without metallurgical plants, there is no recycling for treated bottom ash.

The composition of WtE bottom ash is mainly determined by the original composition of the waste. Some elements, such as zinc, are concentrated during the incineration process in the flue ash and in the finer fraction of the bottom ash. Other elements, like silicon dioxide, normally are not influenced by the process. In summary, the physical and chemical composition of bottom ash is influenced by conditions such as the composition of the original waste, the operating conditions of the facility, the type of combustion process used, and the APC system adopted by each incinerator facility in each region.

2.4 The distribution of metals in bottom ash; the overview of bottom ash recycling potential

The production of bottom ash in WtE plants has become an opportunity for the recycling and material supply industry. After the separation of coarse ferrous and non-ferrous particles, bottom ash still contains in the fine fraction (< 3 mm) valuable metals or trace elements. That is why it is still interesting to do research on the issue of how to get valuable metals out of the bottom ash by an economically and ecologically useful process.

2.4.1 Iron and aluminium

The The most abundant metal contained in bottom ash is iron (Fe). Magnetic separation is the preferred process for recovering iron and magnetite (Fe_3O_4) from bottom ash. The content of iron in bottom ash could reach up to 32.3–39.2 wt.% on particle sizes smaller than 3 mm [Xia **2017**], while metallic iron is only in the range of 3.2 – 9 wt.%. On the other hand, Deike et al. [Deike **2012**] and Chandler [Chandler **1997**] found only about 8–12 wt.% of iron in the fine fraction of bottom ash, and did not find metallic iron at all, because nearly all of the iron was in the form of magnetite (Fe_3O_4).

Another abundant metal in WtE bottom ash, besides silicon, alkali and alkali-earth elements, and calcium, is aluminium. Aluminium originally came from the packaging industries, such as beverage cans, medical packaging, foils, thin sheet metal, etc. [Chimenos **1999**]. Aluminium is contained in almost every particle size. Xia, Yi et al. found that aluminium content was the highest in a particle size larger than 20 mm and in amounts of 21–69.4 g/kg, while in the 20.8–38.6 g/kg range, aluminium was contained in a particle size smaller than 3 mm [Xia **2017**]. Likewise, Deike et al. found in the fine fraction 30–45 g/kg of aluminium and in the coarse fraction (>8mm) about 60 g/kg of aluminium [Deike **2012**].

2.4.2 Copper and zinc

Deike et al. [Deike **2013**] found 0.3–0.4 wt.% of copper and up to 1 wt.% of zinc in bottom ash. The amount of copper in the fine fraction is as high as in the poor copper ores that are mined today. Copper in bottom ash does have the advantage of being mainly metallic, as opposed to natural ores, in which copper is present as sulphide or oxide. Therefore, it makes sense to develop processes whereby copper can be recovered in an economically and ecologically friendly way from bottom ash. In a previous study, the concentrations of copper and zinc depended on the material input of incineration plants [Chimenos **1999**].

Zinc contents in the smaller grain size fraction are higher than in the larger grain size fractions. This is due to the physical properties of zinc, which evaporates at the temperatures reached in the burning chamber and reacts with oxygen to form zinc oxide during the incineration process [Deike **2015**]. Solid particles that are products of the reactions of two gases are very fine particles and that is why most of the zinc oxide is collected in the flue gas filter system. But a certain amount of zinc oxide is also transported into bottom ash and that is why the zinc content in the fine fraction is higher than in the coarser fraction.

2.4.3 Mineral phases

In principle, WtE bottom ash can be used as raw material for road construction and perhaps, if it is clean enough, as raw material for the cement industry and other similar purposes. In Netherlands, bottom ash has been reused as a filler in asphalt for road construction, but the use is limited due to the leaching behavior of copper, molybdenum, antimony, and other metals contained in up to 1% of bottom ash [Born **1997**] (**Figure 2.10**).

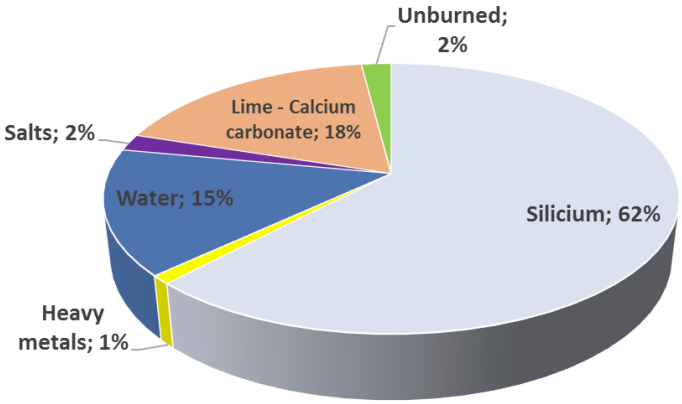

Figure 2.10: The composition of mineralogical of bottom ash [Pecqueur **2001**].

There are reports that certain components of bottom ash have shown a distinct expansion behavior, resulting in the formation of cracks [Pecqueur **2001**]. The swelling is caused by the following reaction:

a. The aluminium metal which oxidizes and form a gel:

With the condition of high pH, (above 10), the metal is dissolved with the emission of H_2 according to the reaction:

$$4\,Al + 16OH^- \rightarrow 4Al_2O^- + 8OH^- + 12e^- \quad \text{.....(2.1)}$$
$$12\,H_2O + 12e^- \rightarrow 6H_2 + 12OH^- \quad \text{.....(2.2)}$$
$$4Al + 4OH^- \rightarrow 6H_2 + 4AlO_2^- \quad \text{.....(2.3)}$$

The formation of gel occurs when the pH dropped to 9-10, aluminium hydroxide formed on the reaction above tends to form $Al(OH)_3$ gel.

b. The formation of ettringite:

This reaction occurred when the materials is saturated with water [LP **1996** and Pecqueur **2001**];

$$Al_2O_3 + 3CaSO_4 + 3Ca(OH)_2 + 28H_2O \rightarrow (CaO)_2(Al_2O_3)(CaSO_4)_3(H_2O)_{31} \quad \text{.....(2.4)}$$

c. The hydration of lime (calcium oxide) and magnesium oxide:

$$CaO + H_2O \rightarrow Ca(OH)_2 \quad \text{.....(2.5)}$$
$$MgO + H_2O \rightarrow Mg(OH)_2 \quad \text{.....(2.6)}$$

2.5 The state of the art bottom ash treatment

The recovery of valuable materials from bottom ash has been discussed mainly with reference to different leaching processes. Many studies

discuss the leaching of copper from bottom ash. Besides copper, other heavy metals contained in bottom ash, such as lead, zinc, and other trace elements, are also treated in terms of leaching.

It has been observed that, during quenching, soluble and dissolution salts of alkali have been formed depending on the washing ratio and the residence time [Marchese **2010**]. Different washing ratios cause different residual alkalinity and affect the pH value of leachates with different metal releases. Lead dissolution causes an increase in pH value. At pH values higher than 11.8, the dissolution–precipitation of Pb to form $Pb(OH)_2$ takes place. This high value of pH is related to the dissolution of $Ca(OH)_2$. The formation of dissolved heavy metals from waste and the subsequent pollution of ground water is the main reason why the use of bottom ash in public road construction is limited in different federal states of Germany. To counter this process, pollutants contained in the leachate should be removed or immobilized before it dissolves. The solidification/stabilization (S/S) process is the proper method to immobilize or stabilize a pollutant. The principle of this process is the use of binders to encapsulate the waste material so that the leachability of heavy metals will subsequently be reduced. Another alternative way to immobilize harmful elements is by using vitrification processes. Immobilization by vitrification of harmful elements and subsequent volume reduction has advantages but it requires high energy consumption [Xiao **2008**].

There are two purposes to which leaching can be put in bottom ash treatment: the removal of heavy metals from the bottom ash, and the recovery of these heavy metals from the leachate [Ferreira **2002**]. The effectivity of a leaching process depends on several factors, such as solvent extraction, the pH value (reagent concentration to dissolve the heavy metals), and the liquid-to-solid ratio during the leaching process. Investiogation of the pH dependence of leaching shows that the higher the pH value the lower the leachability of heavy metals, due to the formation of insoluble hydroxide [Youcai **2002**]. An effective agent for extracting heavy metals is EDTA (ethylene-diamine-tetraacetic-acid), the common reagent used for extraction of heavy metals such as Pb, Cd, Cu, and

Zn [Youcai **2002**]. The methods for the extraction of heavy metals from leachate vary. The recovery/removal of heavy metals from leachate may be obtained by the following procedure:

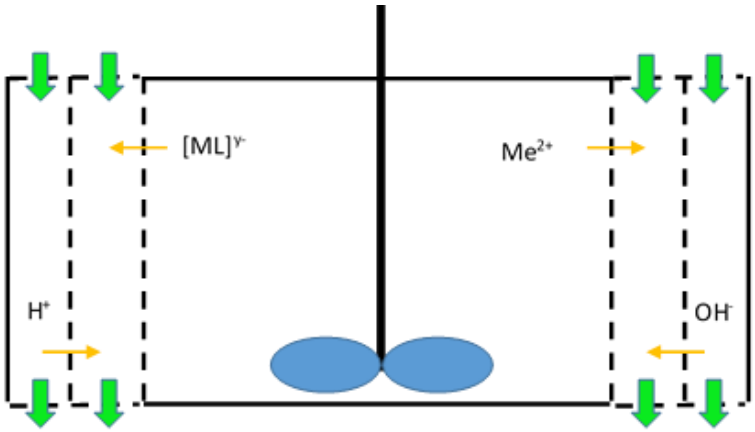

Figure 2.11: The illustration of electrodialytic remediation process referred to [Lam **2010**] which adopted from [Ferreira **2002**].

The basic principle of the electrodialytic remediation process is the use of electric potential to force oxidation or reduction on the surface of an electrode. During the process, the metals are deposited on the cathode surface. A similar process was investigated by Giombattista Traina et al. [Traina **2007**]. The use of electrokinetic remediation by using an open cell with graphite electrode and without enhancing agents (and membrane) showed that the ash pH was increased depending on applied current density and at 2.5–3 mA cm^{-2} the precipitation of heavy metals as hydroxide occurred. After treatment the concentration of pollutant in leachate was reduced by 31–81%.

Therefore, the principal process from previous research has been implemented and improved in this study, which consists of the following steps:

2.5.1 Moisture content removal by drying process

Some methods for recovering valuable metal in bottom ash are substantial. The origin samples used in this research have high amounts of moisture. The current milling and sieving facilities available at the ITM (*Institut*

für Technologien der Metalle, University of Duisburg Essen, Germany) lab are favorable for dried samples. Especially in the sieving facility, the sieving mesh and apparatus are only suitable for dry materials. Wet or high-moisture samples are difficult to sieve due to their agglomeration behavior during the sieving process, especially for finest fractions (starting from particle sizes of 63 µm and smaller). Therefore, a standard test method for drying has been used.

2.5.2 The increasing of degree liberation by milling process

Milling is one of the comminution methods commonly used for physical separation and produces liberated particles. During incineration within a certain temperature range, particles with a lower melting point are melted and combined with other elements to form new compounds that have different compositions than the original ones. That is how physical connections are made between slags and metals and other elements with the potential for physical bonding among the constituents of bottom ash.

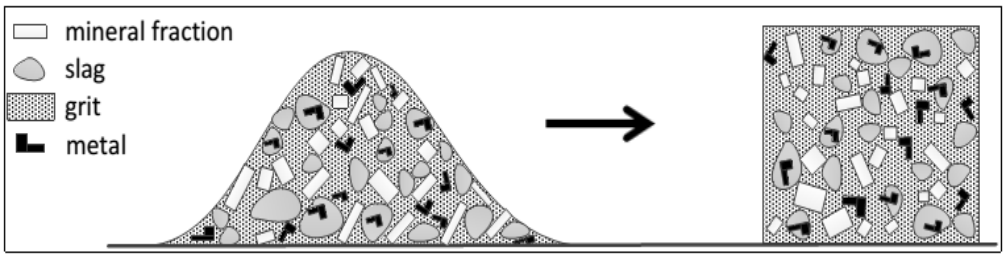

Figure 2.12: Solidification of free-flowing bulk solid after wet extraction [Bunge **2015**].

It has been reported that in the bottom ash from WtE plants, after quenching (**Figure 2.12**), a large number of reactions take place [Bunge **2015**]. On contact with water, soluble and semi-soluble salts (for example $CaCl_2$, Na_2SO_4, KOH, $Ca(OH)_2$) that have concentrations of 2% of grit fraction are dissolved. This process induces the increasing of pH above 12 and triggers reactions with silicates. Minerals are also formed by absorption of carbon dioxide (e.g., limestone) or due to precipitation (e.g., gypsum). The formation of new minerals leads to aggregation of the bottom ash and, during a curing time of several months, the bottom ash will be transformed into a solid block. To counter this

aggregation process and to increase the liberation of physically-bonded particles in slags and metals, comminution with milling is necessary. That is how the recovery of metal fractions is feasible. A further result of ball milling is the increase of fine particle size weight percent. This is important for the next separation process, as the effectiveness of density separation by sluice-box and gold-pan methods depends on particle size. The principle behind the grinding or milling process is to separate the constituents of physically bonded compounds into various liberated-finer particles.

2.5.3 Particle size distribution by sieving process

The main purpose of the sieving process is to classify the milled particles by particle size, so that they can be separated according to density. The principle is to analyze different particle sizes by passing a known weight of sample material through different sized sieves and weighing the amount collected via each sieve to determine the percentage weight in each size fraction. The total weight of samples and the type of movement transmitted to the sieve would affect the effectiveness of the sieving results [Wills **2006**]. The type of particle shape and characteristic should also to be recorded. Some various shapes of particles is described in **Table 2.2.**

Table 2.2: Types of particle shape and its characteristic [Wills **2006**].

Types	Characteristic descriptions
Acicular	Needle-shaped
Angular	Sharp-edged or having roughly polyhedral shape
Crystalline	Freely developed in a fluid medium of geometric shape
Dendritic	Having a branched crystalline shape
Fibrous	Regular or irregularly thread-like
Flaky	Plate like
Granular	Having approximately an equidimensional irregular shape
Irregular	Lacking any symmetry
Modular	Having rounded, irregular shape
Spherical	Global shape

2.5.4 Magnetic Separation

As mentioned previously, up to 10% of the composition of bottom ash, on average, is ferrous materials [CEWEP **2016**]; however, the smaller particle size fractions contain a lower amount of ferrous materials [Xing **2004**] and mainly as iron oxide [Deike **2012**]. The effectiveness of magnetic separation depends not only on how strong the magnet is, but also on how high the degree of liberation is. If a particle is still physically bonded to both magnetic and non-magnetic compounds, the non-magnetic compounds will also be attracted by the magnet. That is why the forces of the magnets have to be optimized. When the magnetic force is too high, the amount of non-magnetic material in the magnetic fraction could likewise be too high. In addition, it is important to reduce the friction between the particles, which can be achieved by conducting the magnetic separation in a fluid.

2.5.5 Density separation by using sluice-box and gold-panning experiment

Density separation is one of the gravity separation methods that principally use the differences in specific densities of particles or minerals to extract the valuable material from the surrounding gangue minerals. The principle of the process is to separate elements or mixtures having different specific gravities by performing a relative movement in response to gravity or other forces usually emitted by viscous fluids such as water or air or sometimes heavy media. These additional forces can be used to disturb the balance of the particles in response to natural gravity. In mineral processing technology, there are several separation methods available, such as sorting, gravity separation, dense media separation, magnetic separation, electrostatic charge, and flotation. The methods, as mentioned previously, often depend on the particle size of the mineral being separated. The effectiveness of each separation method, depending on particle size function, is shown in **Figure 2.13**.

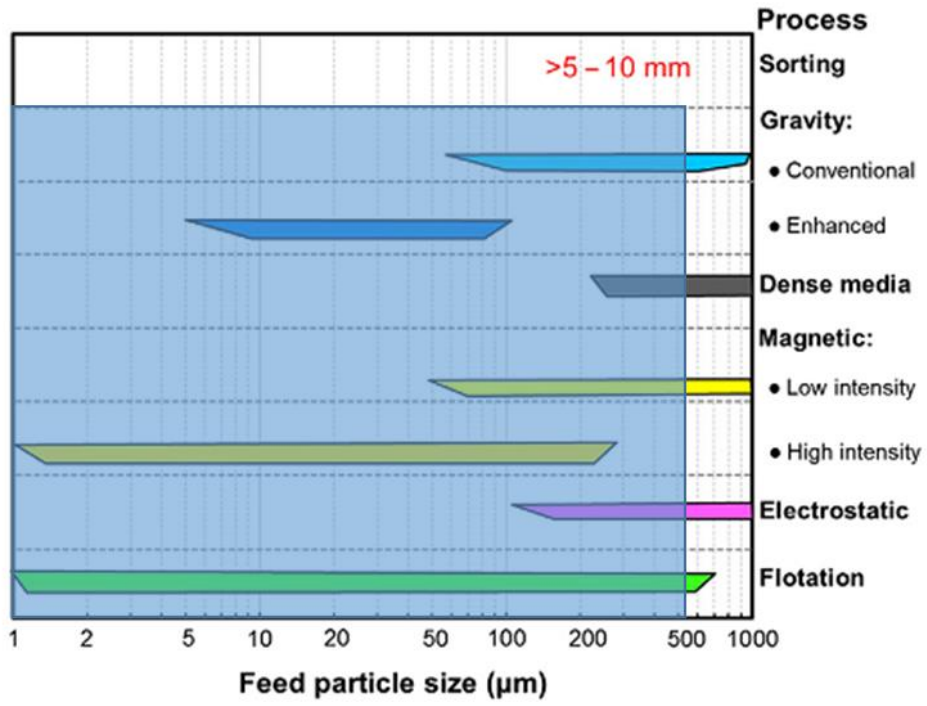

Figure 2.13: The effectiveness of separation method in correspond with particle size range [Wills **2006**].

The highlighted blue colour area on **Figure 2.13** shows the effective separation methods especially for fine particle grain sizes less than 500 µm. The motion of particles in a fluid is dependent not only on its specific gravity, but also on its size; large particles will be affected more than smaller particles [Wills **2006**]. Larger particle sizes will increase the efficiency, while smaller particle sizes are dominated mainly by surface friction, which has a negative effect on commercial high-capacity gravity methods. The sluice-box process (**Figure 2.14**) is one of the techniques of gravity separation. The principle is to separate the particles based on their densities under the force of flowing water. During this process, the valuable materials are trapped in the matting because of their higher densities and tend to sink to the bottom, while the surrounding gangue mineral, due to its lower density, is swept away. Density separation by sluice-box process has been used mainly in the gold-mining industry.

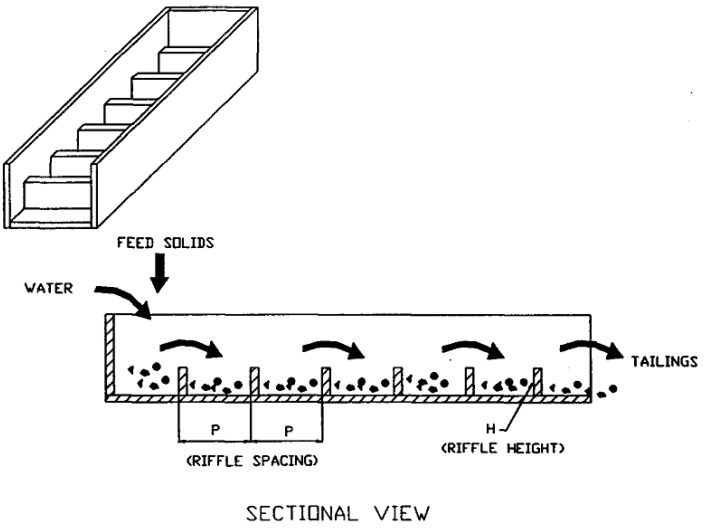

Figure 2.14: The simple illustration of sluice-box separation process [Subasinghe **1992**].

After a sluice-box process, stirring on gold-pan method can improve a further density separation. Heavy particles usually stay in the upper level of the sluice-box. Particles from the upper section of the sluice-box will be separated further by gold-pan separation. Historically, gold-pan has been used manually for decades by gold miners. The water stream in the pan caused by rotation (as the pan is rotated manually) leads to the separation of the gangue minerals from the gold particles. The gold-pan being used for the separation process in this study is shown in **Figure 2.15**.

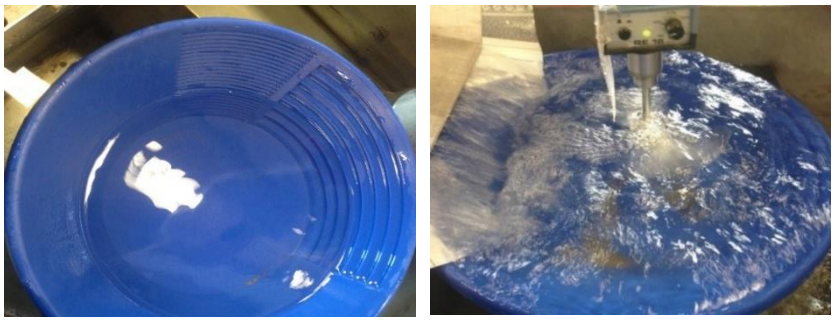

Figure 2.15: The traditional gold-pan (left) and additional stirrer being applied in gold-panning method (right).

This traditional gold-pan process has been modified in the ITM lab, by introducing a water stream with a stirrer, installed in a certain position. The collected particles from the sluice-box process were separated further by this method. The speed used to separate valuable materials from non-valuable materials is limited up to a certain maximum (optimum) speed, beyond which the separation efficiency is reduced.

3 Preliminary and research methodology of bottom ash fine grain size fraction for copper recovery

3.1 Preliminary research

A suitable and economical process for copper recovery from bottom ash, one that can be upscaled on an industrial level, is the objective of this study. Optimal parameters regarding process efficiency, process costs, and environmental benefits were identified. Therefore, information is needed about the characteristics of fine particle bottom ash, such as particle size distribution, the constituent distribution, the content of heavy metals, minerals, magnetic and non-magnetic materials, and various other components. The general flow chart to determine the parameters that are needed, is shown in **Figure 3.1.** In this study, bottom ash samples from different bottom ash treatment companies were examined.

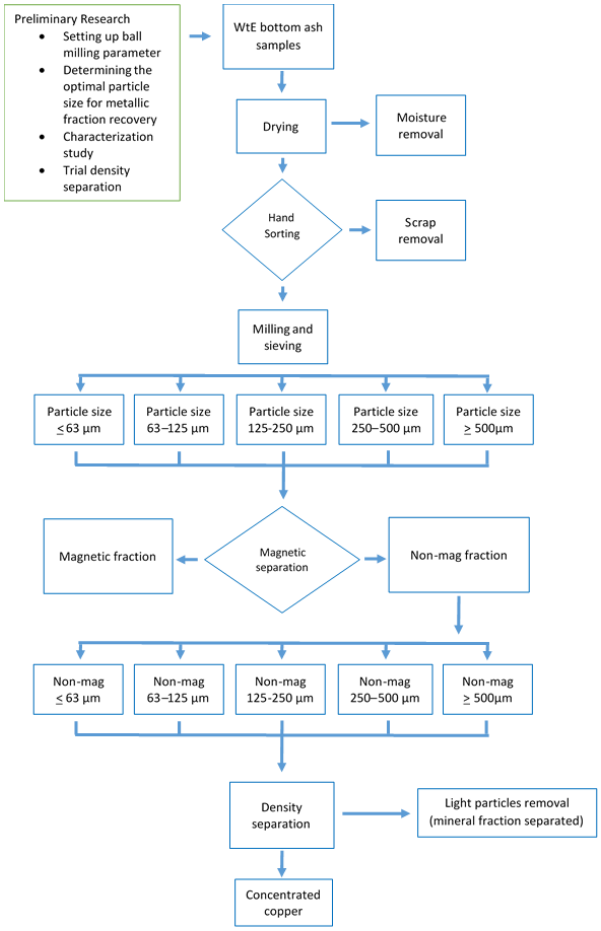

Figure 3.1: The general flowchart process for copper recovery of bottom ash fine particle grain size.

3.2.1 Preliminary ball-milling – magnetic separation process

After a curing time of about 3 months, the prepared bottom ash from plant A had an initial particle size between 4 and 8 mm. At the beginning, a ball-milling process was needed to increase the liberation process. The preliminary research for this study was carried out on particle size fractions of 4 to 8 mm, which had been reduced by ball-milling down to 2-mm particle size. The different grain size fractions, produced in this way, were treated in a density separation process with natrium-polytungstate into light and heavy particle fractions. In **Figure 3.2**, the percentages of light and heavy fractions in the different grain sizes are shown in relation to the total input.

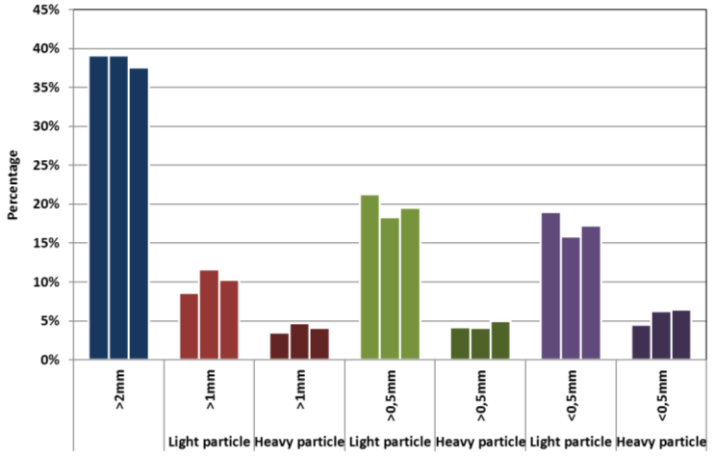

Figure 3.2: The percentages of light and heavy fractions in the different grain sizes.

After separation into light and heavy fractions in the different grain size fractions, the magnetic portions in light and heavy fractions were measured (**Figure 3.3**).

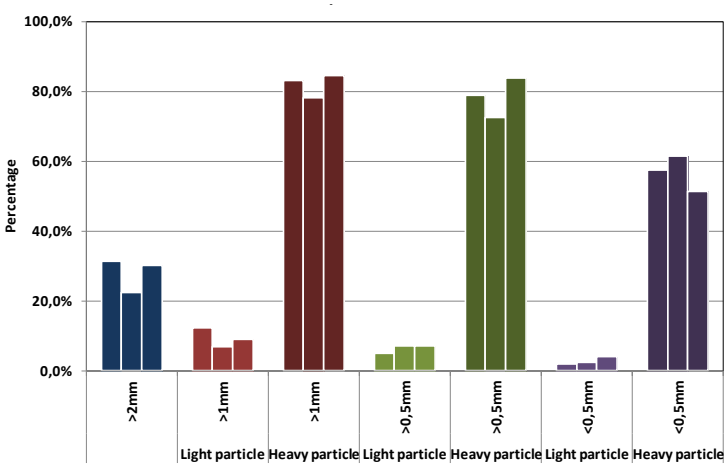

Figure 3.3: Comparison of magnetic and non-magnetic product distinguished by its particle size [Deike **2013**].

From **Figure 3.3**, it can be seen that heavy fractions have high content of magnetic fractions. In the fine fraction, iron is totally oxidized [Deike **2012**] and consists mainly of magnetite (Fe_3O_4). That is why heavy fractions have such high percentages of magnetic fractions. Magnetite ($FeO{\cdot}Fe_2O_3$), which has a spinel structure, belongs to the class of inverse spinels [Trojer **1963**; Kleber **1983**]. The cubic spinel structure of magnetite (a = 0,8374 nm) contains eight stoichiometric units [Trojer **1963**], wherein the oxygen ions are positioned in cubic closed packed structures. In normal spinel structure, 1/2 of the octahedral gaps are filled with trivalent metal ions and 1/8 of the tetrahedral gaps are filled with divalent metal ions [Kleber **1983**]. Each oxygen ion is surrounded by three trivalent and one divalent metal ion. In inverse spinels like magnetite, the divalent metal ions exchange their positions with half of the trivalent metal ions. When magnetite is created from liquid melts (slags), the divalent iron ions (Fe^{2+}) can be replaced by different divalent metal ions like Mg^{2+}, Mn^{2+}, Co^{2+}, Ni^{2+} , etc., and the trivalent iron ions (Fe^{3+}) can be replaced by different trivalent metal ions like Mn^{3+}, V^{3+}, Cr^{3+} , etc. That is why magnetite acts as a collector for tramp elements [Deike **2015**], which can be concentrated easily by magnetic separation in the magnetic fraction of bottom ash, as shown in **Figure. 3.4.**

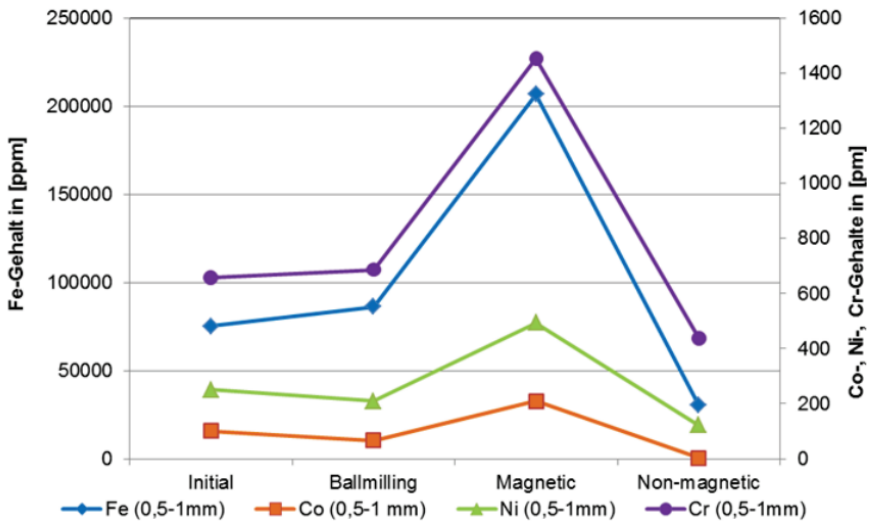

Figure 3.4: The concentration of Co, Ni, and Cr with magnetic separation in bottom ash fine particle grain size [Deike **2015**].

3.2.2 Preliminary density separation with separation with sink-float process

Milled bottom ash was covered with dirt. For initial surface and morphology examination, removal of this dirt was important and therefore bottom ash samples were washed with tooth-cleaning tablets dissolved in distilled water inside an ultrasonic bath for 1 hour at 80 °C. Afterwards, heavy medium separation was done by a sink-float process (**Figure 3.5**). The sink-float process was conducted inside a chamber filled with 300 mL of natrium-polytungstate with a density of 3.0 kg/m³ (**Figure 3.5 – left side**), where the samples were stirred for about 5 minutes to induce the separation process. The sink-float process was conducted for each particle size fraction. Light particles floated and heavy particles sank.

The difference between heavy and light particles can be seen in **Figure 3.5 – right side**. To remove natrium-polytungstate from the light and heavy particles, a filtration process was performed and afterwards the particles were cleaned with distilled water and ethanol and were fired inside a furnace (80 °C) until completely dry. The mixture of natrium-polytungstate and water could be reused for the next operation after its specific density had been adjusted to 3.0 (kg/m³) by drying process. Dried samples were segregated by magnetic separation process into four different samples: heavy-magnetic particles, light-magnetic particles, heavy-non-magnetic particles, and light-non-magnetic particles, as shown in **Figure 3.6**.

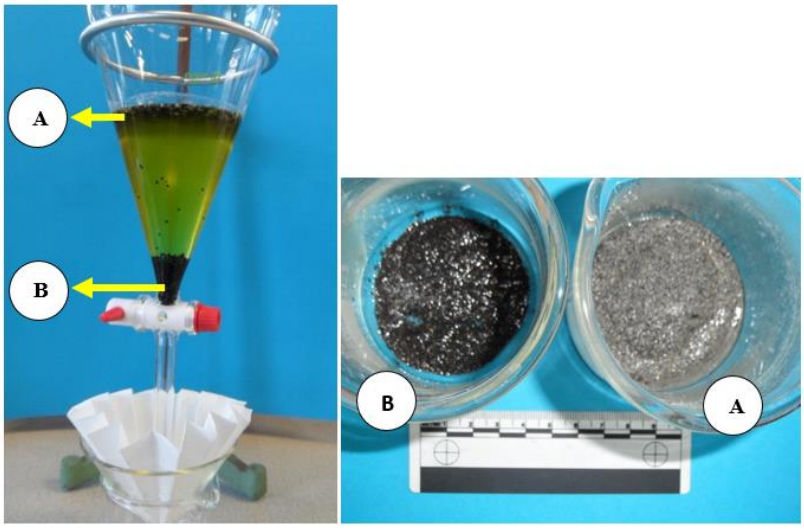

Figure 3.5: The sink-float process (left): 0.5 – 1 mm particle size by using natrium-polytungstate and collected particles (right): (A) light particles, (B) heavy particles.

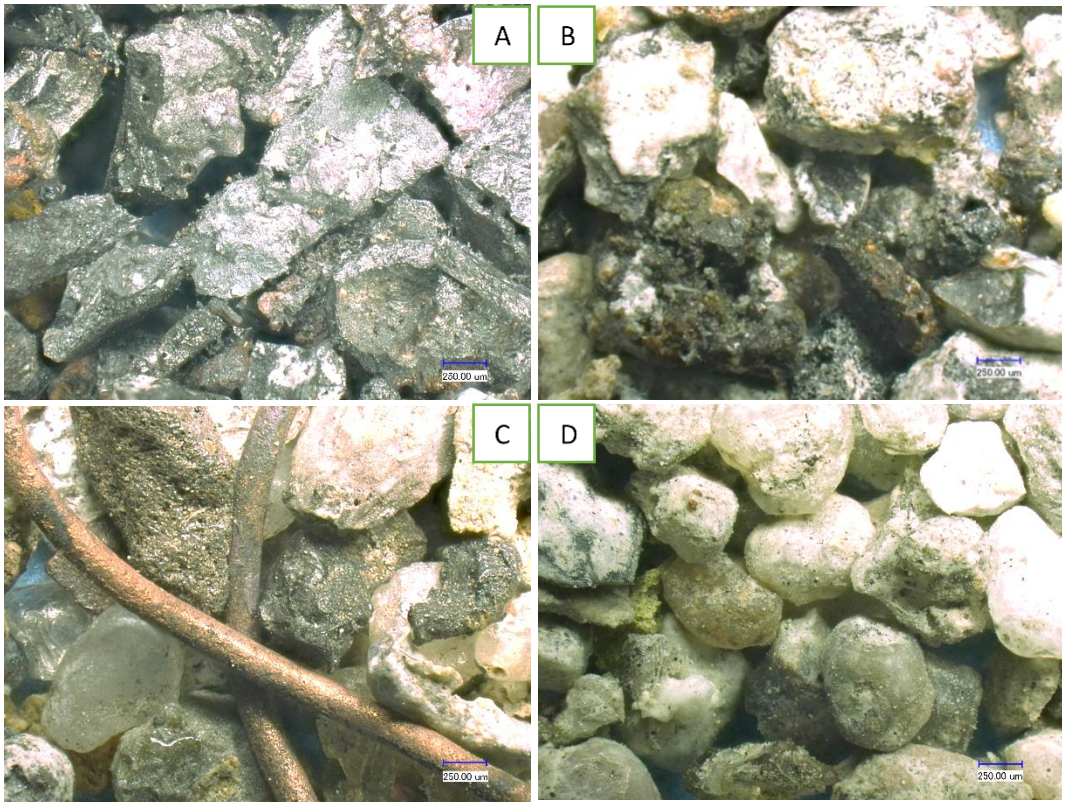

Figure 3.6: Examples of collected 0.5 – 1 mm particles after sink-float process. (A). Heavy-magnetic particles, (B). Light-magnetic particles, (C). Heavy-non-magnetic particles, (D). Light-non-magnetic particles [Deike **2013**].

As shown in **Figure 3.6,** the potential of copper recovery is best done on heavy-non-magnetic particles. It can be clearly seen that collected copper was metallic copper and in the form of wire. The heavy-magnetic fraction was represented by some dark-black colour particles, which sometimes were covered by red-orange layers. The light magnetic fraction commonly contained some dark-black colour particles in association with bright-white particles. By contrast, light-non-magnetic particle fractions mainly consisted of bright white particles. These morphological results are important for further process analysis.

Chemical composition of these collected particles after completion of the sink-float process has been determined by Field Emission Scanning Electron Microscope (FESEM). Because there is no sample preparation before testing, such as mounting, grinding, and polishing, the FESEM results described in **Figure 3.7** mainly explain the particle surface composition, rather than the inner composition of the particles. But starting the particle analyses directly with FESEM very often becomes difficult, as, in FESEM, all the particles look more or less grey (**Figure 3.7 – right side**) and differences are not easily detected. That is

why in this study the particles were first examined via the three-dimensional Keyence microscope, to see the different colours of the particles or to differentiate certain areas on the particle surfaces (**Figure 3.7 – left side**). With this knowledge, it is possible to analyse the particles in FESEM more effectively and purposefully.

In **Figure 3.7.a** and **3.7.c,** a collection of typical heavy particles contained in WtE bottom ash is shown. The heavy magnetic particles (**Figure 3.7.a**) typically appear dark brown or black in color due to the magnetite, whereas the heavy non-magnetic particles (**Figure 3.5.c**) display a brighter colour and very often consist of small parts of copper wire.

In general, nearly almost all the sample surfaces were covered by oxide layers (**Table 3.1**) which contain elements such as iron, sodium, calcium, silicon, etc. In contrast to the small copper wire (**Figure 3.7.d**), which consists mainly of copper and an amount of oxygen much lower than that on the surfaces of the other particles.

Table 3.1: The composition of area (b), (d) and (f) on Figure 3.7.

Element	Weight %.								
	Area (b)			Area (d)			Area (f)		
	Spec. 1	Spec. 2	Spec. 3	Spec. 1	Spec.2	Spec. 3	Spec. 1	Spec. 2	Spec. 3
O	76.01	72.99	75	70.26	9.65	54.44	70.64	57.79	72.83
Na	6.28	6.99	5.87	2.95	--	31.26	11.59	22.30	8.96
Al	1.15	1.75	--	4.44	--	--	0.97	1,53	--
Si	3.02	7.89	2.60	4.31	--	3.98	3.57	2.08	9.41
Mo	--	--	--	--	--	--	--	3.25	--
S	--	0.91	--	--	--	--	1.62	--	1.61
K	--	--	--	--	--	--	--	1.10	0.69
Ca	6.09	5.68	--	6.74	--	1.80	2.37	2.10	6.50
Fe	7.45	3.79	16.53	11.30	--	8.52	9.25	9.85	--
Cu	--	--	--	--	90.35	--	--	--	--

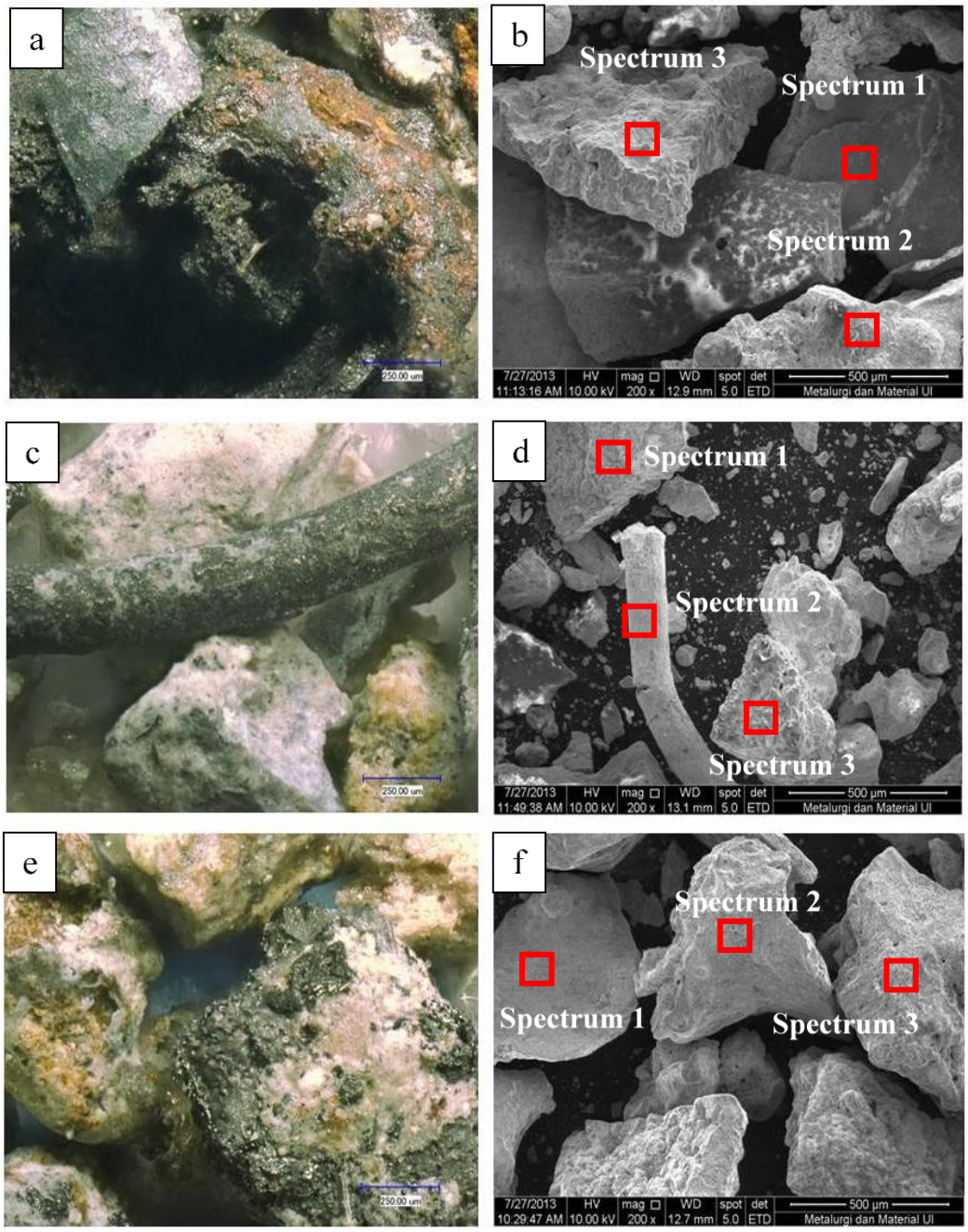

Figure 3.7: Comparison of digital microscope *Keyence*(left side) and FESEM result (right side).

Information about the distribution of different elements on heavy non-magnetic particles (**Figure 3.8)** is provided by element mapping. The distribution of oxygen and silicon shows that silicon and oxygen occur together very often, which indicates silicate-like compositions of these particles. In addition, particles are shown in which the aluminium content, and in some other particles the zinc content, is high. The fact that oxygen is high also indicates the existence of aluminium oxide and zinc oxide in different particles. Moreover,

higher copper and zinc content is detected in the wire-like particle, which indicates that this particle is made of brass.

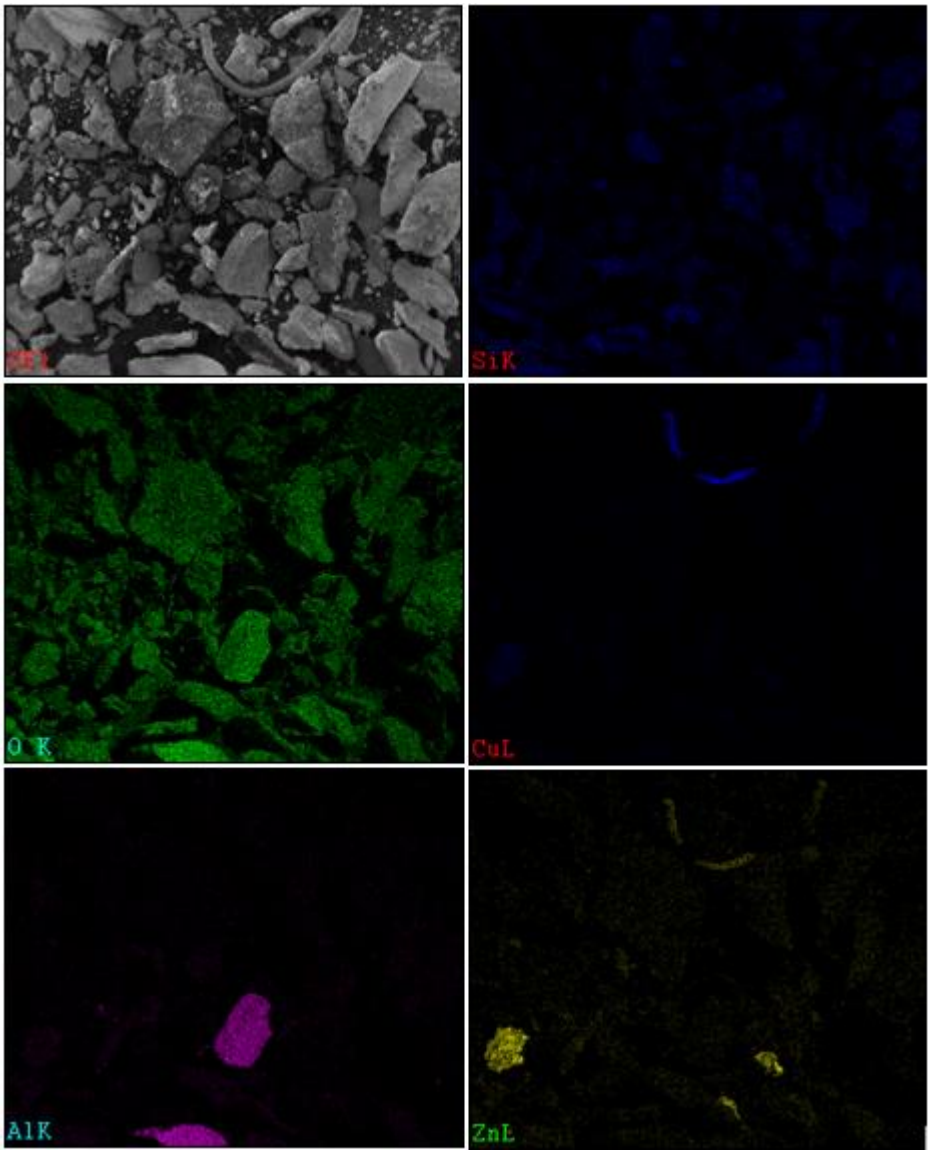

Figure 3.8: Elemental mapping of heavy-non-magnetic particles.

3.3 Moisture content removal by drying process

To estimate the total weight of bottom ash samples that contain valuable materials, it is important to eliminate the moisture content. Several groups of bottom ash with an initial weight of 1 kg were prepared for the drying process. At the end of the drying process, the average total dried bottom ash was recorded. The drying process was conducted inside a Heraeus T5042E furnace for 24 hours. All prepared samples were heated at a temperature of 100–110 °C

for about 24 hours to reduce the moisture content of the samples. The water content of bottom ash was calculated based on equation (3.1).

$$w = \left[\frac{(M_{CWS} - M_{CS})}{(M_{CS} - M_C)}\right] X\ 100 = \frac{M_W}{M_S}\ X\ 100 \quad \text{..... (3.1)}$$

where:

w = water content (%)
M_{CWS} = mass of container and wet specimen (g)
M_{CS} = mass of container and oven dry specimen (g)
M_C = mass of container (g)
M_W = mass of water ($M_W = M_{CWS} - M_{CS}$) (g)
M_S = mass of solid particles ($M_S = M_{CS} - M_C$) (g)

Dried bottom ash weight after the drying process was recorded so that water content of the samples could be recorded. The water content calculation was referred from Standard test method for laboratory determination of water (moisture) content of soil and rock by mass, as shown in equation (3.1).

3.4 The increase of liberation degree by milling process

The milling process is useful not only for enhancing the liberation process but also for particle size reduction, for mixing-blending purposes, and for particle shaping. Grinding media are used in this milling process, based on the impact process principle. The impact on particles from contact with grinding media and with the chamber wall deforms particles, which are finally fractured into smaller sizes. In this research, the grinding media used were several steel balls that were inserted together with the bottom ash in the chamber. The ball-milling process was conducted for one hour with a weight ratio 1:2 for samples versus steel balls. The rotation of the ball-milling process was also changed every 30 minutes. The weight of the samples being used in each chamber was about 200 grams and the combined weight of the steel balls was 400 grams. The milled product was then sieved for classification by particle size difference. The milling process for bottom ash from plant A was mainly conducted by ordinary ball milling, as shown in **Figure 3.9**.

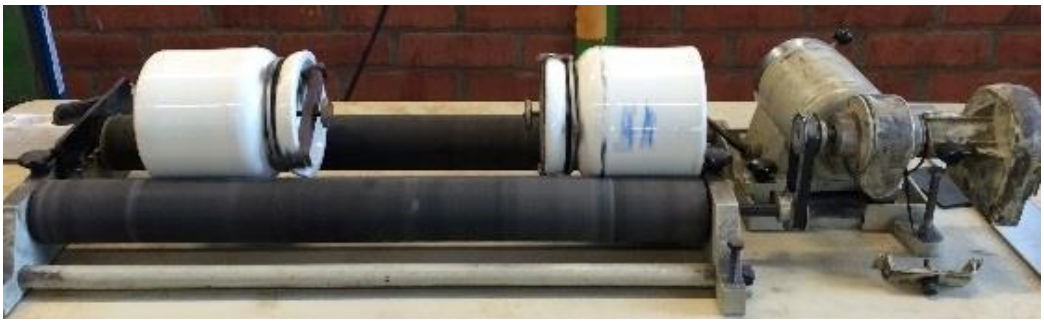

Figure 3.9: Ball milling process conducted by rotary ball mill on lab scale.

In later operations, especially on bottom ash from plants B and C, the milling process was carried out by disc mill, as shown in **Figure 3.10**. The use of milling by Retsch disc milling has shown a tendency to recover metallic fractions easier, in particle sizes $\geq$ 500 µm (which are discussed later, in the next chapter). This disc-milling equipment has two different milling compartments, which differ in their capacity.

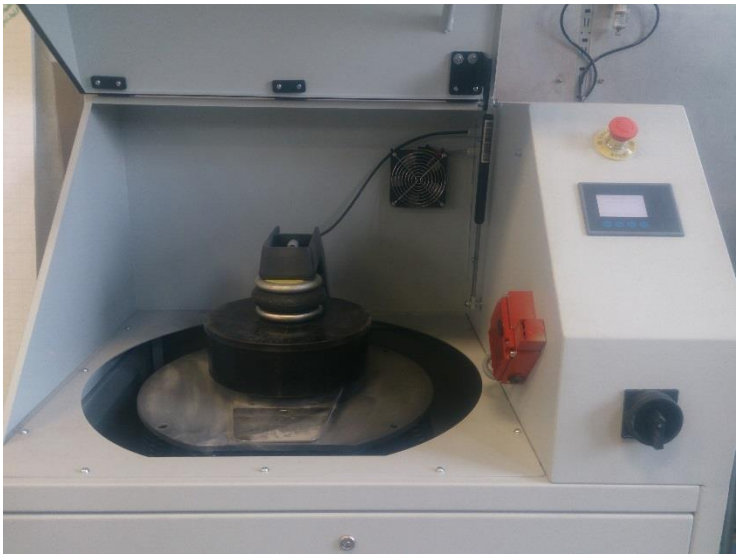

Figure 3.10: *Retsch* disc milling equipment.

3.5 Particle size distribution and classification by sieving process

The initial bottom ash used in this study had a particle size in the range 4 to 8 mm. The liberation process was conducted by ball-milling process, which produced a smaller particle size. The mesh numbers used in this study were classified into 500, 250, 125, , and $\leq$ 63µm. Mesh number 500 µm contains all particles that have particle grain sizes $\geq$ 500 µm, 250 µm all particles that have grain sizes in the range of 250–500 µm, and mesh number $\leq$ 63 µm contains particle grain sizes in the range $\leq$ 63 µm. The weight of each particles size was recorded. The smaller particle size was expected, having a higher weight of samples, to show that the liberation by ball-milling process was successfully done. However, in later discussion, it will be explained that the ball-milling parameter with samples-to-steel-ball weight ratio of 2:1 for 1 hour was not optimum, due to the abundance of 500-µm particle size even after ball milling. This shows that the ball-milling process produced unsatisfactory results; therefore, in later operations (on bottom ash from plant B and plant C), liberation was done only with disc-milling equipment (**Figure 3.10**).

The sieving process in this research was conducted with a Retsch AS 300 vibratory sieve shaker, corresponding to DIN ISO 3310-1 standard. The sieving process lasted for five minutes with an amplitude of 0.7 mm and with an interval process of 15 seconds. **Figure 3.11 shows** the sieving machine. As the process finished, each fraction was weighed automatically with the scale on which the sieves were located and the measured data was automatically saved in the connected computer.

Figure 3.11: Sieving process by using *Retsch* vibratory sieving machine type shaker AS 300.

3.6 Magnetic Separation

The ferrous materials that were still contained in fine bottom ash fraction were separated magnetically. Magnetic separation is an important step, because copper is contained mainly in the non-magnetic fraction and can be concentrated in this way. Initial magnetic separation was conducted after sieving, and was achieved by manual magnetic separation on laboratory scale made from NdFeB material, at a magnet strength of 42–45 Mega Gauss Oerstat. After magnetic separation, the classified samples were distinguished by particle size and their different magnetic properties.

In the course of this study, a magnetic separation process in combination with a sluice-box construction was developed and installed. Magnetic separation was done in a modified sluice box (**Figure 3.12)**, with several electromagnets below the bottom of it. In addition, different barriers were positioned in the sluice box, in order to be able to adjust a targeted flow of the fluid to form a zig-zag water pattern.

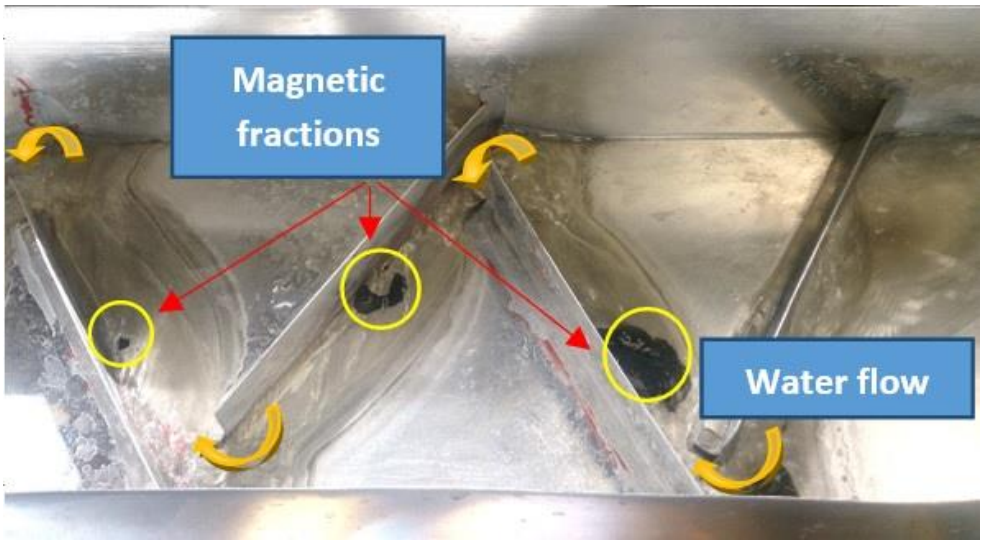

Figure 3.12: Wet magnetic separation by using the combination of sluice box experiment and installed some electromagnets on the bottom of the sluice box.

The use of wet magnetic separation was useful for fine particle grain size materials, because bottom ash with a particle size ≤ 250µm tends to agglomerate, so that in dry condition a mixture of non-magnetic and magnetic agglomerated particles are attracted all together by the magnet and at the end the magnetic fraction still contains many non-magnetic particles. In wet magnetic separation, on the other hand, there is no agglomeration and the magnetic fractions stay collected in the sluice box, in different steps at those points where the electromagnets are positioned, and non-magnetic particles are easily washed away with the zig-zag water flow, as can be seen in **Figure 3.12**.

3.7 Density separation by using sluice-box and gold-pan process

In general, valuable materials have higher densities than other materials. That is why, after magnetic separation, valuable materials can be separated with different methods of gravity separation. Very often water and air are used in such separation techniques as media to reduce the friction between the particles. In this study, water has been chosen as a fluid medium to separate heavy particles from light particles. The water pressure used in the separation process was 50 L/min. The main density separation in this study was divided into two processes: initially by sluice-box method, then continued by gold-pan process.

3.7.1 Sluice-box experiment

Sluice-box is the common density separation process in gold mining technology. The sluice-box principle is the removal of gangue minerals, which have lower densities than the valuable minerals embedded therein. The sluice-box experiment was built downstream (**Figure 3.13)**, Area 1 being the highest and Area 6 the lowest area, followed by a water container. The separation happens because of the water turbulence that is created near the riffle area in combination with a matting system in which valuable materials are trapped while gangue minerals are washed away and collected in the water container. Each area contains particles of different densities: the lower the area, the lower are the particle densities. The sluice-box process was conducted for 1 hour with a water flow of 50 L/min.

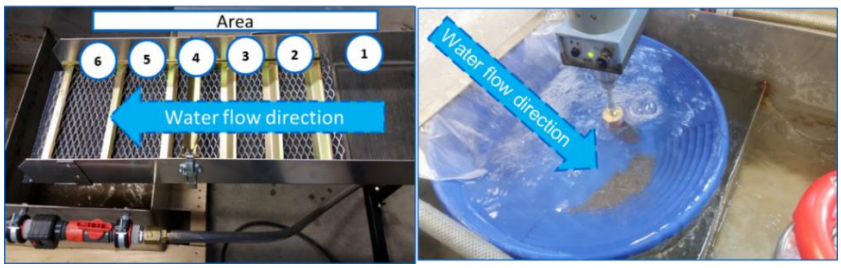

Figure 3.13: Density separation by using sluice-box experiment (left) and gold-pan (right).

Bottom ash samples were poured into the sluice box near Area 1. The water was recirculated by a water pump. According to experimental results in this study, samples that were effectively separated and consist of many valuable materials were only those smaller than 500 µm. Particle sizes smaller than 125 µm contain less metallic particles, whereas sample that have particle sizes larger than 500 µm were not effectively separated by this method. The process lasted for 1 hour, then all particles trapped in the matting were collected and dried. The dried samples were observed by digital microscope to analyse the morphologies of the samples. The sluice-box process with the matting system was used only for the separation of bottom ash from plant A, because the process with current parameters consumed a lot of time, and discharging of all the trapped materials from the matting system was relatively complicated.

3.7.2 Gold-pan Experiment

To improve the density separation results after a sluice-box experiment, another density separation is needed. In this study, a gold-pan experiment was used in addition to the modified sluice-box process (**Figure 3.14)**. The aim of this experiment was the removal of lighter particles by the combination of pressurized and stirred water in the gold pan itself. When gold-pan experiment was used in addition, the riffle and matting system were removed from the sluice box and a stirrer was positioned as shown in **Figure 3.13 (right side).** When the water pump was switched on, pressurized water recirculated and the prepared samples were poured in the upper area of the sluice box, so that all the particles moved with the water into the gold pan. The very light particles were easily washed away while many heavier particles stayed in the gold-pan, and after several minutes the particles were in a stagnant condition, concentrated at certain places in the gold pan. After switching off the water pump, all the spread-out particles were collected in the center of the gold pan. After starting the water pump again, further separation proceeded. This process lasted for 1 hour.

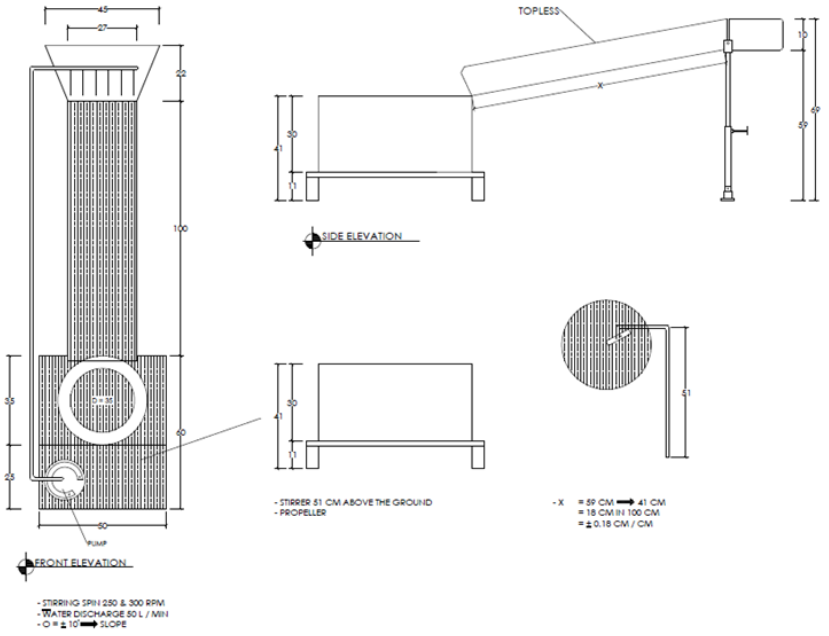

Figure 3.14: The schematic modification of sluice-box and gold-pan experiment on lab scale.

A modification of the sluice-box/gold-pan experiment can be seen in **Figure 3.14**. The sluice box was set at a 45° angle with the water container, and

the gold pan was positioned exactly straight downstream from the sluice box. A stirrer was also placed on the right side (**Figure 3.15**) of the gold pan. The gold pan itself was also positioned 45° to the water container. The angle of the gold pan relative to the water container is the most important parameter; if it is not in correct position, this will affect the result.

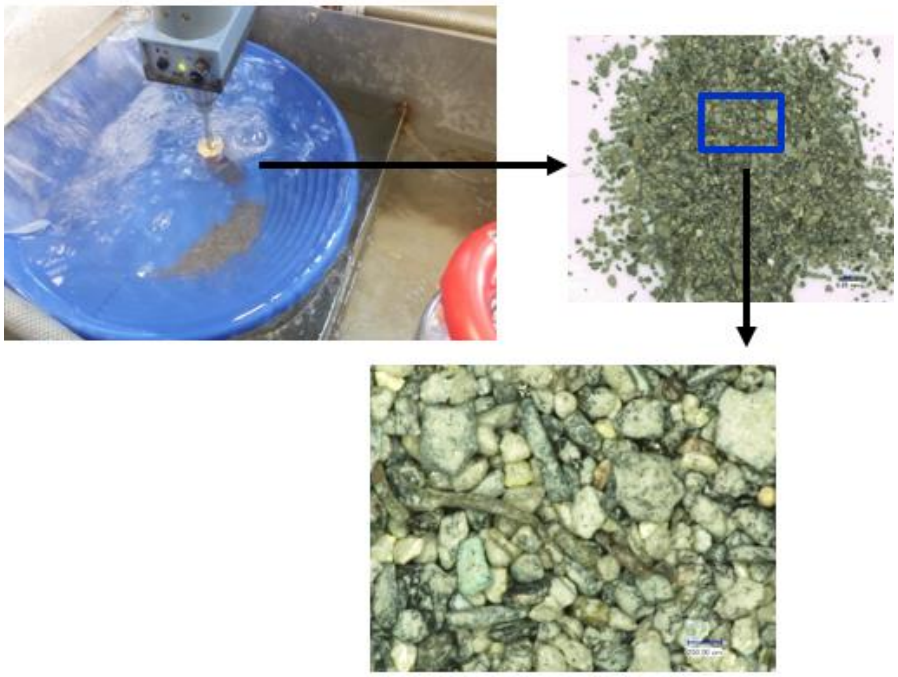

Figure 3.15: The heavy and non-magnetic particles produced by gold-pan experiment.

The stirrer was set at a constant speed during gold-pan process. There were two different stirring speed parameters: 250 rpm and 300 rpm. After a 1-hour process, both heavy and lights particles from both magnetic and non-magnetic fractions were collected. These samples were dried inside the Heraeus furnace. The recovery of metallic copper was expected from the heavy-non-magnetic particles, which stayed in the gold pan, as shown in **Figure 3.15**. The metallic copper was concentrated after the gold-pan experiment, mostly in the form of wire covered with a layer of dirt. Nevertheless, a small number of light particles were still collected among the gold-pan products.

3.7.3 An additional separation, vacuum separation

In this study, the use of a separation chamber connected to a vacuum cleaner was tried, to counter the contamination of light particles that were still found after the gold-pan process in the heavy fraction. The basic principle of

vacuum separation is also density separation; however, the medium used is air sucked through the filter bag. The schematic process for this is shown in **Figure 3.16** (below):

Figure 3.16: Vacuum separation experiment simple design.

The sample being separated is placed on the left side of the bottle, while the right side of the bottle is being sucked by the vacuum cleaner. The separation principle is the removal of light particles, which are expected to be sucked into the filter bag during the process. The expected result is that the valuable materials would stay in the chamber.

3.8 Characterization of fine particle size WtE bottom ash

For microscopic examination, samples were taken from the particle-size fractions to be examined, embedded in epoxy resin, and observed by light microscopy in reflected light. Individual particles were also examined with a digital microscope. This approach, compared with conventional microscopy, has the advantage that in a such deeper particles can be photographed in a field of uniform depth and the corresponding different colours observed. Using these images, it was possible, in the subsequent SEM images, to analyse the areas with different colours in a target-oriented way.

3.8.1 The morphological examination of fine particle bottom ash with digital microscope

The observation of particle morphology was performed on a Keyence digital microscope VHX-500F and a Leica DM4000 M-LED microscope (**Figure 3.17**), both of which are available in the ITM laboratory. At every step of the experiment, the shape, colour, and physical appearance of the particles were captured by these digital microscopes. The initial and treated samples were

observed and their morphological appearance and the results were recorded. With the digital microscope, it is possible to check irregularities that would not be detectable in a normal photograph.

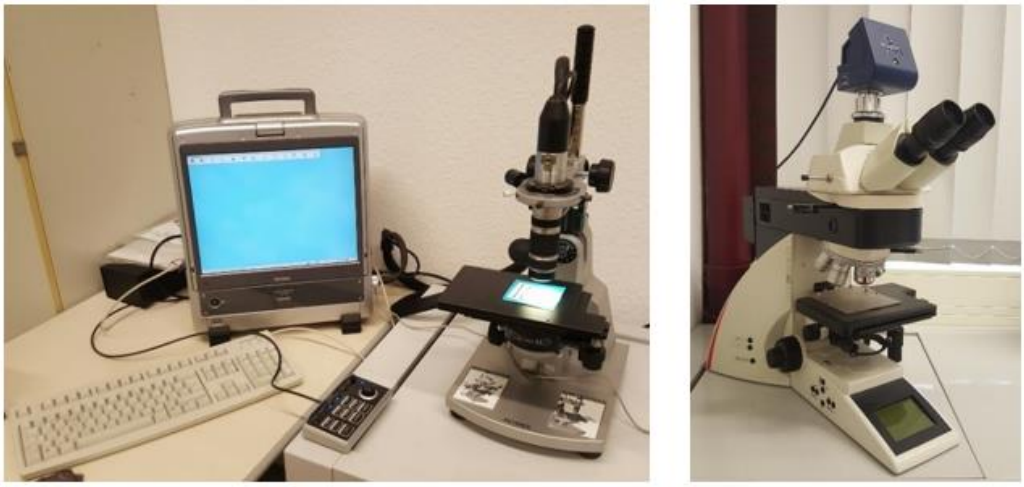

Figure 3.17: Digital microscopes being used for morphological examination. (a). Keyence VHX-500F (left) and (b). Leica DM4000 M-LED (right).

In addition to discovering the metallographic structures inside a sample, an examination using an optical microscope was also done. The aim of this examination was to learn the morphology of the particle and to determine which aspect of it should be characterized via scanning electron microscope (SEM) and energy dispersive X-ray spectroscopy (EDS). For examination by SEM, the sample being used for examination needed to be prepared in a special way to ensure the electrical conductivity of the sample. Therefore, a mounting process was performed on the sample by using conductive filler materials. The mounting used in this study was cold mounting. A 30-gram epoxy and 30-gram conductive filler were combined and stirred together until a good shape with few bubbles was achieved.

In this study, the sample was started to polish with 600-µm silicon carbide abrasive grinding paper for eight minutes using a SAPHIR 550 WITH RUBIN 520 type ATM grinding-polishing machine, as shown in **Figure 3.18**. The pressure used in this step was 25 N (not too high, to avoid the risk of an increased amount of surface damage). After grinding, the sample was polished with diamond abrasives ranging from nine microns down to one micron, to remove

the damage done during grinding but still maintain the flatness of the sample. Three such polishing steps were done, with each step finished in four minutes using 30 N pressure.

Figure 3.18: Grinding – polishing machine type of SAPHIR 550 with RUBIN 520.

3.8.2 Scanning Electron Microscope (SEM) and Energy Dispersive X-Ray Spectroscopy (EDS)

The SEM instrument used to characterize the material is shown in **Figure 3.19,** which also include EDS. The sample that was used in this characterization was separated through gold-pan experiment and embedded in epoxy resin. This sample was also examined with digital microscope before characterized with SEM-EDS.

Figure 3.19: SEM instrument which include electron column, sample chamber, EDS detector, electronic console and visual display monitor.

4 Characterization of bottom ash after milling, sieving and density separation process

One of the most important questions to answer in this study is: In which particle size can copper be recovered most effectively. It was found that a particle size fraction in the range of 125–250 µm is the suitable particle size for metallic copper recovery performed by this method. However, particle sizes ≤ 63 µm and ≥500 µm were not explored, because of the limited ball milling and sieving at that time, considering that samples with particle size ≥ 500 µm needed to be re-ball-milled in order to recover the valuable materials by this separation method.

4.1 Elemental distribution as a function of particle grain size

Ball milling is an important part of this research, because it initiates the physical liberation of particles by the impact process between steel balls, chamber walls, and particles. The effect of liberation is seen after sieving, with the classification into different grain size fractions.

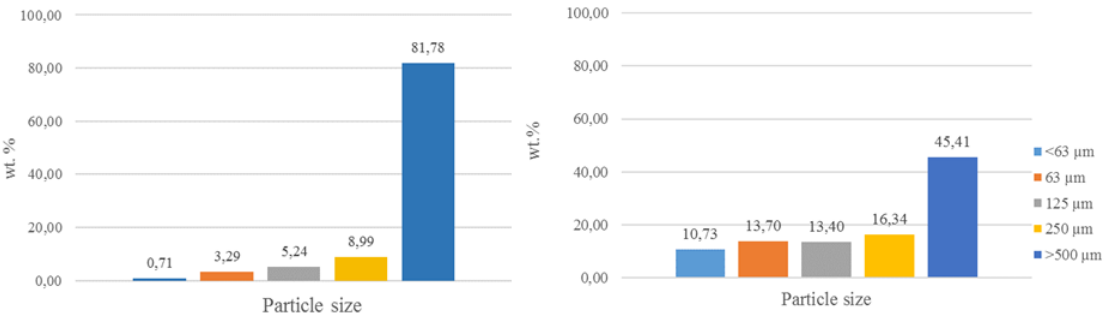

Figure 4.1: The particle size distribution profile of before ball milling (left) and after ball milling (right).

As shown in **Figure 4.1**, bottom ash mainly consists of grain size fractions > 500 µm before ball milling. After ball milling with a 2:1 ratio of ball mill and sample, fractions ≥ 500 µm decreased and the smaller grain size fractions increased. The very fine grain size fractions (≤ 63 µm and 63 µm) had different contents of magnetic and non-magnetic fractions, as shown in **Figure 4.2**. The smaller the grain size, the higher the percentage of magnetic material.

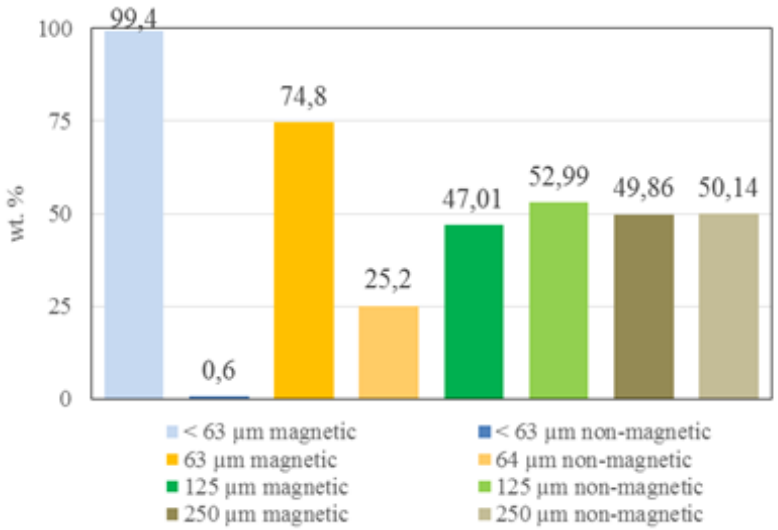

Figure 4.2: The distribution of magnetic and non-magnetic fraction according to its particle size.

In contrast to the very fine grain sizes (≤ 63 µm and 63 µm), the percentages of magnetic and non-magnetic fractions in larger grain sizes (250 µm and 125 µm) were distributed more evenly, with nearby ratios of 50%/50%.

In **Figure 4.3**, the contents of aluminium, silicon, calcium, and iron (the typical slag-formers) are shown as a function of grain size. The aluminium content is more or less evenly distributed in all grain sizes. In contrast, a clear correlation of higher silicon content and higher iron content in larger grain sizes was seen. As opposed to iron and silcon, the calcium content of larger grain sizes was lower and in smaller grain sizes was higher.

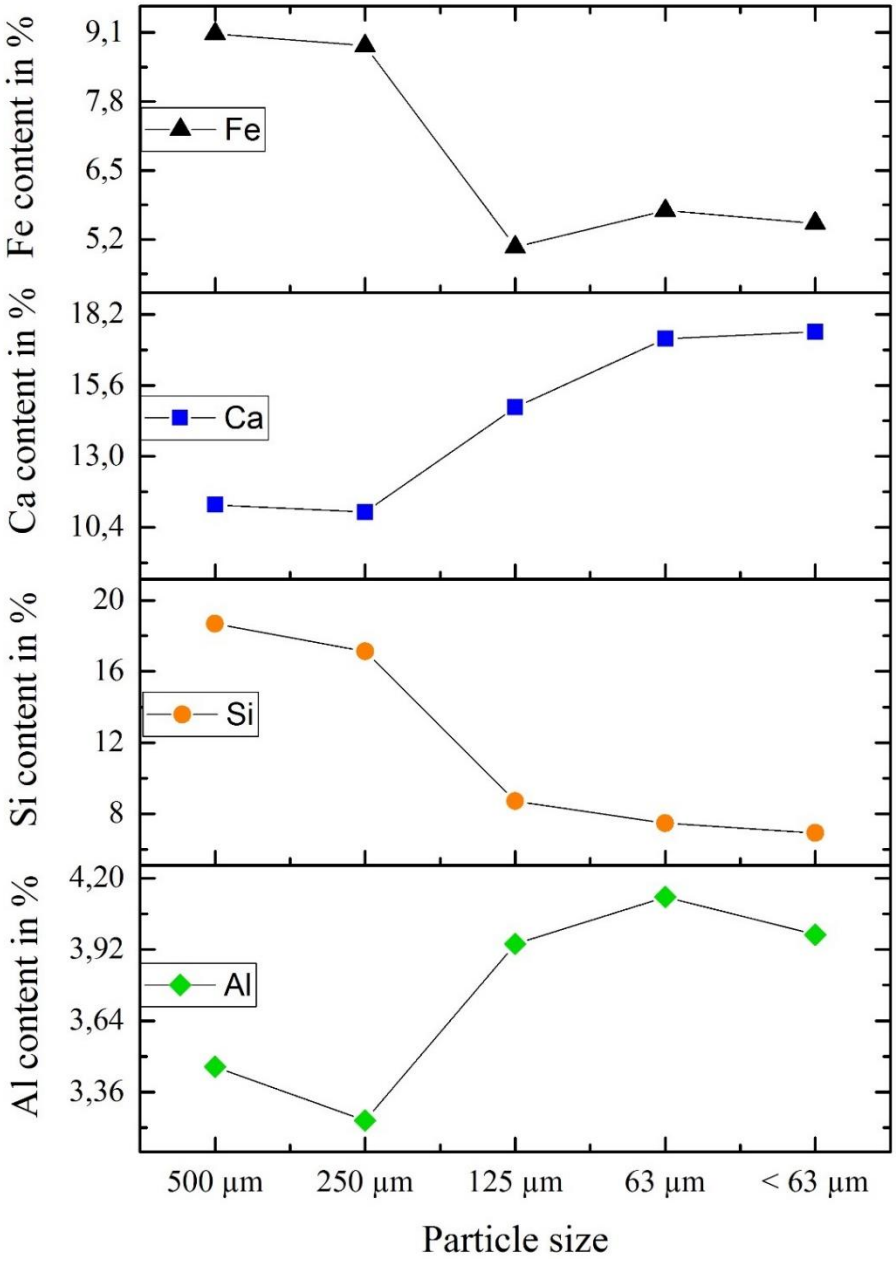

Figure 4.3: The dominant elements contained in WtE fine particle bottom ash distinguished by its particle size after ball milling – sieving processes.

As shown in **Figure 4.3**, silicon concentration tended to be higher with larger particle size. Iron concentration, showing similar behavior, was found at 90,000 ppm in larger particle size but decreased to 50,000 ppm in smaller particle size. Contrary to this was the concentration of calcium, which was higher in smaller particle size. Calcium content reached 175,000 ppm in particle size less than 63 µm while only 112,000 ppm of calcium was found in 500-µm particle size.

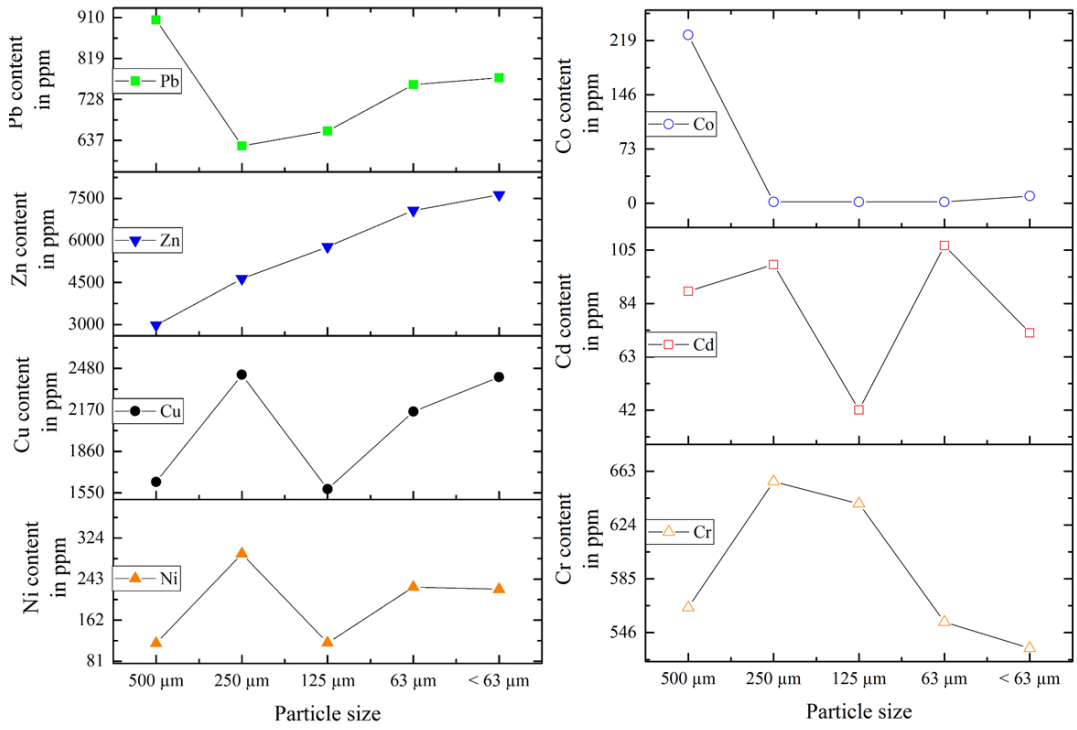

Figure 4.4: The concentration of valuable elements after sieving process, in bottom ash fine particle grain size.

The behavior of high-density elements (the valuable materials) contained in the fine-particle bottom ash according to particle size difference showed an interesting tendency. In fine-particle grain size, as shown in **Figure 4.4**, the concentration of nickel did not differ with different particle sizes, while the concentration of zinc increased with decreasing particle size.

As depicted in **Figure 4.4**, the concentration trends for zinc and copper as a function of grain size clearly show a different pattern. The zinc content increased in the small particle size fractions up to 7600 ppm, while the copper content was more or less constant at about 2000 ppm in all grain size fractions.

The distribution of different elements in different grain size fractions is shown in **Figures 4.5** to **4.9**. The oxygen and calcium mapping show that these elements mainly occur together, which indicates the existence of calcium-oxide. In addition, silicon can be identified together with calcium and oxygen; at these positions, not always but very often, the existence of calcium-silicates can be assumed. In **Figure 4.5** (grain size fraction > 500 µm), at position 1, higher silicon, oxygen, and zinc contents can be identified, which indicates the existence of a zinc-

silicate particle. In **Figure 4.6** (grain size fraction 250–500 µm), the distribution of calcium, silicon, and oxygen is very similar to that in **Figure 4.5**. Particles with higher silicon and lower calcium content in combination with oxygen are also identified in **Figure 4.6**. In **Figure 4.6,** the existence of an iron oxide particle at position 1 can be identified. In comparison to **Figure 4.5,** the number of aluminium-containing particles is higher in **Figure 4.6**. At position 2, a particle mainly containing silicon and oxygen is shown.

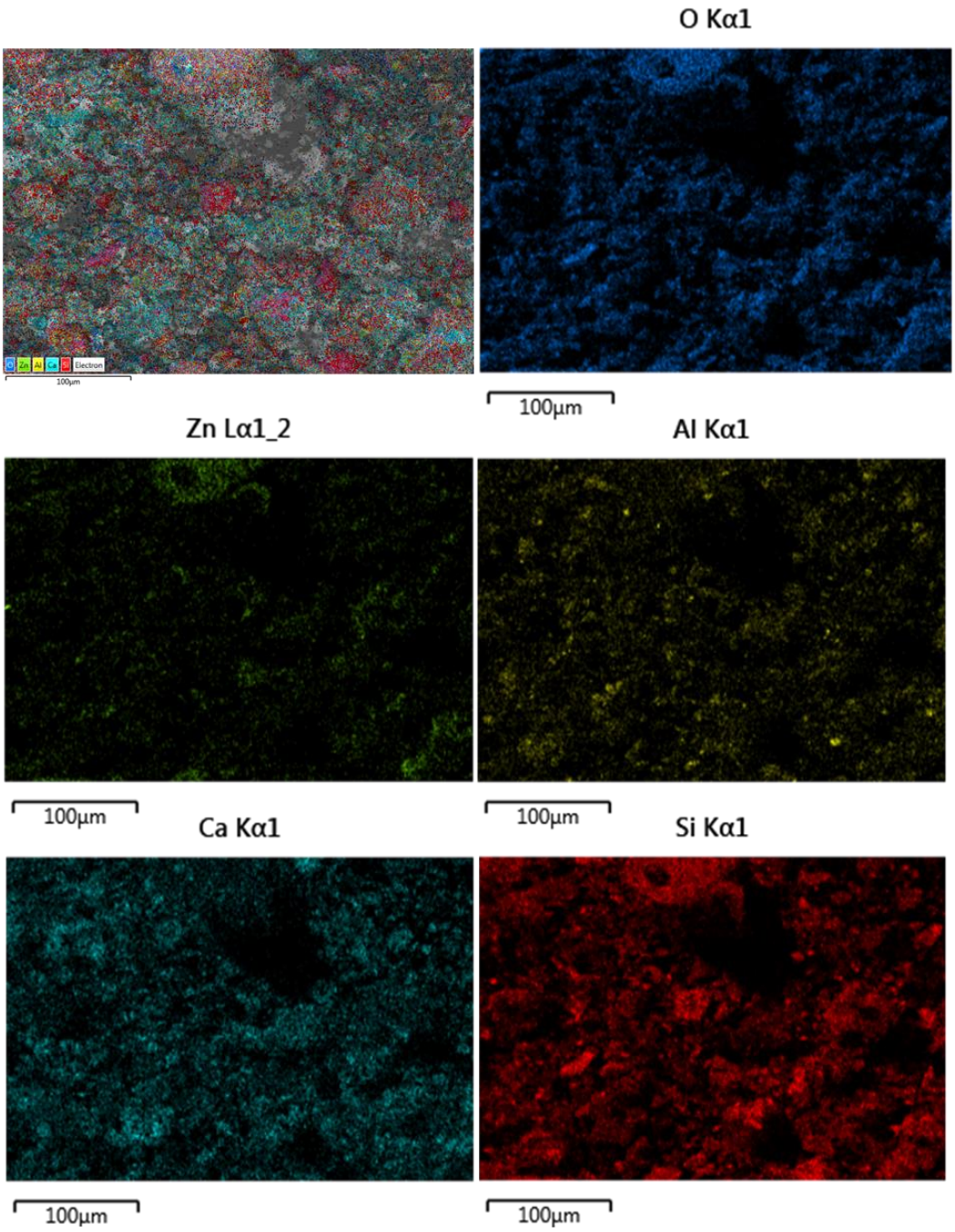

Figure: 4.5: The overview of elemental mapping of the ball milled and sieved sample. Typical of 500µm after ball milling – sieving sample.

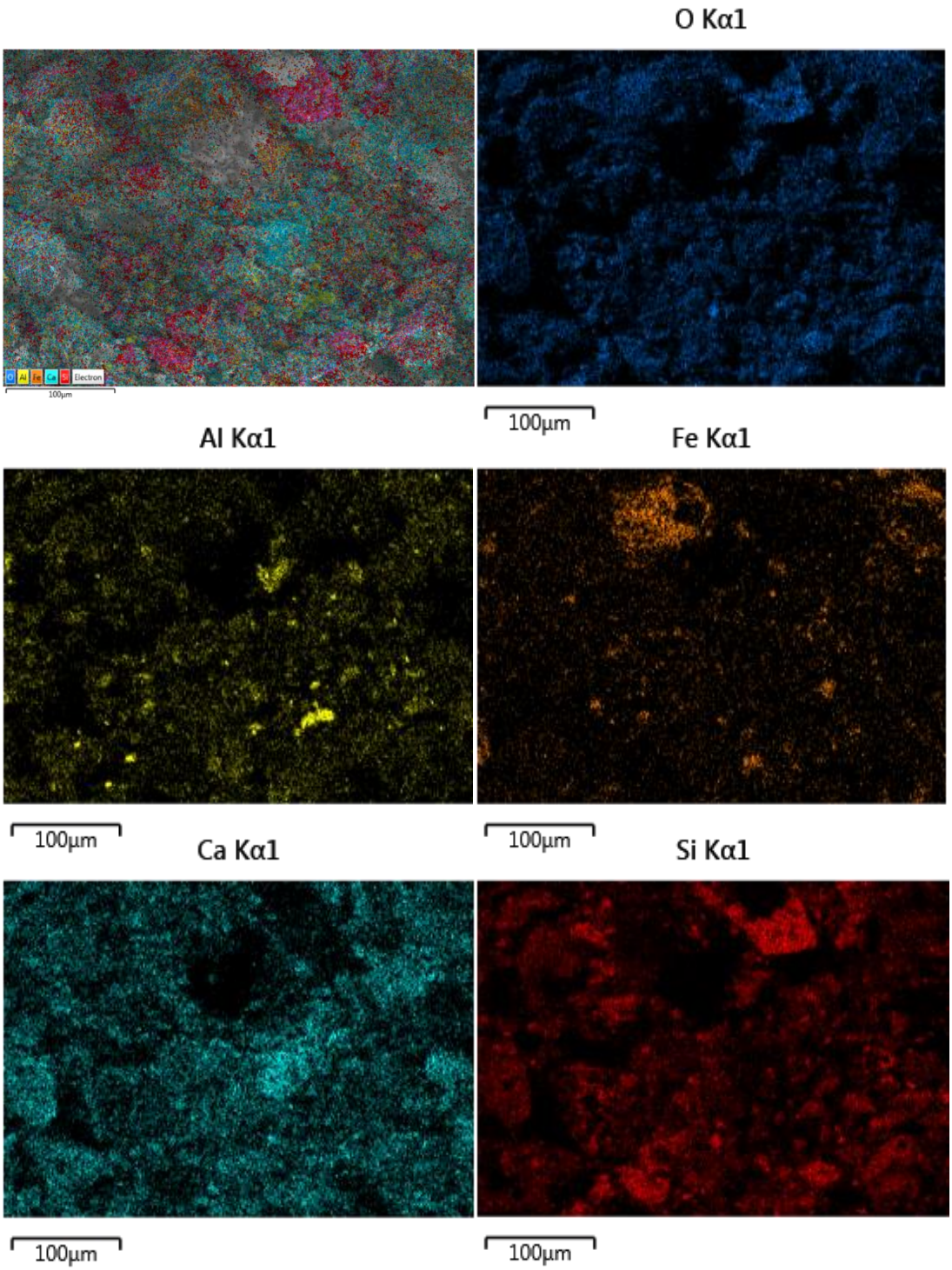

Figure 4.6: The overview of elemental mapping of the ball milled and sieved sample. Typical of 250µm after ball milling – sieving sample.

The frequent common presence of calcium, aluminium, and oxygen (**Figure 4.7**) indicates the formation of calcium aluminates also in the 125–250 µm grain size fraction. From steel metallurgy [Oeters **1989**] it is known that calcium aluminates have higher sulphur solubilities the higher the CaO%/Al_2O_3% ratio. That

is probably why higher sulphur content can be seen in the region, where calcium aluminates exist.

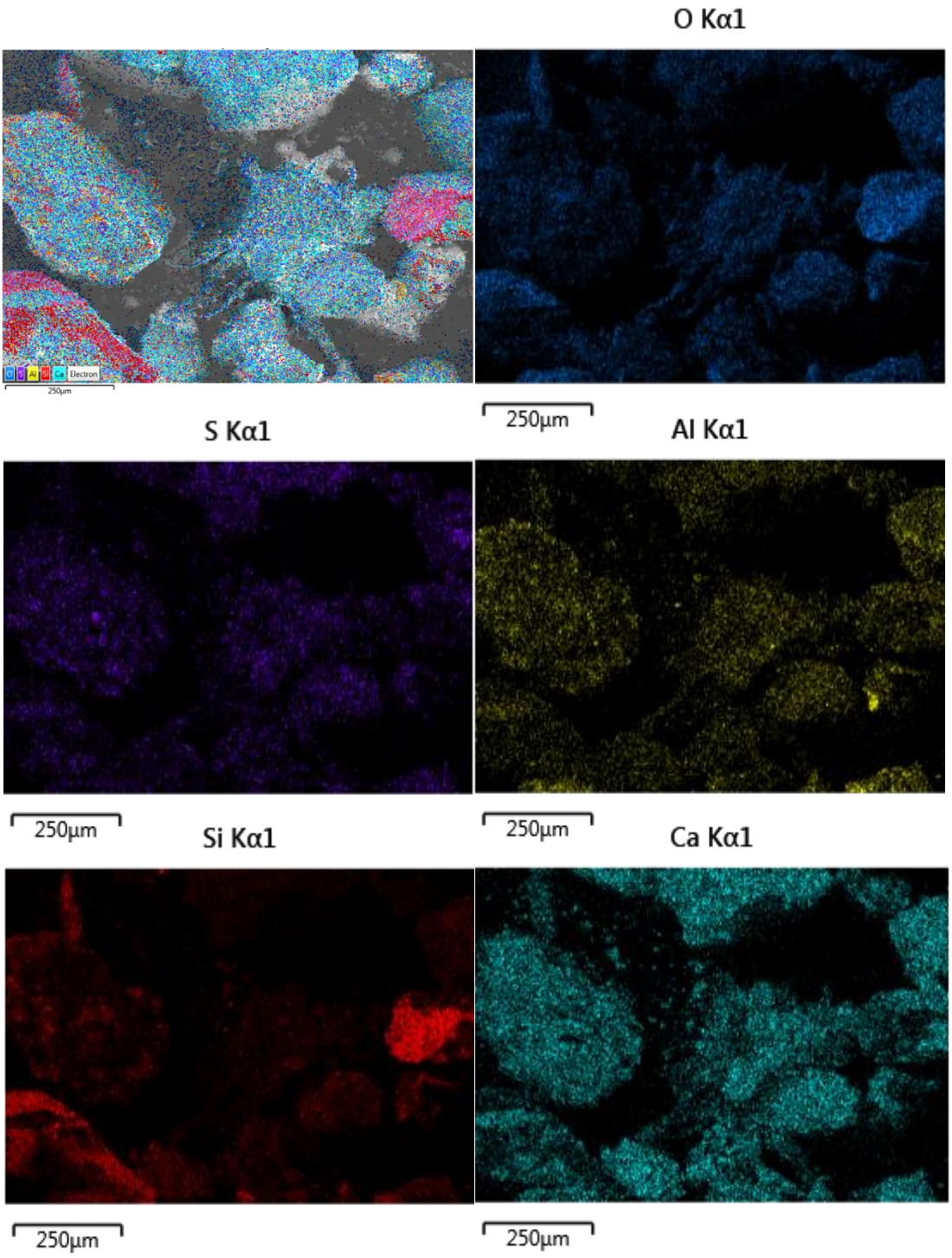

Figure 4.7: The overview of elemental mapping of the ball milled and sieved. Typical of 125µm after ball milling – sieving sample.

In **Figure 4.8**, more or less the same distribution of elements is shown as in **Figure 4.7**. In the center of **Figure 4.8,** it can be seen that higher silicon contents exist together with calcium, aluminium, and oxygen and that in this area the sulphur content is less.

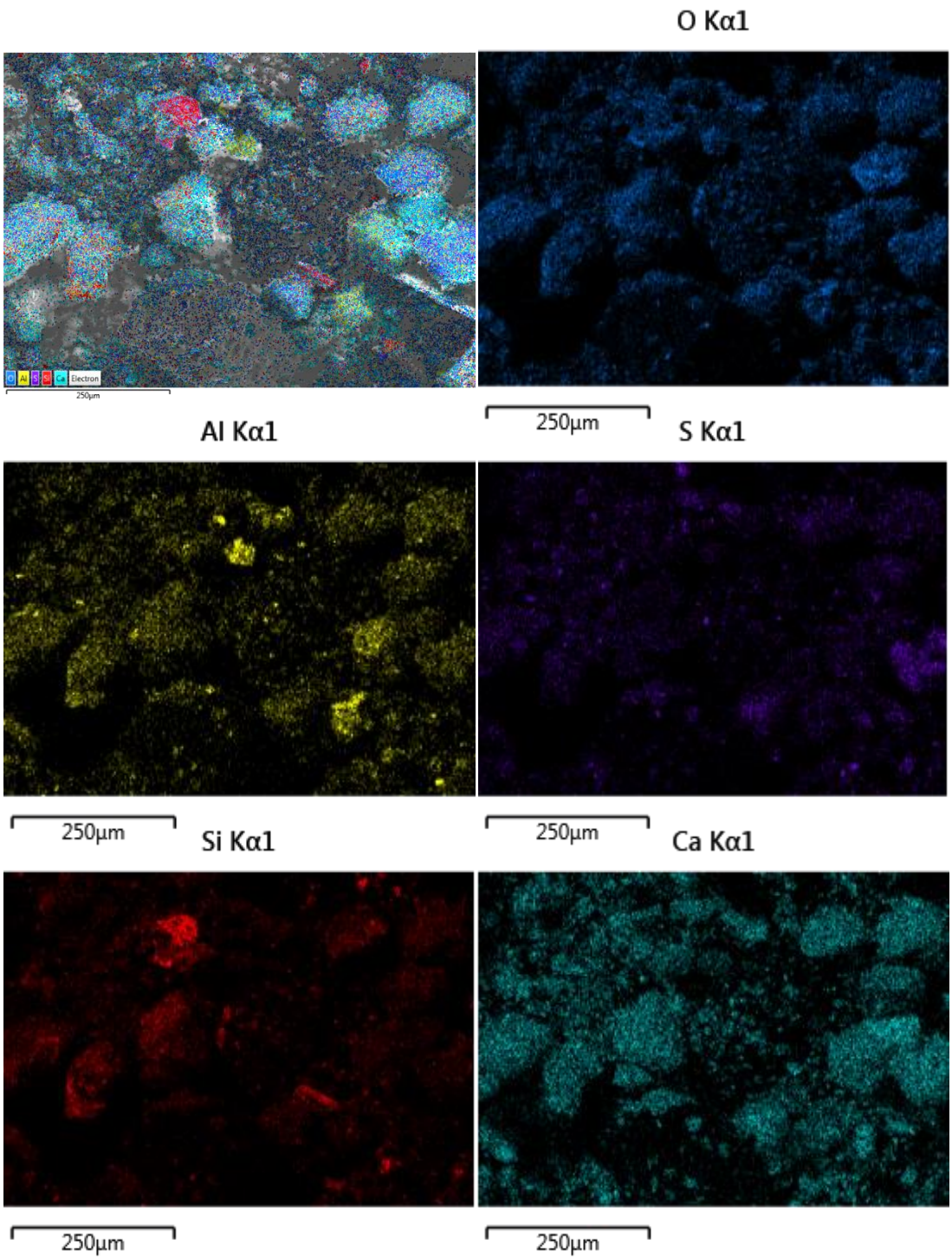

Figure 4.8: The overview of elemental mapping of the ball milled and sieved sample. Typical of 63µm after ball milling – sieving sample.

The element distribution shown in **Figure 4.9** (grain size fraction < 63 µm) is very similar to the distributions in **Figures 4.5** to **4.8**, where it is shown clearly that sulphur is connected with pure calcium-oxide or calcium aluminates. In slag particles where the silicon content is higher, the sulphur content is less.

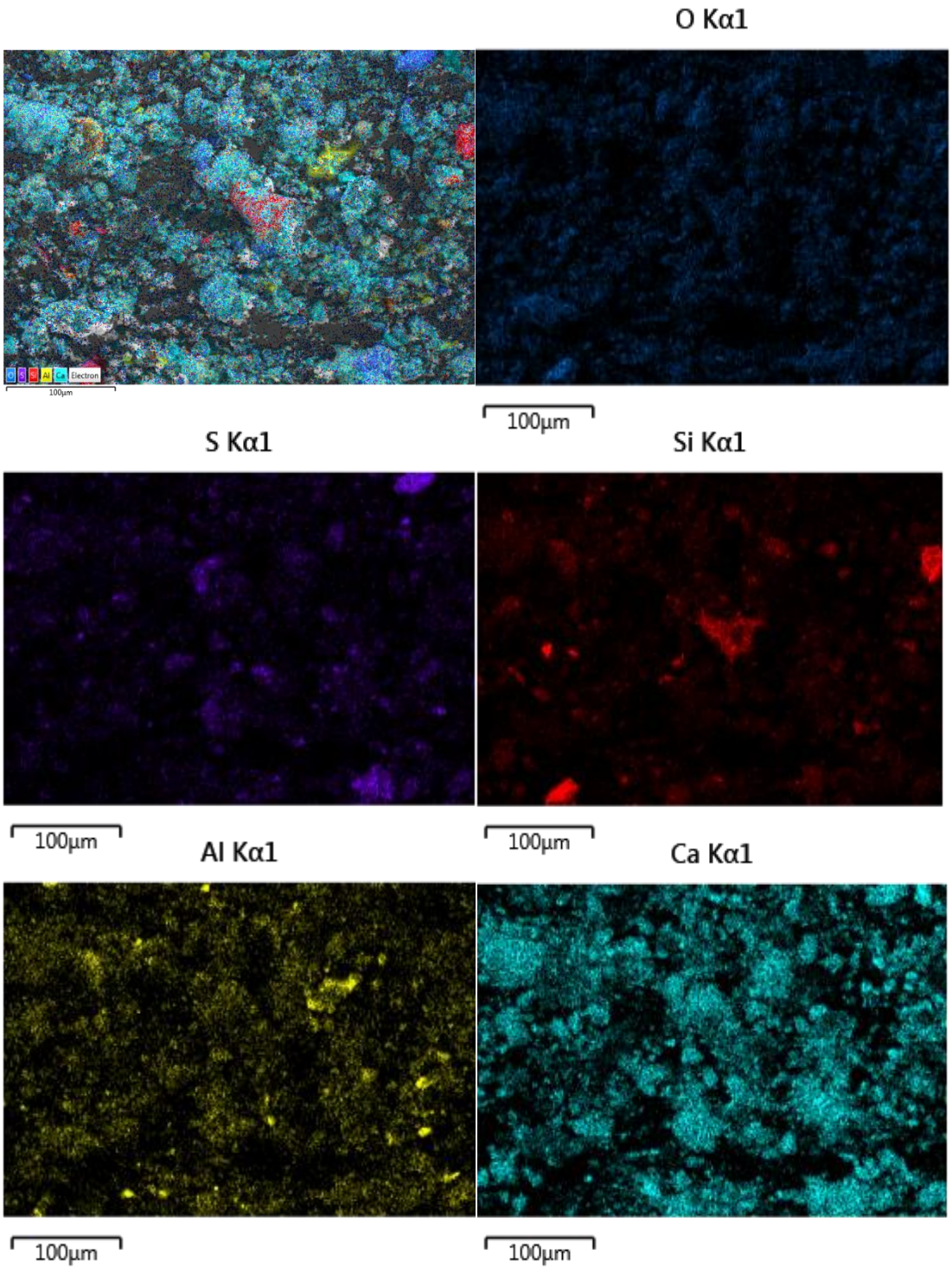

Figure 4.9: The overview of elemental mapping of the ball milled and sieved. Typical of <63µm after ball milling – sieving sample.

4.2 The characterization of magnetic and non-magnetic fraction

As shown in **Figure 4.2,** in fine grain sizes the contents of magnetic fractions are higher than thoses of non-magnetic fractions. The results were determined by a dry manual magnetic separation process. In **Figure 4.10,** the

contents of elements in magnetic and non-magnetic fractions, taken from another bottom ash sample, are shown relative to the grain size fractions. It can be seen clearly that the contents of nickel, cobalt, and chromium are significantly higher in the magnetic fraction than in the non-magnetic fraction. Nevertheless, dry magnetic separation has the disadvantage that non-magnetic particles adhere to magnetic particles or get caught between them, so that they too are removed in the magnetic separation process. That is why for this study a semi-continuous wet magnetic separation process, based on a modified sluice-box process, was developed (subsection 3.6), after the results and the handling of the manual magnetic separation had been considered.

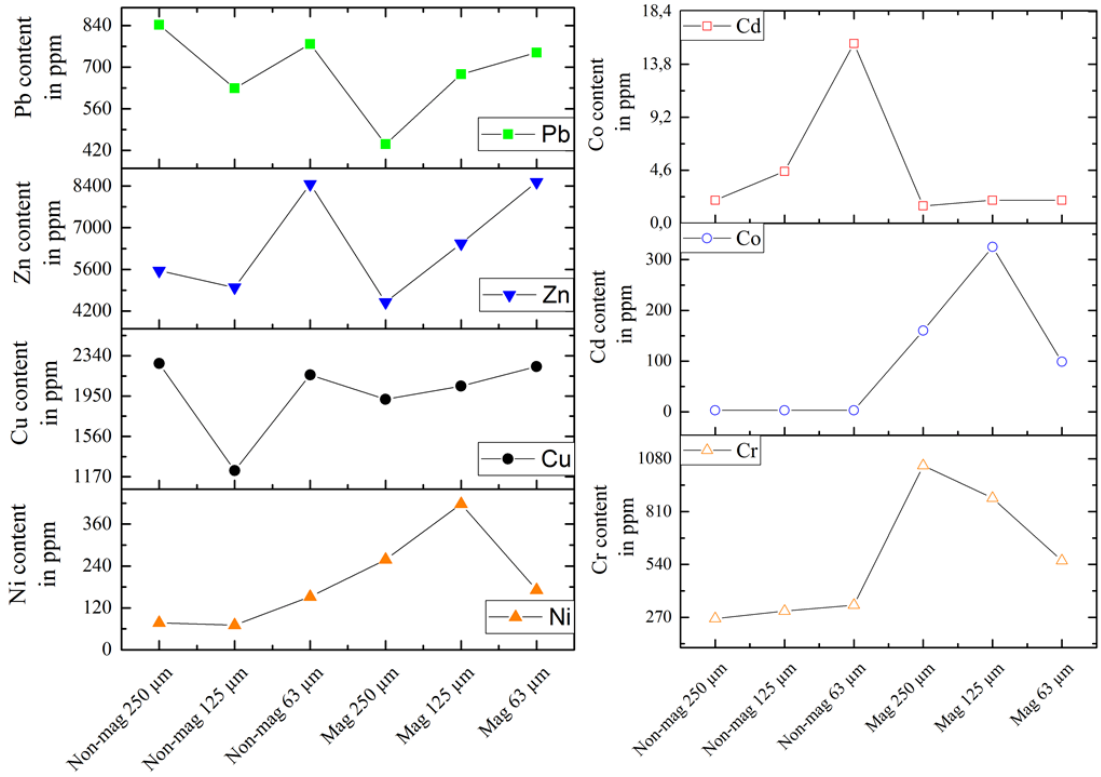

Figure 4.10: The tendency of some valuable elements after magnetic separation distinguished by its particle size different.

This wet magnetic separation process was conducted in sluice-box equipment, without the matting system but with electromagnets placed under the sluice-box, while the water circulation system was kept the same. During this process, magnetic particles were separated by the magnetic forces of the electromagnets keeping the particles fixed in the sluice box, while the other particles were easily transported to the water container. This magnetic particle was then collected and kept in the Heraeus furnace until completely dried. The

compared results of XRF tests from wet and dry magnetic separation in 63–125 µm grain size fraction are shown in **Figure 4.11**:

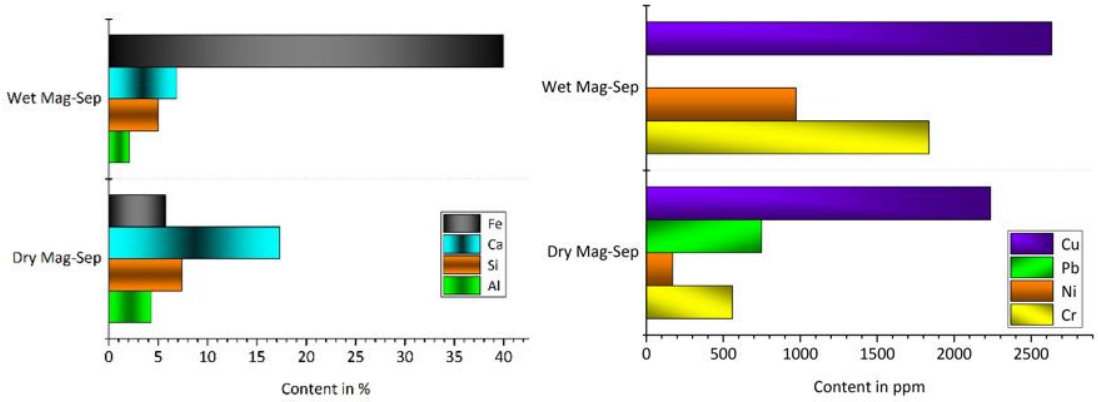

Figure 4.11: The chemical composition comparison of bottom ash magnetic fraction with wet and dry magnetic separation process in the particle size ≤ 125µm.

The wet magnetic separation process showed its potential (**Figure 4.11**) for use in the concentration of elements such as chromium and nickel, together with iron. In **Figure 4.11,** it is shown that the enrichment of iron with wet magnetic separation is much more effective than dry magnetic separation. Because chromium and nickel are essentially dissolved in iron, the contents of these elements are also higher with wet magnetic separation. In addition, as is shown in **Figure 4.11**, lead is reduced drastically in the magnetic fraction with wet magnetic separation. Some non-magnetic elements such as Ca and Si are reduced to below 10%. For larger particle size, dry magnetic separation is still feasible.

An interesting result is the unexpected high concentration of copper in magnetic fraction, in amounts of > 2000 ppm. The reason for this will be explained in the next chapter.

4.2.1 Magnetic fraction in comparison to after sieving sample composition

According **Figure 4.3**, the bottom ash being used in this research contained ferromagnetic elements such as nickel and cobalt. As expected, the contents of these elements are higher in the magnetic fraction after magnetic separation process. In addition, chromium is the only element that was increased significantly in the magnetic fraction (**Figure 4.10**), from about 550–660 ppm up to 800-1000 ppm.

The contents of diamagnetic elements such as Cu, Zn, Pb, and Cd have different patterns than the ferromagnetic elements. With the exception of zinc, where the known enrichment in the smaller grain size fraction can be seen, no clear tendencies depending on the grain size fraction can be seen for the other elements. Initially, the magnetic separation conducted in this research was done manually and in dried conditions, but with the development of semi-continuous wet magnetic separation technology it was possible to improve the separation results. From this result, it can be seen that wet magnetic separation is favorable mainly for very fine particle grain size.

4.3 The characterization of heavy particles from non-magnetic particles after SLB process

In context of recycling, copper contained in fine particle size of bottom ash does have the potential to be recovered, due to its economic value in the market. In **Figure 4.12** the concentration of elements trapped in zone 2 and 3 during sluice box process (**Figure 3.13**) with matting system are shown. Valuable compounds or elements separated with sluice-box process are usually trapped in the upper zones 2 and 3.

In **Figure 4.13**, typical particles in two different grain size fractions (63 – 125 µm, 125 – 250 µm) from different steps of separation [Prayogi, Pratiwi and Larasati **2016**] are shown. In the first row the original material is shown and in the second row the non magnetic fraction can be seen before using sluice-box process.

The zone number 2 in sluice-box process (third row) contained always the valuable compounds, such as metallic particles. Typically, the lower zones in the sluice-box always contain more white particles which are assumed as mineral particles.

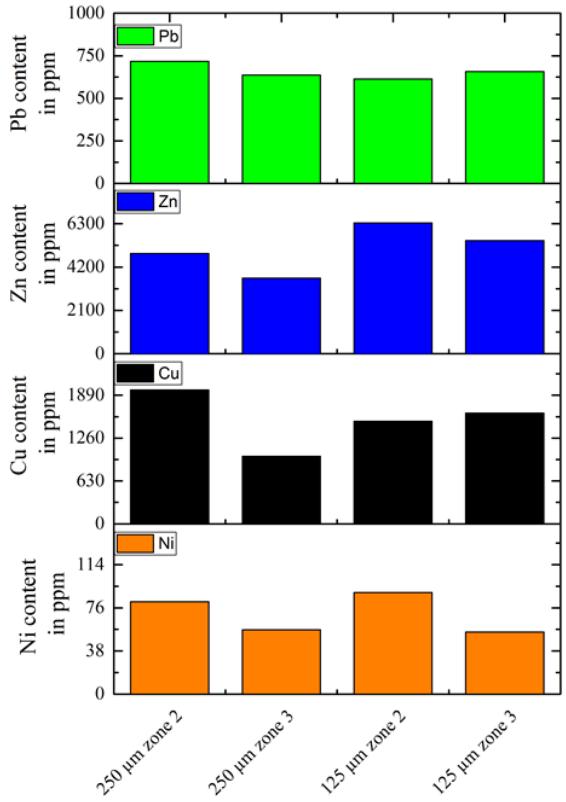

Figure 4.12: The concentration of Cu, Ni, Zn and Pb on collected particles in zone 2 and zone 3 after sluice-box process for non-magnetic fraction distinguished by its particle size different.

The main reason why no particles in grain sizes 63–125 µm and $\leq$ 63 µm after sluice-box and gold-pan process are shown, is because of the tendency of these particle sizes to be easily swept away by water flow; therefore, in this particle size range, the sieving process was not conducted.

The main goal of this study was to find ways in which copper could be recovered easily and at low cost from the fine fraction of bottom ash. As shown in **Figure 4.13**, copper is contained in the separated fractions from sluice-box process (zones 2 and 3) and in the heavy non-magnetic fraction collected in gold-pan process (fourth row). That is why these fractions are the most interesting ones relative to the recovery of copper. In the light non-magnetic fractions (fifth row), the number of visible copper particles is not zero, but is strongly reduced.

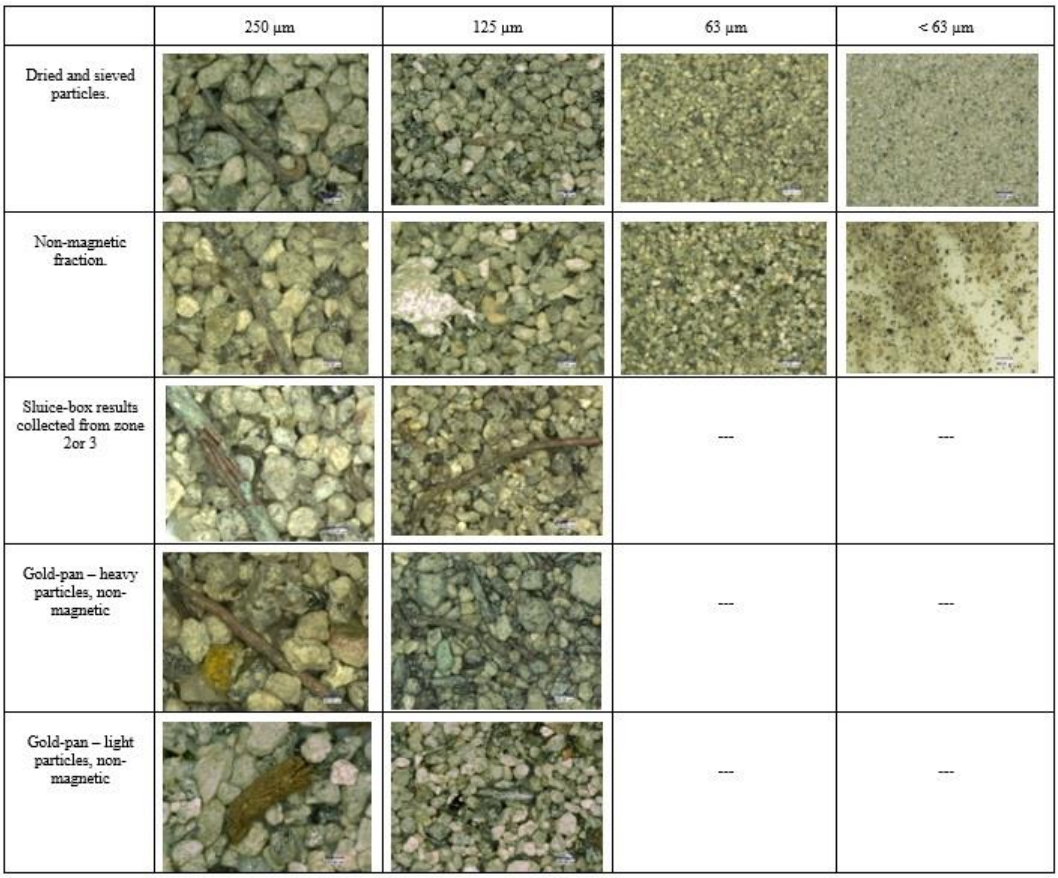

Figure 4.13: The morphology of fine particle bottom ash on each process, which focussed in non-magnetic fraction.

The collected particles in the gold-pan were embedded in epoxy resin, which could be observed in an optical microscope (**Figure 3.17**). Some results are shown in **Figure 4.14** (right side)**.** Metallic particles that have been polished have a bright appearance in microscope observation, while other metallic particles are darker in appearance, from grey to black. All embedded and polished samples were examined with SEM, and the EDS result are shown in **Table 4.1.**

Analyses no. 1 to 4 show the compositions of metallic particles (bright colours in optical microscopy); particles no. 1 to 3 consist of copper, and particle no. 4 is nearly pure tin. Because of the grey colour in optical microscopy, it was clear in advance that these particles were not metals. The detailed chemical compositions of these particles show that nearly all particles, with exception of particle no. 5, have higher oxygen content, an indication that these particles are oxides of varying composition. Particle no. 5 is embedded in particle no. 4, but has a different composition. As in particle no. 4, the tin content is also high in particle no. 5, but in addition the antimony content is much higher. In particle no. 5 the high chlorine

content is particularly striking, but it seems that it does not indicate a stoichiometric chlorine compound; for example if it were antimony chloride ($SbCl_3$), the chlorine content would be 46.5% of chlorine.

For all the other particles (no. 6 to no. 10), higher oxygen content is typical. It seems probable that particle no. 6 consists partly of titanium dioxide (M (TiO_2) = 79.8 g/mol), which means a stoichiometric Ti/O ratio in weight percent of 1.49. Regarding this ratio with a titan content of 49.29 wt.%, an oxygen content of 33.08 wt.% could be expected, lower than it was measured. EDS is a semi-quantitative analysis method, which is why it is very seldom that pure stoichiometric compounds can be measured with normal measuring techniques. For example, It could be possible that oxygen in higher quantities is located at the surface of a sample, due to the way the sample was prepared or because parts of oxygen are in compounds with other elements.

Particle no. 7 consists mainly of zinc oxide (M (ZnO) = 81.4 g/mol), which means a stoichiometric Zn/O ratio in weight percent of 4.09. Regarding this ratio with a zinc content of 65.90 wt.% an oxygen content of 16.11 wt.% could be expected, which is not so far away from 22.6 wt.%, as measured.

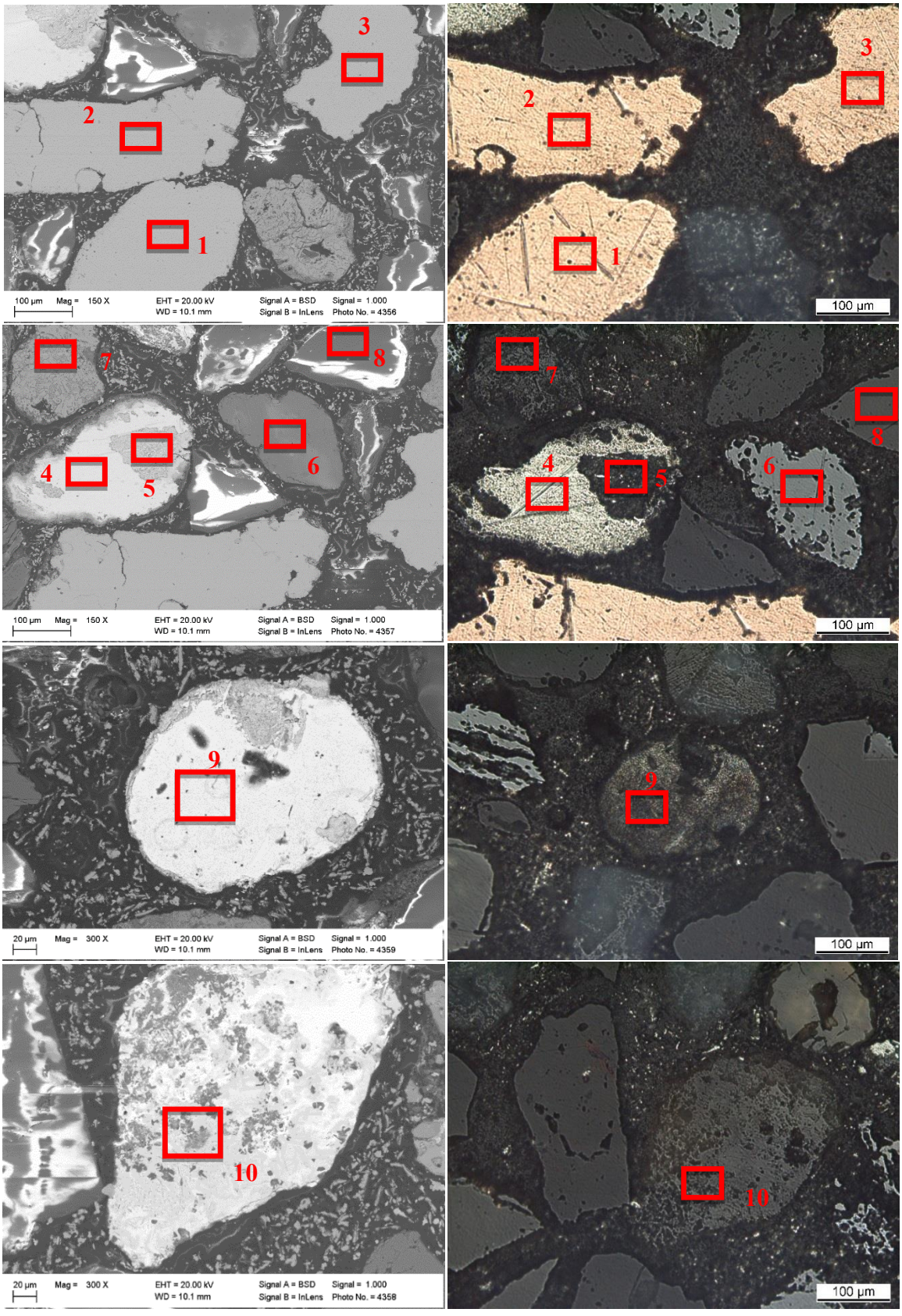

Figure 4.14: Typical of non-magnetic fraction heavy particles collected on the gold-pan: Scanning electron microscope results (left) compared to *Leica* optical microscope (right).

Table 4.1: EDS Analysis on selected area in SEM results in Figure 4.6.

Area	C	O	Cl	Br	S	Si	Na	Ca	Ni	Cu	Sn	Zn	Sb	Al	Fe	Pb	Nb	Ti	As	V
1	5.34	0.99	-	-	-	-	-	-	4.20	89.47	-	-	-	-	-	-	-	-	-	-
2	4.01	0.92	-	-	-	-	-	-	3.91	91.16	-	-	-	-	-	-	-	-	-	-
3	7.84	1.05	-	-	1.19	-	-	-	3.82	86.09	-	-	-	-	-	-	-	-	-	-
4	3.13	-	-	-	-	-	-	-	-	-	96.87	-	-	-	-	-	-	-	-	-
5	5.96	5.27	7.57	-	-	-	-	-	-	2.74	61.27	-	15.77	-	1.42	-	-	-	-	-
6	2.29	46.34	-	-	-	-	-	-	-	-	-	-	-	-	-	-	0.64	49.29	-	1.45
7	5	22.60	-	-	-	-	-	0.72	-	2.57	-	65.90	-	3.21	-	-	-	-	-	-
8	20.71	44.04	-	-	-	-	-	-	-	-	-	-	-	35.25	-	-	-	-	-	-
9	-	8.06	-	-	-	-	-	-	-	-	-	-	-	-	-	91.94	-	-	-	-
10	2.39	24.49	-	2.35	-	9.31	1.44	8.60	-	-	-	-	-	-	1.37	48.67	-	-	1.38	-

Particle no. 8 consists partly of aluminium oxide dioxide (M (Al_2O_3) = 102 g/mol), which means a stoichiometric Al/O ratio in weight percent of 1.13. Regarding this ratio with an aluminium content of 35.25 wt.%, an oxygen content of 31.2 wt.% could be expected, lower than as measured.

Particle no. 9 consists probably of lead oxide (M (PbO) = 223.2 g/mol), which means a stoichiometric Pb/O ratio in weight percent of 12.95. Regarding this ratio with a lead content of 91.94 wt.%, an oxygen content of 7.1 wt.% could be expected, which is not so far away from the 8.06 wt.% that was measured. It seems that particle no. 10 is probably a mixture of CaO-SiO_2-PbO. The stoichiometric oxygen content of such a mixture would be 19.28 wt.%, which is not so far from 24.49 wt.% oxygen that was measured.

The collected particles in the gold pan comprised many kind of particles, including some light particles that still were collected with the metallic fraction. To evaluate their chemical compositions, an element mapping was conducted on some non-magnetic particles after separation by gold-pan process. The results of element mapping of these non-magnetic particles are shown in **Figure 4.15**.

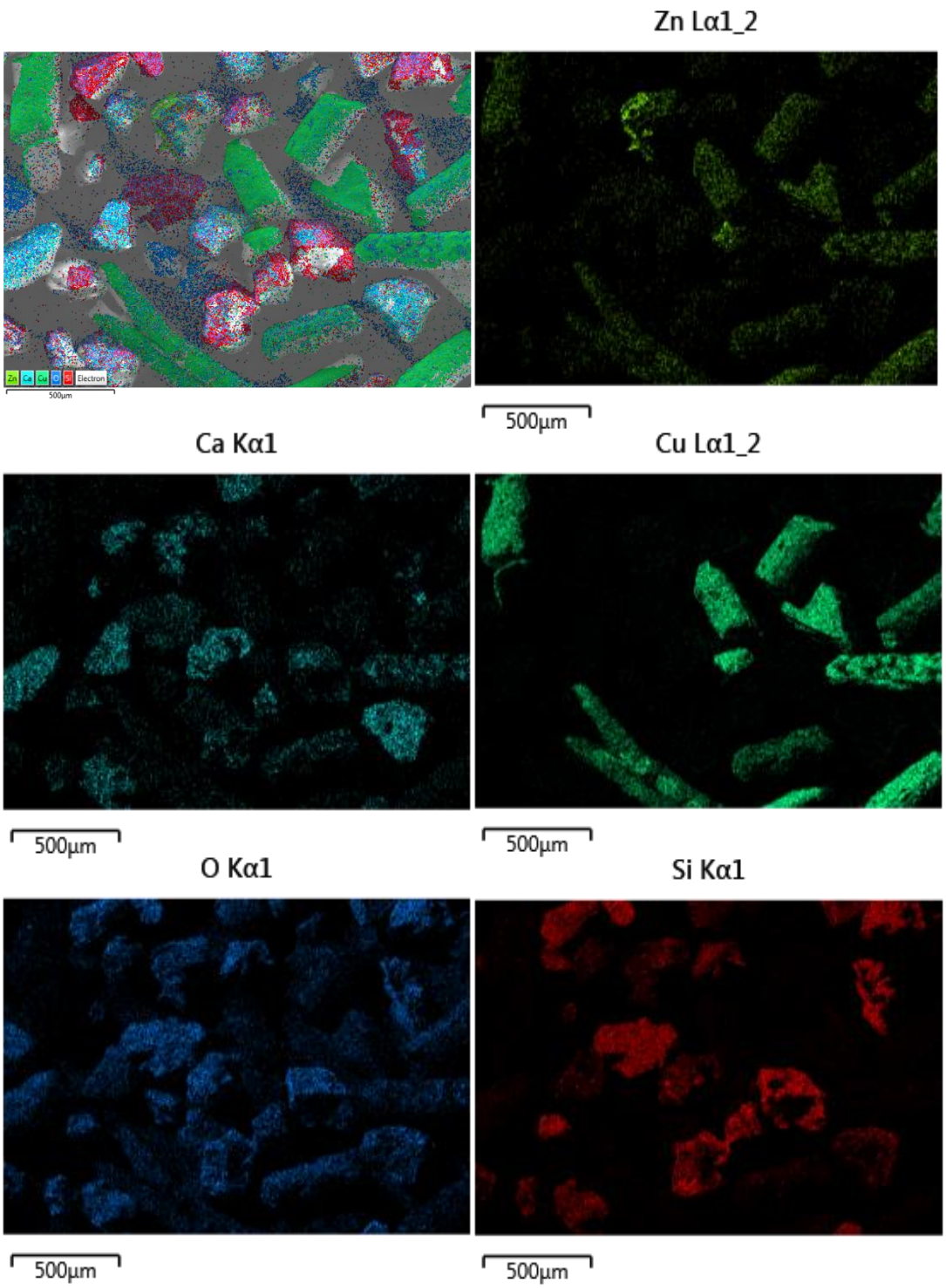

Figure 4.15: Elemental mapping observation of collected heavy particles in gold-pan, metallic copper as in the form of wire has been concentrated in this fraction together with SiO_2 (glass) particles.

In **Figure 4.15,** it is shown that copper mainly occurs together with zinc, which indicates brass particles. Silicon is often combined with oxygen alone, but also together with calcium and oxygen, which indicates, on the one hand, pure silicon dioxide particles and, on the other, slag-like particles of $CaO\text{-}SiO_2$.

Samples produced by gold-pan process usually contain in addition to the metallic particles, light mineral particles such as calcium oxide, silicon dioxide, and solid mixtures of both. It is necessary to separate these mineral phases from the metals fraction. That is why an additional vacuum separation was implemented after the gold-pan process. After being separated by vacuum separation, the non-magnetic particles were washed with 100 g/L citric acid to get clean particles so that light particles could be easily distinguished from metallic particles (**Figures 4.16 and 4.17**).

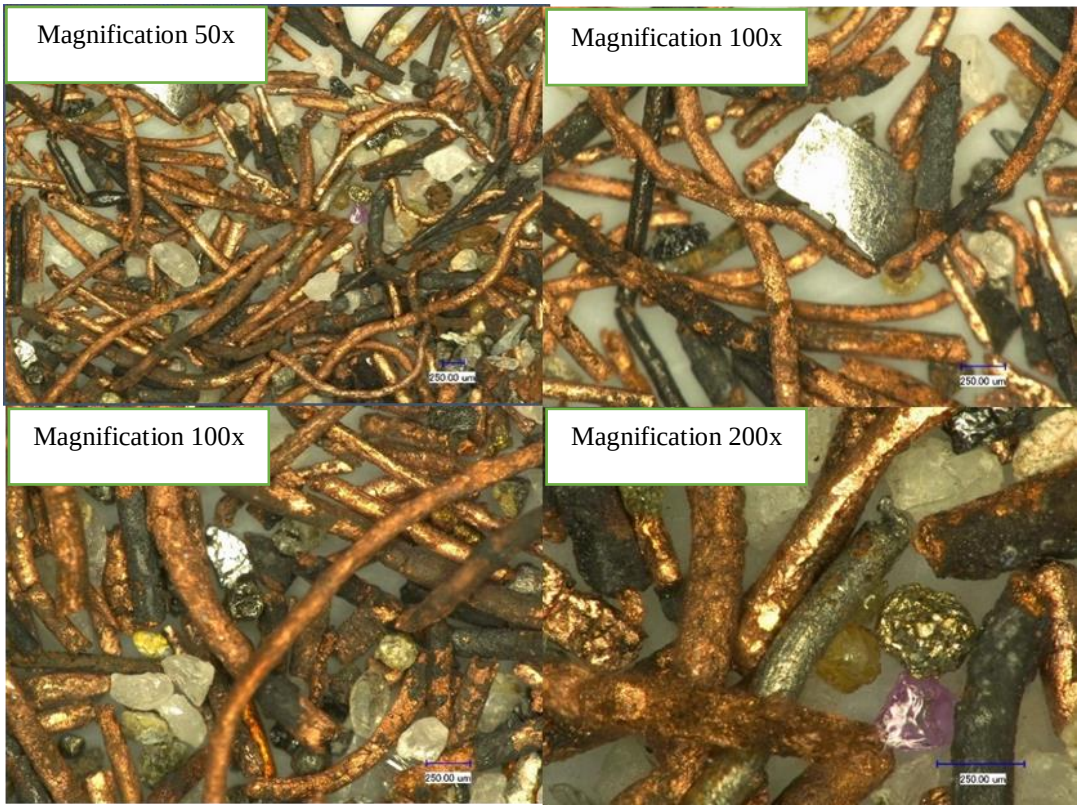

Figure 4.16: Collected heavy particles after gold-pan – vacuum experiment on bottom ash particle size 125µm, 100 g/L citric acid washed.

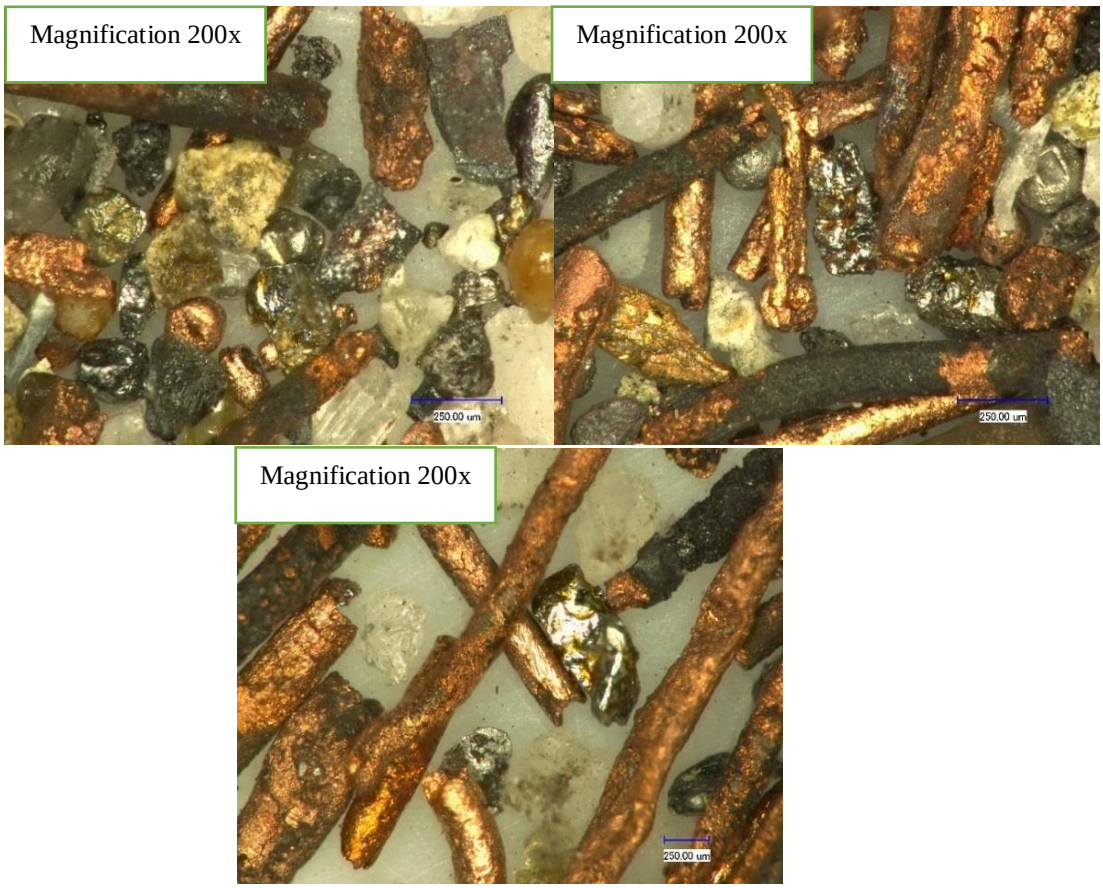

Figure 4.17: Other heavy particles collected together with copper on bottom ash particle size 125µm, 100 g/L citric acid washed.

The combination of sluice-box and gold-pan processes together with vacuum separation process was as effective as sink-float separation with natrium-polytungstate, but much cheaper. This combination process would produce metallic copper at the end of the process, and it would be possible to transfer this technology to a larger industrial process. That would not be possible with the sink-float technology with natrium-polytungstate as shown in **Figures 4.16** and **4.17**; other metallic fractions would also be separated. Other heavy particles aside from copper could be determined by their different shape and colour in comparison to copper. Metallic copper, very often in form of wire, has a bright orange colour, sometimes covered by a spotted dark layer, whereas other heavy particles have a bright to dark silver colour, or bright yellow colour together with various shapes, from rounded to irregular. These metallic fractions were predicted as lead, brass, tin, and others, which could be still covered by oxide layers.

4.4 Collected heavy particles and its characterization

The results of this study reported so far show that an enrichment of metals is possible with ball milling, sieving, and washing with a combination of sluice-box and gold-pan processes. Here it is important to know that the effectivity of metal enrichment is dependent on the grain size fraction. The enrichment of valuable metals contained in bottom ash from plant A were compared in two grain size fractions (125–250 µm and 250–500 µm) and the results can be seen in **Figure 4.18**. As has been shown, the enrichment of chromium and cobalt in the magnetic fraction after sluice-box and gold-pan process is more effective in the 125–250 µm grain size fraction in comparison to the 250–500 µm grain size fraction. The same can be seen with the non-magnetic fraction. The copper, zinc, and lead content are higher in the 125–250 µm grain size fraction than the 250–500 µm grain size fraction.

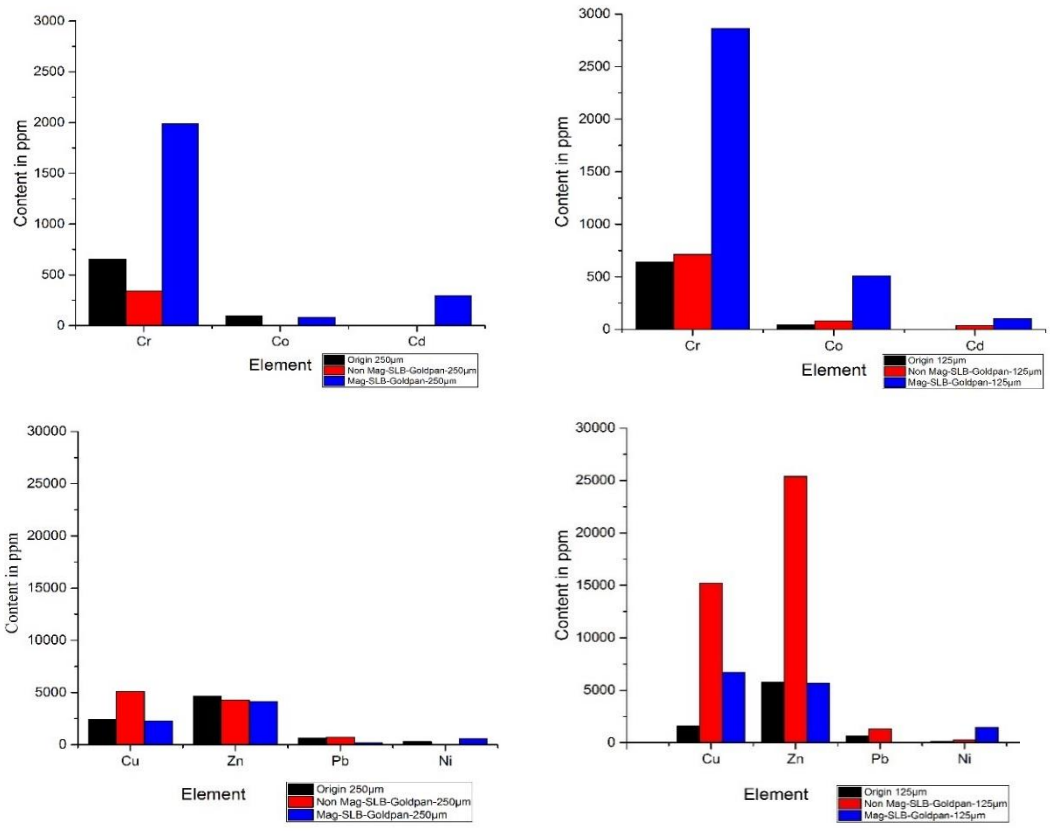

Figure 4.18: The comparison of collected heavy metals after gold-pan experiment. 250 – 500µm particle size (left) and 125 – 250µm particle size (right).

There are some elements that significantly increased after gold-pan experiment, namely, copper, zinc, and chromium. The most interesting is the

recovery of copper itself. The copper in this study had metallic form, as proved in **Figures 4.8** to **4.11**. The valuable materials contained in bottom ash plant A can be seen in **Figure 4.12**; with density separation, the copper concentration could be increased. The comparison of particle size difference showed that certain particle sizes can determine suitable/optimum copper recovery. In this case, particle size in the range of 125–250 µm is preferable for copper recovery.

4.4.1 The effect of density separation on high-density elements contained in bottom ash

There are two basic parameters that should be considered with respect to recovery of valuable elements by density separation in this study. First, the enrichment of valuable metals depends on the grain size and, second, the separation effectiveness with gold-pan process depends on the stirring speed. In **Figure 4.19,** it is shown that the stirring speed in gold-pan process has a stronger effect in the 250–500 µm grain size fraction than in the 125–250 µm grain size fraction. When a higher stirring speed is used in larger grain size fraction, the content of valuable metals retained in the gold pan is reduced. Therefore, it can be assumed that more particles due to higher velocity have left the gold pan. In smaller grain size fraction (125–250 µm), this effect can only be seen in copper separation and not in the other elements. It appears that the effectiveness of this separation method is limited to a certain speed.

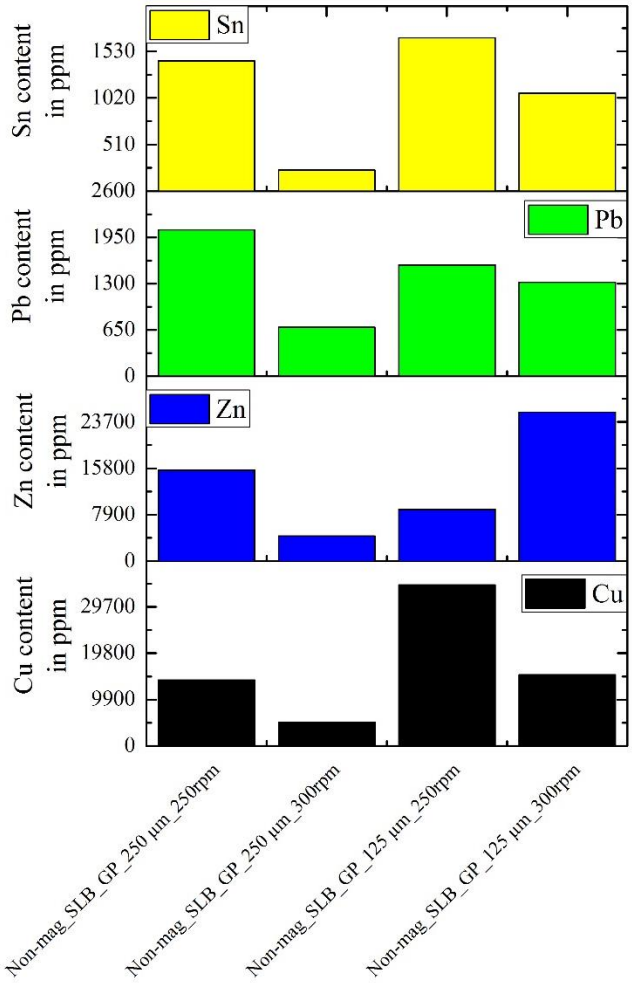

Figure 4.19: The effect of stirring speed different on collectability Cu, Zn, Pb and Sn.

4.5 Collected light particles and its characterization

Silicon, calcium, aluminium, magnesium, and titanium are the five most abundant elements in fine particle bottom ash. Almost all of them are collected among the light particles, both magnetic and non-magnetic fraction. Silicon dioxide, calcium oxide, and aluminium oxide alone and together were abundant in light particles in this study. According to Li [Li **2016]** and Pan [Pan **2008**], bottom ash has the potential to be reused as secondary material for cement production purposes, but, aside from the heavy metals concentration in bottom ash, the chloride level would cause a serious problem in the cement kiln.

The use of bottom ash in the cement industry needs to meet certain criteria. The essential parameter of the reusability of bottom ash in the cement industry is its chemical composition, which will affect cement quality and

mechanical properties. According to Jill R. Pan et al., the use of bottom ash in cement production is ideal for use in Type II Portland cement, which could be used in construction of roads or dams [Pan **2008**]. The general composition of Type II Portland cement is listed in **Table 4.2** (below).

Table 4.2: The typical Portland cement composition [Pan **2008**].

Compounds	**Content in %**
CaO	60
SiO_2	15-25
Al_2O_3	3-8
Fe_2O_3	0.5-6
MgO	0.1-4

In comparison with the composition of Portland cement, listed in **Table 4.2,** the composition of bottom ash (**Figure 4.3**) in this study has met the requirements for cement production, with the exception of lime (calcium oxide) content, which is still lower than required in cement composition. The problem of the reusability of bottom ash is the heavy metal content and the presence of sulphur and chlorine.

Yinming Li et al. [Li **2016**] reported that heavy metals affect cement quality and create environmental problems because of the leachability of heavy metals and the possible contamination of groundwater. That is why the elimination of heavy metals such as copper, zinc and lead and the removal of sulphur and chlorine are essential if we are ever to reuse fine particle bottom ash as raw material in the cement industry.

As shown in **Figure 4.20.a,** the smaller particle size fractions, after ball milling and sieving, contain much higher amounts of chlorine and sulphur. In **Figure 4.20.b,** the sulphur and chlorine content in non-magnetic fraction are shown **(Figure 4.20.b – left side)**, which is caused after magnetic separation. It can be seen that the suphur and chlorine content in the finer grain size fractions is higher. The same tendency as in the original material can be seen in the non-magnetic fraction. After washing in the sluice-box process, the sulphur and chlorine content is reduced drastically on the different grain size fractions (125–250 µm and 250–500 µm). In

Figure 4.20.c, a further reduction of sulphur and chlorine can be seen after the gold-pan process. As seen in **Figure 4.20.c**, there is no big difference between the sulphur and chlorine content in the different grain size fractions retained in the gold pan and in the grain size fractions transported out of the gold pan. Sluice-box and subsequent gold-pan processes were separation processes assisted by pressurized water, which means that there was intensive contact between the water and particles containing sulphur and/or chlorine, resulting in the dissolution of sulphur and chlorine from the minerals.

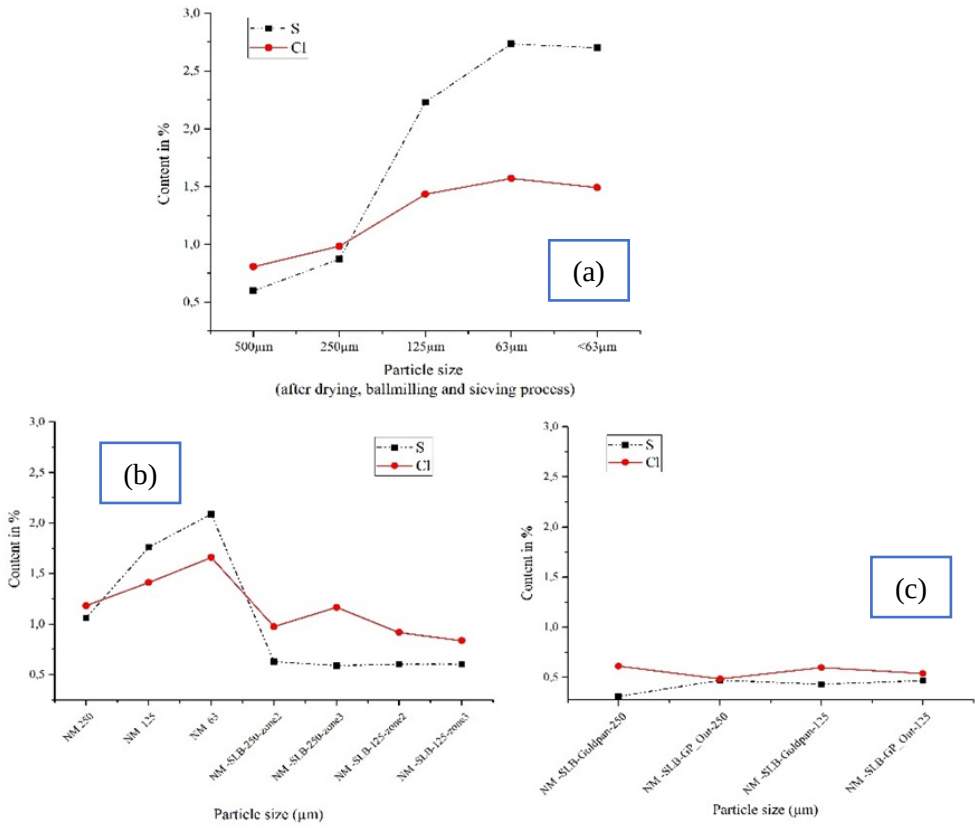

Figure 4.20: The behaviour of Cl and S concentration during processes.

(a). After sieving from ≥ 500µm – ≤ 63µm, (b). After magnetic separation for particle size 250 – 125µm and (c) After sluice-box – gold-pan process for particle size 250 – 125µm.

However, to be able to reuse this material in cement production, the concentration of the both elements must be reduced to below 100–200 ppm. In addition, the most important elements that need to be reduced for usage in cement production are Cr, Co, Ni, Cd, Pb, Cu, Zn, and Sn. These elements should be reduced to 100 ppm. The contents of important trace elements in the light fraction are shown in **Figure 4.21,** after different treatment steps. There is no real reduction of copper in the light fraction after sluice-box and gold-pan processes, compared to

the copper content after vacuum treatment. The same can be seen for the other elements, with the exception of zinc, where a further reduction after the vacuum process can be measured. Small differences in the contents of elements have to be interpreted very carefully, because the measurement accuracy of XRF at very low levels is highly dependent on the calibration procedure and is sometimes limited:

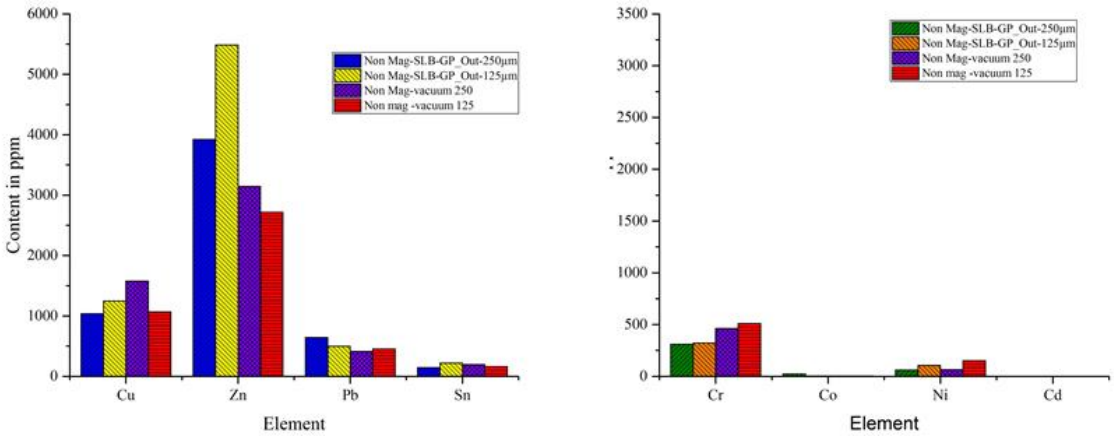

Figure 4.21: The concentration of high-density elements on collected light particles.

It seems that the Co, Ni, Cd, and Sn content are reduced down to very low levels in the light fractions, and might meet the cement raw material requirements, but, because of limited measurement accuracy of XRF, these values have to be checked by an analysis method other that XRF to be sure of the results. It seems that the most problematic elements are copper, zinc, and lead, if the separation sequence (ball milling → sieving → magnetic separation → sluice-box process → gold-pan process → vacuum treatment) is used. Therefore, a further separation process is required to reduce their concentrations to acceptable levels.

4.5.1 The effect of density separation on light particles bottom ash

After magnetic separation, the light fraction of fine particle bottom ash commonly contains aluminium oxide, silicon dioxide, calcium oxide, and some other oxides (alkali elements, etc). These compounds are abundant, compared to heavy metals. As shown in **Figure 4.3,** after ball milling and sieving of the original material, the aluminium oxide content is normally stable for every particle size. Silicon dioxide tends to have the lower content with decreasing particle size, by contrast with calcium oxide, which is enriched by the reduction of particle size.

What happens with the above-mentioned elements during sluice-box and gold-pan process is shown in **Figure 4.22**. When the magnetic fraction is treated in sluice box and gold pan, it can be seen that contents of aluminium, silicon, and calcium retained in the gold-pan are lower than the contents of the material transported out of the gold-pan. This effect is independent of grain size. If the non-magnetic fraction is analyzed, the same behavior is displayed by calcium, but the behavior of silicon is different. In the non-magnetic fraction, the silicon content in the gold pan is higher than the silicon content in the fraction transported out of the gold pan.

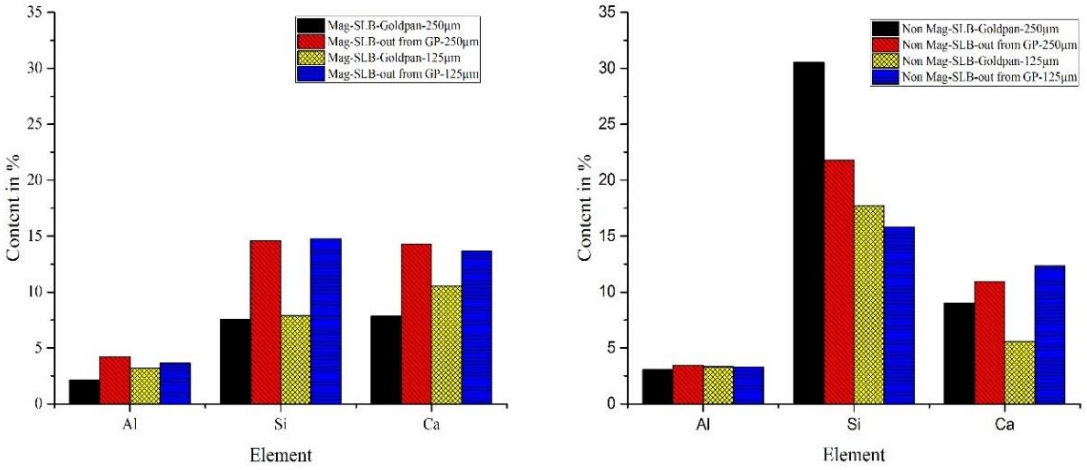

Figure 4.22: The content of Al, Si and Ca on gold-pan product in the particle size 250µm and 125µm with stirring speed 250 rpm for 1 hour.

The result of the gold-pan experiment provides an opportunity for reusability of bottom ash in the cement industry, especially for non-magnetic particles that float out of the gold pan (the suitable particle size is 125 µm because it has higher calcium oxide content). As described in **Table 4.2**, the cement industry requires 60% calcium oxide.

4.5.2 The effect of stirring speed to the light particles separation

In **Figure 4.23**, no real effect of stirring speed on separation of light non-magnetic particles is shown. Perhaps it shows that a lower stirring speed has the effect of higher silicon content in the larger grain size fraction, but it could also be an accidental effect, which would have to be checked again.

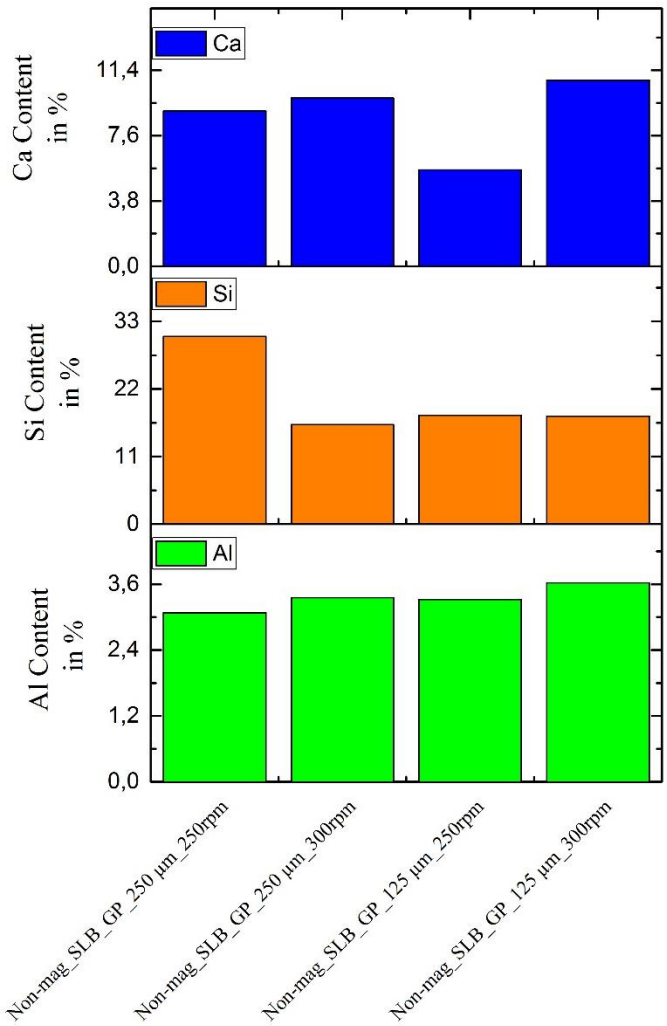

Figure 4.23: The content of Al, Si and Ca on sieved, magnetic separation and sluice-box – gold-pan 125 and 250µm products with different stirring speed parameter; 250 and 300 rpm for non-magnetic fraction.

The collected light particles after gold-pan process were also treated with the vacuum process to separate the light compounds (e.g., Si and/or Ca compounds) that still were collected together with the heavy particles. The removal of these light compounds was successfully achieved and was proved by Keyence microscope results together with element mapping in **Figure 4.24**, which shows that the particles mainly consist of calcium, silicon, aluminium, and oxygen, and that some particles also contain smaller amounts of sulphur.

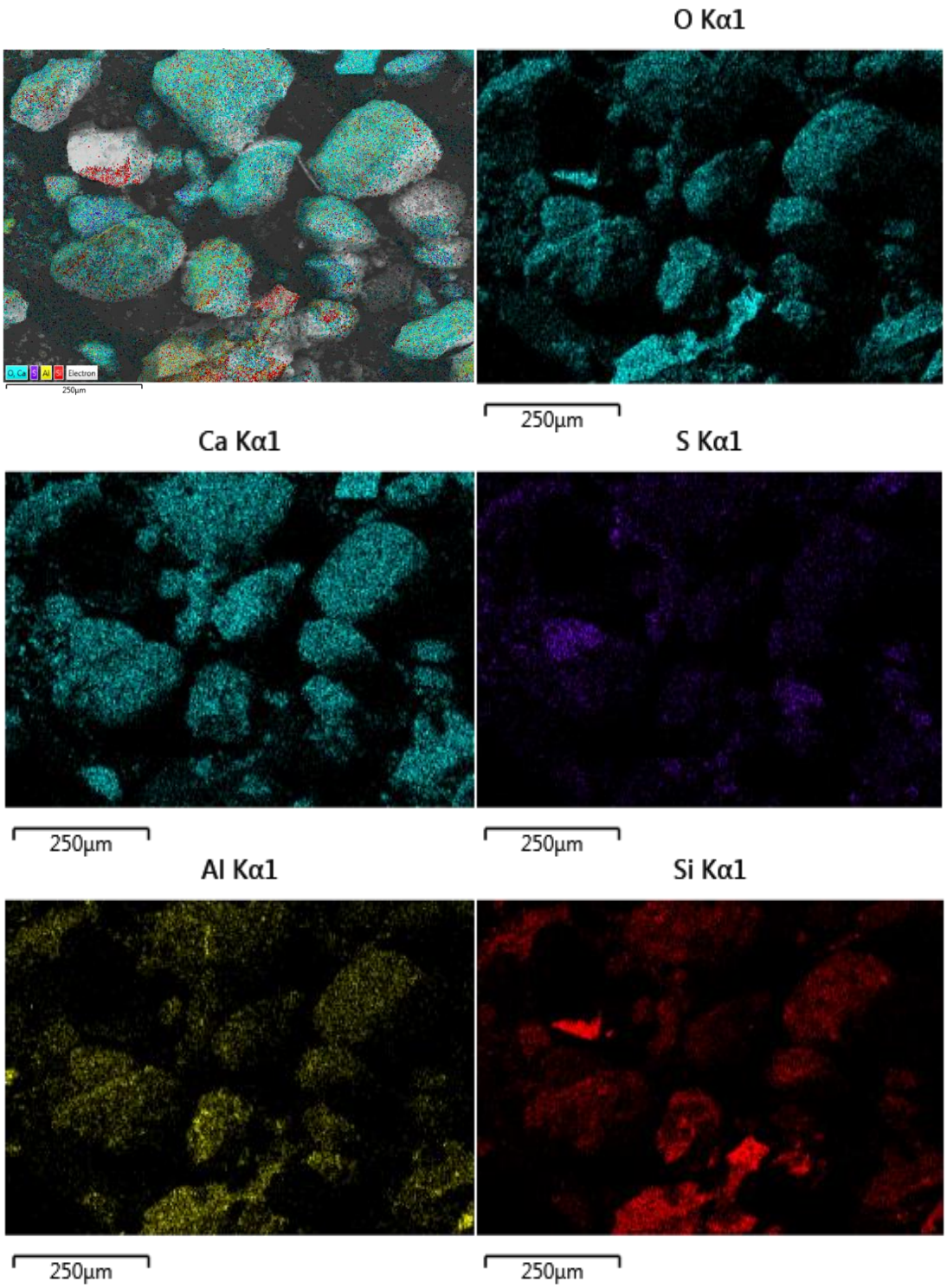

Figure 4.24: The elemental mapping of collected light particles after gold-pan and continued with vacuum process product 125 – 250µm non-magnetic particles.

In another particle (**Figure 4.25**), beside the normal composition of CaO-Al_2O_3-SiO_2, the appearance of zinc together with silicon and oxygen indicates an oxide mixture of ZnO-SiO_2 in this fraction. As it clearly seen, the collected zinc in this fraction is non-metallic zinc.

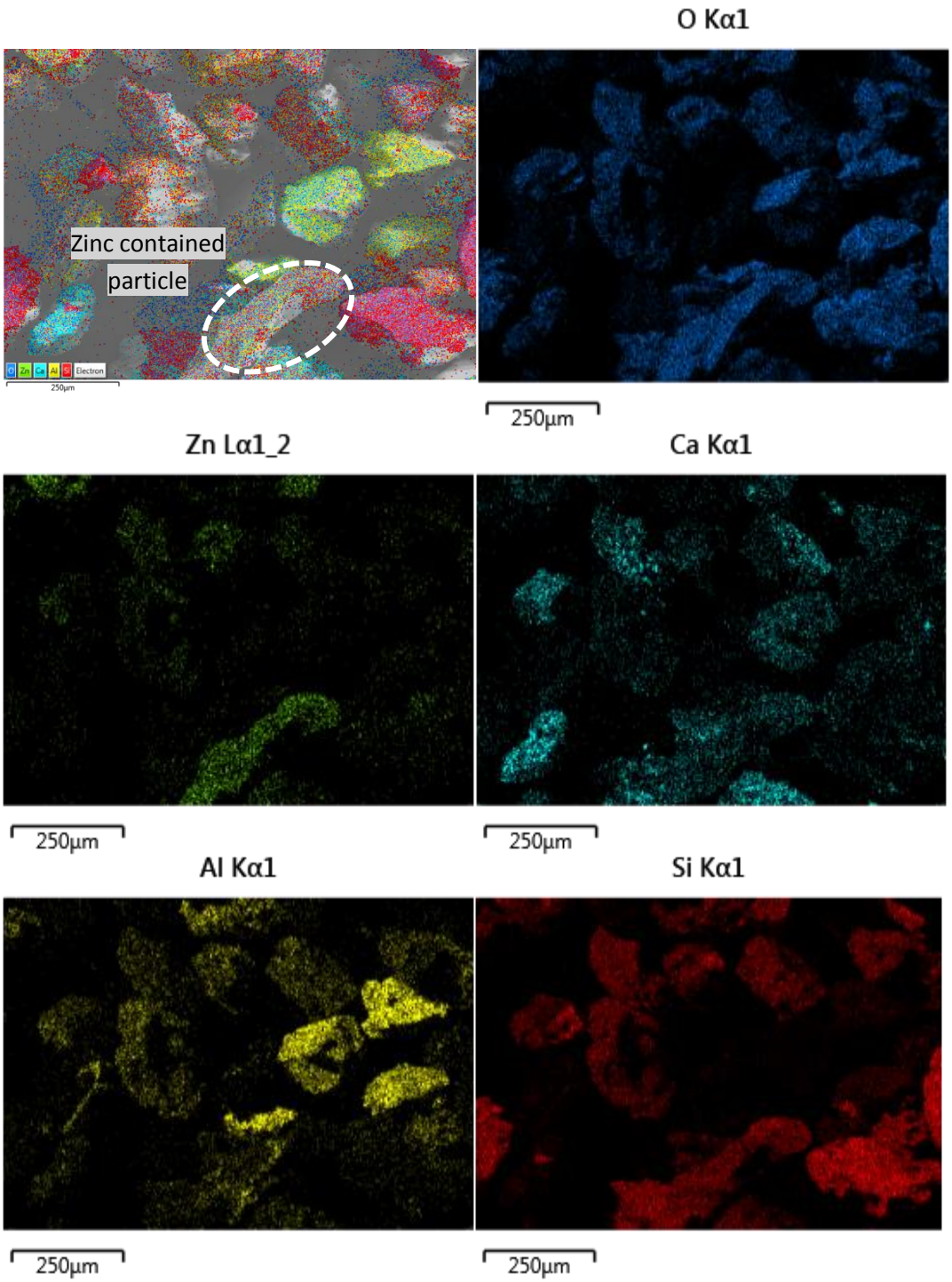

Figure 4.25: The concentration of zinc in collected light non-magnetic particles.

4.6 Material balance

To estimate the metallic fraction contained in bottom ash fine fraction, every fraction starting from ≤ 63-µm up to ≥ 500-µm particle grain size should be treated with the method described in this research and the calculated recovery from bottom ash documented. Previously it was discussed that particle size ≥ 500

µm is difficult to treat, therefore this fraction should be re-milled to reduce its particle grain size. Bottom ash samples from WtE plants B and C were used to determine the material balances presented here. Different particle grain sizes from the two incineration plants were used. The original grain size from plant B was a larger grain size than that from plant C. The particle grain size difference plays the main role in determining preliminary treatment or separation. These samples have been treated by the following steps:

- Drying
- Scrap removal (hand sorting)
- Breaking and magnetic separation (manual magnetic separation)
- Milling and sieving
- Wet magnetic separation and density separation with gold-pan process

The mass balance from material input to sieving is shown in **Figure 4.26,** including the loss of material after the separation process. From this data, the metallic fraction and the recovery could be calculated after each process step.

The approximately amount of metallic copper could be estimated from the following table which showed the concentration of copper and other valuable elements as XRF analysis results.

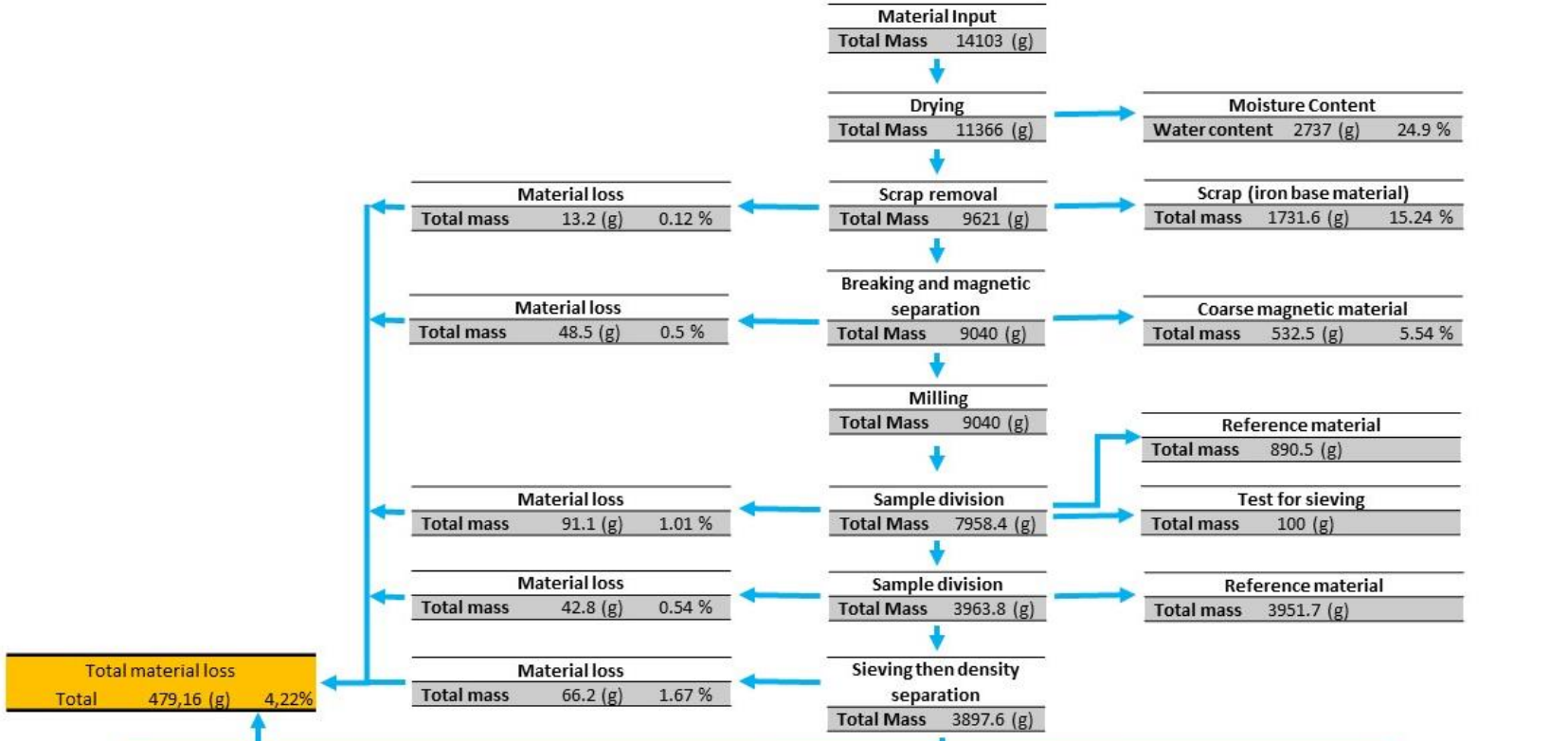

Figure 4.26: Material recovery after all processes of the bottom ash from plant B separation.

As shown in **Figure 4.26**, the original sample used in this part was fresh bottom ash from incineration plant B, which contained high humidity that should be reduced by drying process. Initially, the sample had a particle size up to 250 mm. In comparison to a sample from incineration plant A, this sample contained many large scraps, which were separated by hand-sorting. The remaining sample was physically separated by a breaking process, continued with magnetic separation manually by hand and in dried condition. Magnetic particles and non-magnetic particles were separated. The non-magnetic particles were further physically liberated by milling process. To produce samples that are as representative as the initial sample, a sampling process was conducted as noted by "sample division" in the **Figure 4.26**. Afterwards classification was done by sieving process. That sample with particle size $\geq$ 500 µm was re-milled again. Samples that were noted as reference material were then examined by XRF test or other characterization methods. The total loss of materials was recorded and at the end more than 95% of material was recovered.

In order to reduce the content of some ferromagnetic elements, such as iron, nickel, and cobalt, probably contained in magnetite or other magnetic oxides, magnetic separation was once again conducted by wet magnetic separation process in each grain size fraction. Magnetic particles produced by wet magnetic separation (**Figure 4.27**) were particles with a high density and specific dark-brown colour. In comparison to magnetic fraction, particles with a brighter colour are typical for non-magnetic fractions, because non-magnetic fractions contained more quartz/glass/SiO_2 and calcium compound particles. Valuable materials like copper were mainly contained in the heavy non-magnetic fraction as metallic particles. Metallic copper was usually to be found starting from particle size 63–125 µm or larger (**Figure 4.27**). For the finest particle grain size ($\leq$ 63µm), in general, no metallic copper could be recognized by digital microscope.

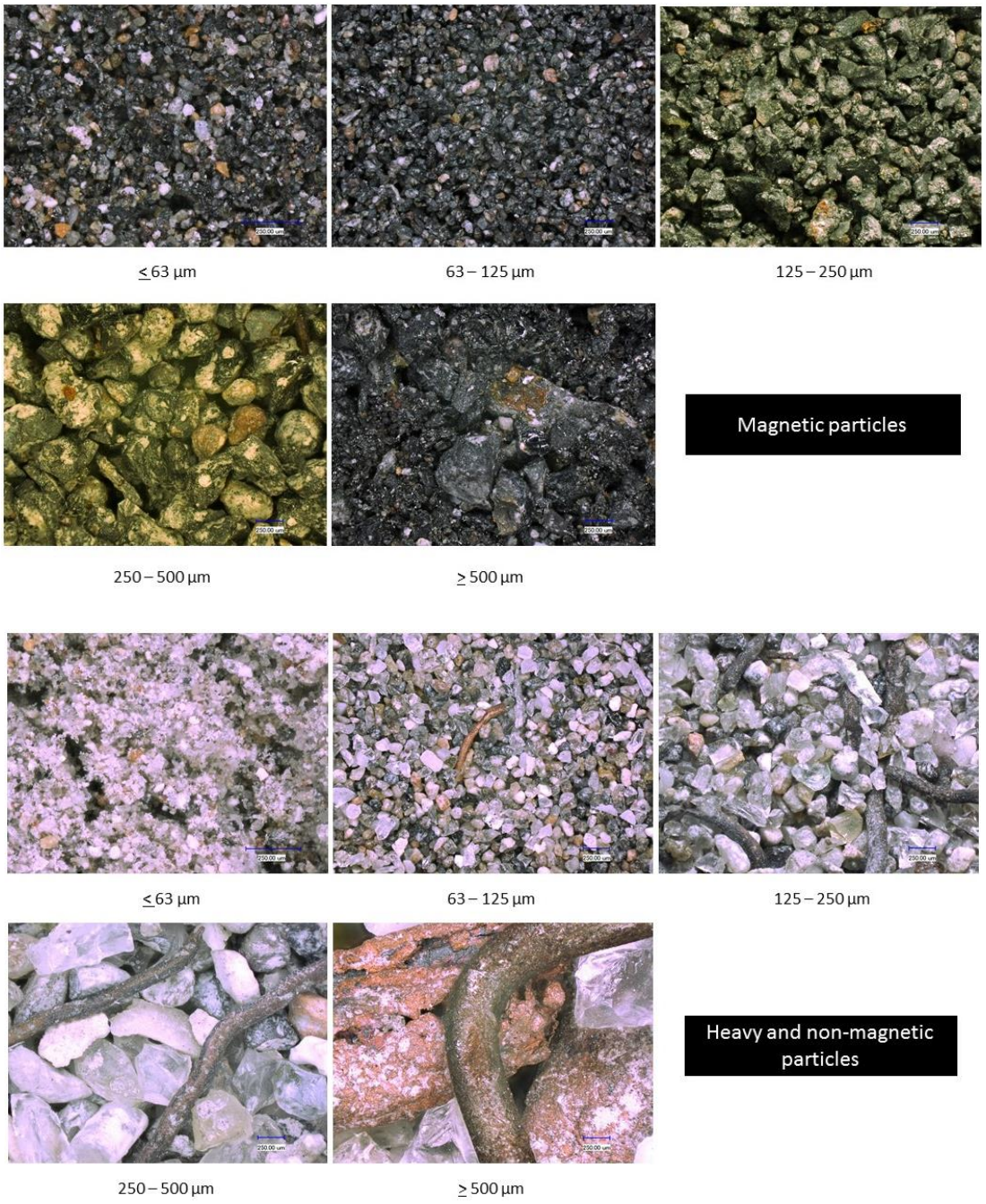

Figure 4.27: The characteristic heavy fraction products from bottom ash plant B observed by *Keyence* digital microscope.

In general, no valuable metals can be detected by optical microscopy in the non-magnetic light fraction of bottom ash (**Figure 4.28)**. It can be seen from Figure 4.28 that the non-magnetic light fraction consists essentially of smaller and larger stone-like particles, depending on the grain size structure.

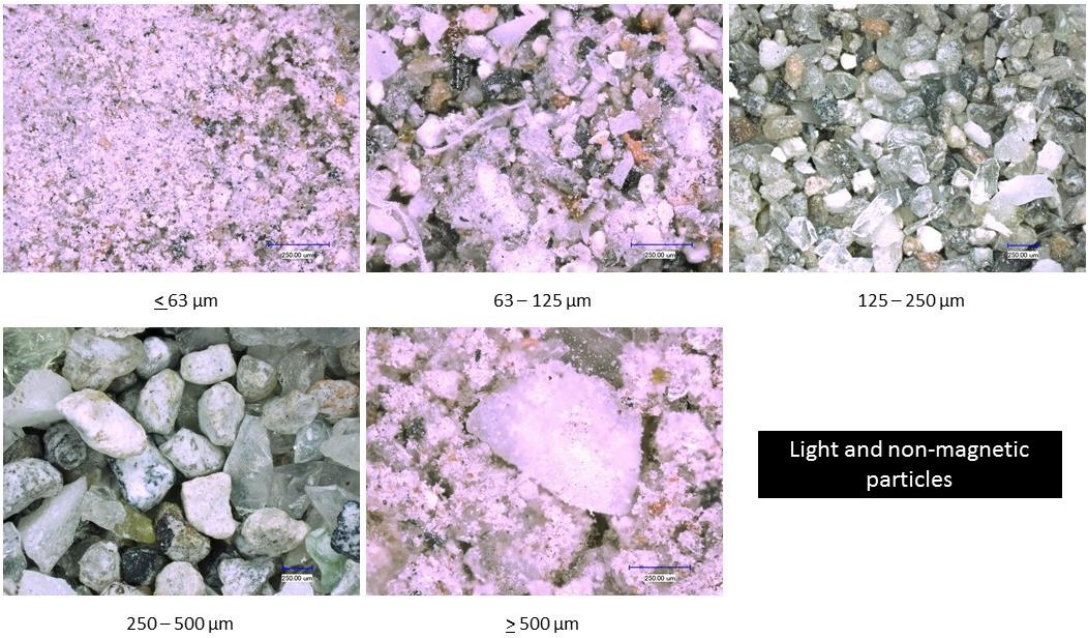

Figure 4.28: The characteristic light fraction products from bottom ash plant B observed by *Keyence* digital microscope.

In order to get information about the chemical composition of light non-magnetic particles, heavy non-magnetic particles, and magnetic particles, XRF analysis was done on these fractions (**Figure 4.29**).

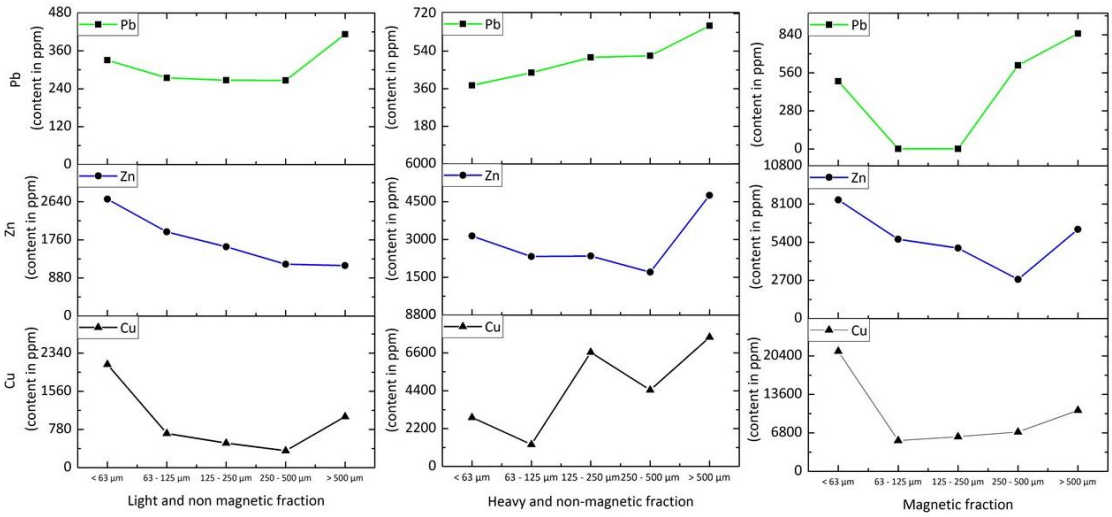

Figure 4.29: The tendency of high density element such as Cu, Zn and Pb in magnetic fraction, light-nonmagnetic fraction, and heavy-nonmagnetic fraction.

In **Figure 4.29**, it can be seen that unexpectedly lower amounts of lead, zinc, and copper are still contained in the light non-magnetic fraction. In the heavy non-magnetic fractions the lead, zinc, and copper content in general is higher than in the light non-magnetic fractions. A clear tendency is seen, that the copper content increases with the grain size fraction. It seems that the zinc content is more or less constant over the different grain sizes. Larger brass particles (bright yellow

colour) could be the reason for the higher zinc content in the larger grain size fraction.

The higher zinc and copper content in the magnetic fraction is surprising and was not expected before. Copper is normally enriched in the heavy-non-magnetic fraction, but this time copper has also higher concentrations in the magnetic fraction (**Figures 4.30** and **4.31**).

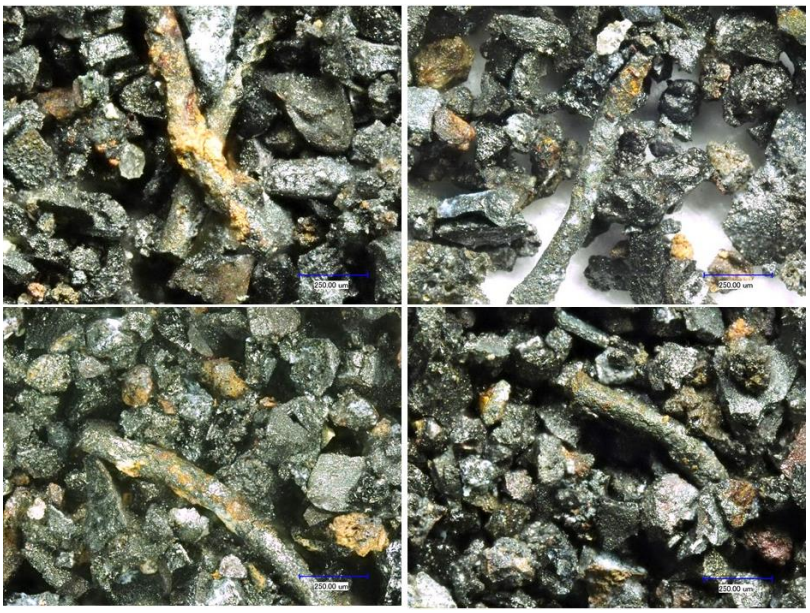

Figure 4.30: The source of copper containment in magnetic fraction (*Keyence* observation for particle size 125 – 250µm).

Figure 4.31: The source of copper containment in magnetic fraction (*Keyence* observation for particle size 250 – 500µm).

The reason why copper content in magnetic fractions is possibly physically bonded copper wire with some magnetic-compounds like iron oxide

(magnetite) is shown in **Figure 4.32** and **Table 4.3**. Because copper is mainly contained as metal in the form of small cable remains in the different grain size fractions of fine bottom ash, the variations of chemical analyses can be very high, because copper is ductile and therefore it could be difficult to get a uniform copper distribution, especially in very fine grain size fractions.

This is seen with the comparison of optical microscope and SEM results in **Figure 4.32**. In optical microscopy, the copper-rich phase has a bright yellow-orange colour inside the grey matrix of iron oxide. It seems difficult to separate this kind of copper physically, as it is already in small particle size. This explains the appearance of copper even in small magnetic fractions.

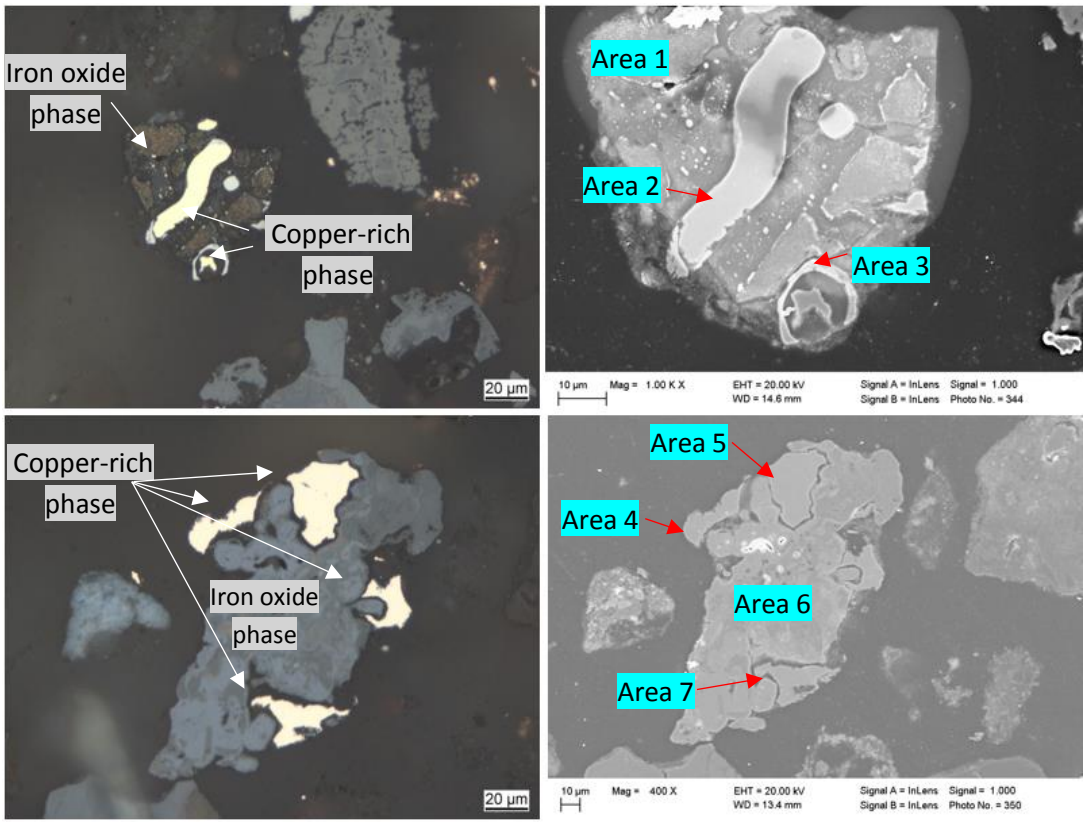

Figure 4.32: Copper containment in magnetic fraction (63 – 125 µm). The comparison results from *Leica* microscope (left) and SEM (right).

From EDS analysis (**Table 4.3**), it can be seen that the particle in area 3 is no oxide but a metallic mixture of different elements based on iron and copper. In areas 1 and 6, oxides with higher iron and copper content are shown. In the other areas, no oxygen was detectable, which indicates the existence of metal structures. This is in accordance with results of optical microscopy, in which metals can easily be detected because of their reflection behavior.

Table 4.3: EDS Analysis on selected area in SEM results in Figure 4.30.

Element	Weight %.						
	Area 1	Area 2	Area 3	Area 4	Area 5	Area 6	Area 7
O	28.20	-	-	-	-	20.55	-
Br	-	6.64	-	-	-	-	-
Na	6.21	-	-	-	-	-	-
Al	8.61	-	-	-	-	-	-
Si	13.32	-	-	-	-	-	-
P	1.65	-	8.28	-	-	-	-
Nb	4.54	-	-	-	-	5.67	-
K	3.43	-	-	-	-	-	-
Cr	1.33	-	-	-	-	-	-
Sn	-	4.05	6.61	-	-	-	-
Sb	-	-	9.95	-	-	-	-
Fe	14.53	2.55	35.89	2.41	1.98	35.80	1.62
Cu	18.18	86.76	39.27	97.59	98.02	37.98	98.38

4.7 Comparison of bottom ash fine particle grain size from two different incineration plants

There was some improvement in methodology that initially showed up mainly in the magnetic separation method, going from dry magnetic separation to wet magnetic separation, because the fine particle size would easily be agglomerated, causing some non-magnetic particles to become attached to the magnetic particles. Wet magnetic separation is also an easy process to conduct. The process was applied to bottom ash from incineration plant C, too. Initially, the bottom ash from plant C had a smaller particle size than that from plant B, ranging up to 8-mm particle grain size. The results from plant B separation showed that there were still large amounts of light particle contamination in the heavy non-magnetic particle size $\geq$500 µm. Some methods have been developed to solve this problem. This is the main reason for comparison between incineration plants B and C, which will be described in this section.

As mentioned before, samples from plant C have smaller particle sizes than the samples from plant B. That is why some modification was made to its separation process. The main process is still the same as shown in **Figure 4.26**; however, some process steps have been skipped (for example, scrap removal and breaking process were not to be applied in the separation process for samples from plant C). The separation method for bottom ash from plant C would be conducted

by the following process: drying, milling, wet magnetic separation, density separation, and an additional process for particle size > 500 μm to improve the separation of the metallic particles collected in this fraction. A detailed flowchart of the separation process is shown in **Figure 4.33**.

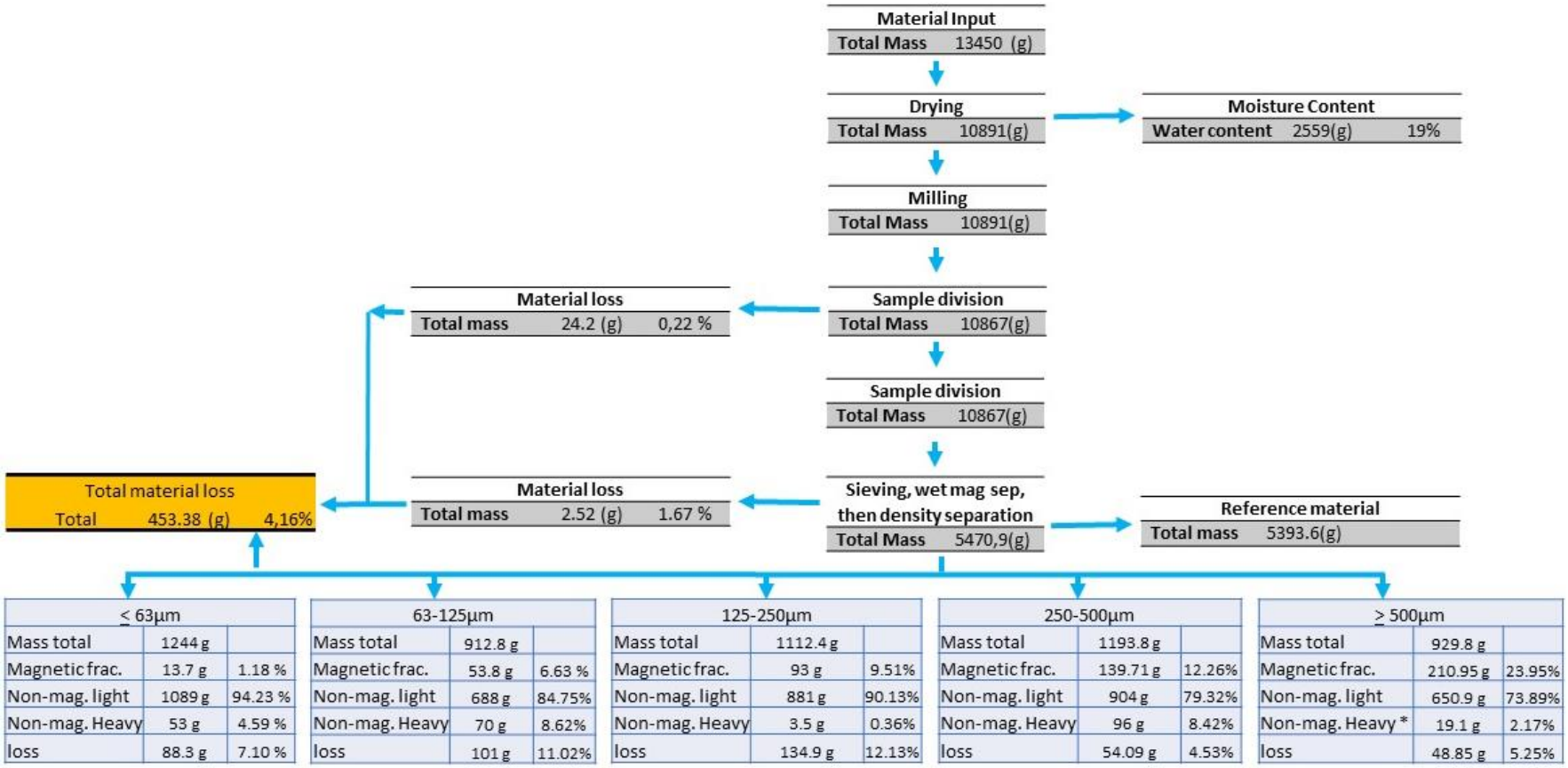

Figure 4.33: Material recovery after all treatment processes for bottom ash of plant C.

(*Improvements have been applied in this fraction, compared to **Figure 4.26**)

The major difference between the bottom ash from plant B and that from plant C is the content of scrap (iron-base material). Bottom ash from plant B contained many scrap materials, which then were removed by hand-sorting. This could be the reason for lower magnetic fraction content in the particle size ≤500µm, compared to bottom ash from plant C, which originally had smaller particle sizes and was directly milled down to a particle size below 500 µm. From **Figure 4.33**, it can be seen that the quantity of magnetic fraction increases with increasing grain size fraction.

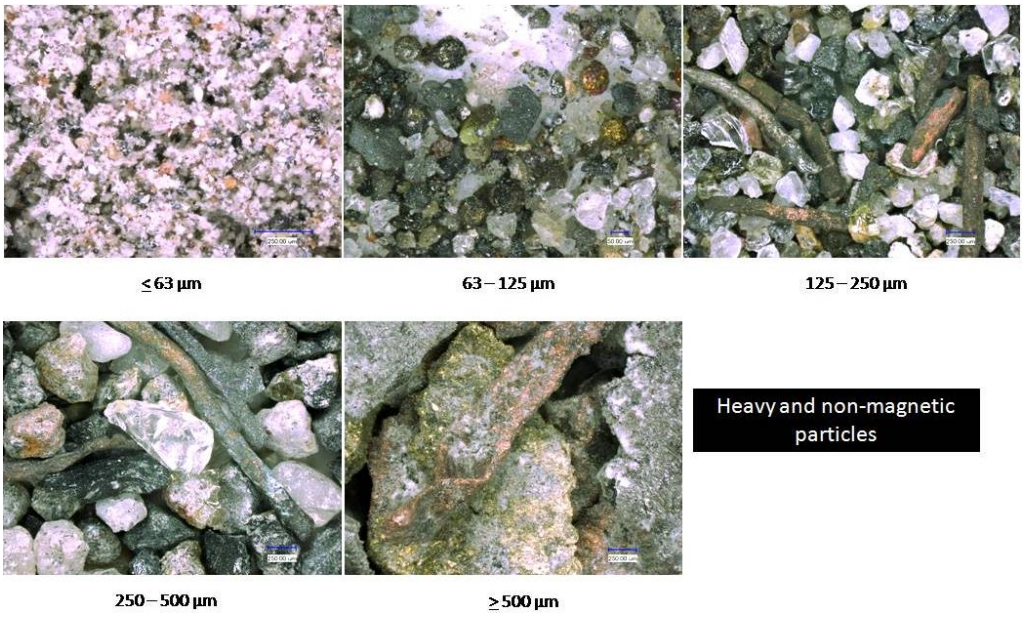

Figure 4.34: The characteristic heavy fraction products from bottom ash plant C observed by *Keyence* digital microscope.

According to Keyence microscope examination, the presence of metallic particles (**Figure 4.34**) could be seen starting from ≥ 63-µm particle grain size. The larger the grain size fractions, the higher the content of metallic particles. However, due to milling, some metallic particles could be fractured and collected in the smaller particle grain size, for example, as shown in particle size 63–125 µm in **Figure 4.34**.

The improvement that was implemented in the bottom ash from plant C was the use of wind separation, especially for particles ≥ 500 µm. Before wind sieving, the particles were re-milled for an additional 2 to 4 minutes. The milling time depended on the quantity of coarse particles previously contained in fraction ≥ 500 µm. The more coarse particles there are, the longer the milling time required.

The bottom ash of plant C contained many coarse particles, so 3 to 4 minutes milling time was applied to flatten the metallic fraction. Due to the longer milling time, the ductile metallic particles became flat and the brittle particles of light minerals such as glass were cracked into smaller pieces. The method for improving metallic fraction recovery contained in grain size fraction ≥ 500 µm is as follows:

- Re-milling process
- Re-sieving into several particle size (≥ 1 mm, 1 – 0.7 mm and ≤ 0.7 mm)
- Density separation with vacuum-process

After the aforementioned process (re-milling, re-sieving, and vacuum process), metallic particles were successfully concentrated and the weight percent of ≥500-µm metallic particles showed a similar tendency as other grain size fractions with heavy non-magnetic particles in the range < 10 wt.%.

The reason for the weight reduction of heavy non-magnetic fraction in particle size ≥ 500 µm was the reduction of glass and other mineral particles that can be further separated by re-milling, re-sieving, and vacuum process. Heavy non-magnetic particles in ≥ 500-µm fraction of bottom ash from plant C contained more coarse particles. That is why re-milling was performed for 3 to 4 minutes in a disc mill machine. Afterwards, this particle was sieved into three different sizes (≥ 1 mm, 1–0.7 mm, and ≤ 0.7 mm). The appearance of heavy non-magnetic particles after re-milling and re-sieving of former ≥500-µm fraction is shown in **Figure 4.35**.

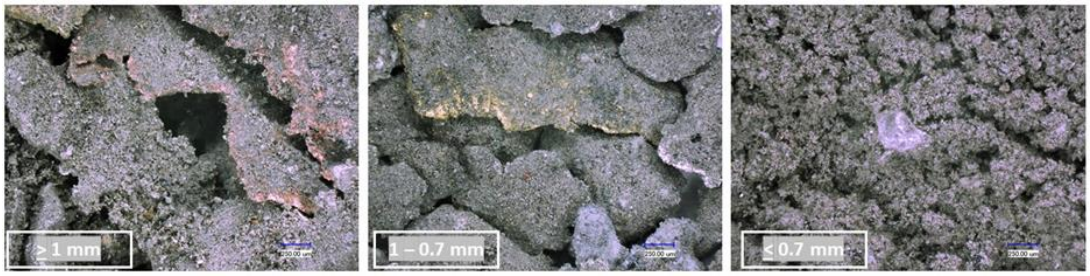

Figure 4.35: The flattened metallic particles of heavy non-magnetic product of ≥ 500µm fraction (bottom ash from incineration plant C) after re-milling and re-sieving.

With re-milling and re-sieving, metallic particles were separated in the larger fractions successfully and the concentrations of glass particles were reduced in these fractions. The metallic particles collected in larger grain size fractions

(starting from ≥ 0.7-mm particle size) consists of metallic copper, brass, and aluminium particles, which are flat because they have a higher ductility compared to brittle particles such as glass and other mineral particles. Glass and other mineral particles were collected in the smaller particle grain size (≤ 0.7 mm). The problem is still mixed flat aluminium particles together with metallic copper and brass. The vacuum process is able to separate light (aluminium) particles (**Figure 4.36.a)** from other heavy non-magnetic particles, as shown in **Figure 4.36.b.**

Figure 4.36.a: The products of light non-magnetic product of ≥ 500µm fraction (bottom ash from incineration plant C) after re-milling, re-sieving, and vacuum process. Most of metallic particle in this product is flattened aluminium-(oxide) particles.

Figure 4.36.b: The products of heavy non-magnetic product of ≥ 500µm fraction (bottom ash from incineration plant C) after re-milling, re-sieving and vacuum process. Most of metallic particle in this product is flattened metallic copper and brass particles.

The re-milling, re-sieving, and vacuum process of ≥500-µm heavy non-magnetic particles results in a concentration of valuable metals such as metallic copper and brass. However, it has to be considered that, after too much milling, it could happen that the edges of the flattened metals, as shown in **Figure 4.36.b,** will break. This could be why metallic particles are still contained in the smaller particle grain size fraction. Therefore, it is necessary to optimize the milling process relation to the metal content at the beginning.

5 Discussion of the results

5.1 An overview of fine particle size WtE bottom ash characteristic

Nowadays, bottom ash is an important material that has the potential to become a continuous source of raw material in the future. The bottom ash composition was originally determined by the material input (feeding waste materials before combustion process) composition. During the incineration process, all compounds were exposed to high temperatures [Bunge **2015**]. The transformation of bottom ash occurs once it is in contact with the extractor. When the bottom ash is leaving the combustion process, it becomes involved in reactions between the components in slag and in water. During the aging process, various conversion processes occur, such as the hydration process, the formation of salts, and others reported in the literature [Beck **2005** and Pfrang **1999**]. The reactions during quenching and the storage-aging process have the main role of determining the major composition of the solid residue. The problem is the release of heavy metals and/or heavy metal compounds afterwards. The constituents of bottom ash distinguished by particle size from coarse to fine particles have been investigated. Chimenos et al. [Chimenos **1999**] have reported that bottom ash is mainly composed of glass, minerals, magnetic metals, unburned organic matter, paramagnetic materials, and metals.

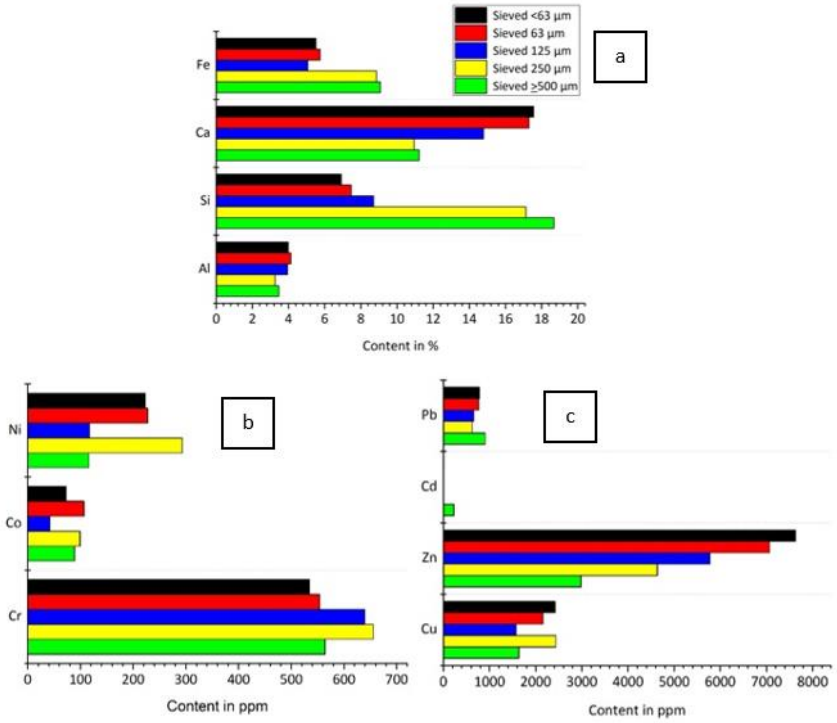

Figure 5.1: The composition of fine particle bottom ash distinguished by particle size different.

The essential elements or compounds contained in bottom ash were compounds of Al, Ca, Si, and Fe, as shown in **Figure 5.1.a**; the distribution of compounds from Al relatively showed no difference in particle size. Fe tends to have higher concentrations in higher particle sizes, while Si and Ca compounds have unique behaviors. Si tended to have lower concentrations on reducing particle size, mainly depending on the concentration of silicon dioxide in the feeding material. During the incineration process, in the case of Si concentration, it seems there was no reaction affecting Si concentration, in contrast with Ca concentration, which was enriched by the smaller particle size of bottom ash. As has also been investigated by Deike et al. [Deike **2012**], during the reaction with water, calcium contained in bottom ash when leaving the combustion process might be forming calcium hydroxide and calcium carbonate due to reaction with water or carbon dioxide, with the following reactions:

$CaO + H_2O \leftrightarrow Ca(OH)_2$ ..... (5.1)

$$\Delta G\ (298\ K) = -57840\ \frac{J}{mol}$$

$$\Delta H\ (298\ K) = \ -65166\ \frac{J}{mol}$$

$CaO + CO_2 \leftrightarrow CaCO_3$ ..... (5.2)

$$\Delta G\ (298\ K) = \ -130938\ \frac{J}{mol}$$

$$\Delta H\ (298\ K) = \ -177697\ \frac{J}{mol}$$

$Ca(OH)_2 + CO_2 \leftrightarrow CaCO_3 + H_2O$ ..... (5.3)

$$\Delta G\ (298\ K) = \ -73118\ \frac{J}{mol}$$

$$\Delta H\ (298\ K) = \ -112531\ \frac{J}{mol}$$

From a previous study [Deike et al. **2012**], the formation of calcium hydroxide could be possible due to the reaction of lime with water, as shown in the equation above. The negative value of the Gibbs standard enthalpy shows that the reaction takes place under standard conditions at room temperature (irreversible reaction). The negative value of the standard reaction enthalpy (at room temperature) shows that this is an exothermic reaction. This reaction takes place already during the aging time [Knorr **1999** and Deike **2012**] in de-slagging process. Free lime (CaO) can also react in the presence of carbon dioxide (CO_2) to form calcium carbonate at room temperature, as described in equation (5.1). And the combination of reaction (5.1) and (5.2) leads to reaction (5.3), which is also an exothermic reaction. This reaction (in addition to various other potential reactions) can be explained by the fact that calcium hydroxide contained in fresh bottom ash regresses in the course of aging [Johnson **1991**].

This reaction mechanism explains the observation c that in bottom ash, in the course of aging [Knorr **1999**], concentrations of calcium carbonate (calcite) were increased. This (and similar kinds of) reaction is why the temperatures in bottom ash increase during aging. It is assumed that the rates of these thermodynamic reactions at standard conditions are very much determined by the kinetic conditions.

It is therefore understandable that the smaller particle size has more surface contact with water or carbon dioxide, so that more calcium hydroxide and calcium carbonate are produced in the smaller particle size than in larger particle size. The reason for calcium enrichment in the lower particle size fraction could be explained by this mechanism. Furthermore, when bottom ash comes out of the combustion process, the weathering of bottom ash has occurred. According to some research [Meima **1997** and Gouman **2007**], there are three major steps of weathering. Each stage has a specific characteristic pH value (**Figure 5.2**) that is mainly controlled by the calcium minerals and the partial pressure of CO_2. These stages are [Meima **1997**]:

- Unweathered bottom ash

  In this stage, the reaction takes place when dry bottom ash first comes into contact with water in the quench tank. The reactions involved in this process are hydrolysis of some oxides and dissolution and precipitation of hydroxides and salts. An increase in pH value with resulting strong alkaline condition (pH of 12) is the final result.

- Quenched/non-carbonated bottom ash

  In the next stage, pH value is decreased to 10–10.5 by the formation of ettringite (the formation of ettringite can be seen in equation (2.4) in subsection 2.4.3), gibbsite, and gypsum; when three of these minerals coexist, there is no degree of freedom left and the pH is stable at a value of 10. Due to further hydrolysis, some secondary minerals begin to precipitate, such as amorphous Fe/Al-(hydr)oxide, hydrous aluminosilicates, etc.

- Carbonated bottom ash

  In the further stage, the pH value is decreased to 8–8.5 by absorption of CO_2 and precipitation of $CaCO_3$ or calcite.

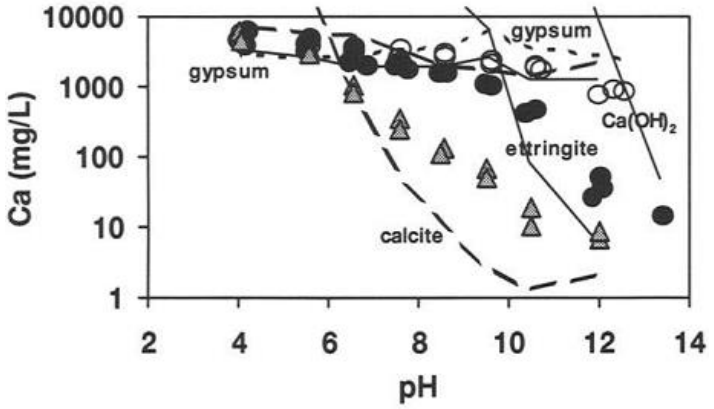

Figure 5.2: The illustration of the change Ca-leaching as the weathering continue or the pH dependency [Meima **1997**].

As investigated by Jeannet A. Meima et al. **1997**, bottom ash is composed of metastable solids (**Figure 5.2**), when weathering takes place, which also depends on the pH value; the concentration of calcium was the main determinant of the pH value, under current conditions. Once it dissolves the calcium compound to $Ca(OH)_2$, this will turn the bottom ash pH strongly alkaline and cause a further reaction.

Table 5.1: The effects of carbonation and weathering on some elements solubility, and its compound forming mechanism [Meima **1997**].

Element	Unweathered bottom ash , pH > 12		Quenched/non-carbonated bottom ash, pH 10 - 10,5		Carbonated bottom ash, pH 8 - 8,5	
	Controlling mechanism	Identified species	Controlling mechanism	Identified species	Controlling mechanism	Identified species
Ca, SO_4, CO_3	Solubility-control by portlandite and gypsum	Anhydrite, calcite, portlandite, complex (Ca) silicate	Solubility-control by ettringite and gypsum/anhydrite; solubility control by calcite	Ettringite, anhydrite, gypsum, calcite, CaO, whitlockite, $CaHPO_4$, complex (Ca) silicate	Solubility-control by calcite and gypsum	Anhydrite, gypsum and calcite
Al	Solubility-control by hydrous Al-silicate	Complex silicates	Solubility-control by gibbsite or amorphous $Al(OH)_3$	Gibbsite, corrundum, AlO, elemental/alloy, complex silicate, $MgAl_2O_4$	Solubility-control by gibbsite or amorphous $Al(OH)_3$	Amorphous $Al(OH)_3$
Fe	--	Magnetite, hematite, pseudobrookite	Solubility-control by ferrihydrate	Hematite, wustite, maghemite, goethite, pyrite, pseudobrookite, magnetite, ulvospinel, hercynite, jacobsite, chromite	Solubility-control by ferrihydrate	Magnetite, hematite, wustite, maghemite
Mg	Solubility-control by brucite	Complex silicates	Solubility-control by brucite or magnesite	Magnesite, dolomite, $MgSO_4.2H_2O$, sepiolite, complex silicate, $MgAl_2O_4$,	Solubility-control by Mg-calcite, sepiolite or dolomite	--
Si	Solubility-control by hydrous Al-silicate	Quartz, glasses, complex silicates	Solubility-control by walrakite or amorphous SiO_2	Quartz, glasses, hydrous Al-silicate, complex silicate	Solubility-control by illite or amorphous SiO_2	Hydrous Al-silicate, quartz, illite, complex silicate
Na, K, Cl		Complex-(Na/K) silicate	--	Halite, sylvite, complex-(Na/K) silicates		--
Mo	Solubility-control by powellite	--	Solubility-control by powellite	$CaMoO_4$	Sorption to ferrihydrate	$CaMoO_4$, Pb/Mo rich particle
Cu	--	Metallic/alloy	Organic complexation and solubility-control by tenorite or $Cu(OH)_2$	Metallic/alloy, CuCl, $NaCuPO_4$, complex silicate	Organic complexation and sorption to amorphous $Al(OH)_3$	Cu/O-phases (e.g. Cuprite, tenorite), metallic alloy, complex silicate, Cu/Ca/O-, Cu/Fe/O-, Cu/Al/O-, Cu/Al/O/S/Ca-, Cu/S-phases, sorbed to neoformed clay
Pb	--	Metallic/alloy	Solubility-control by cerrusite or $Pb(OH)_2$, or sorption control	Complex silicate, PbO	Sorption control or solubility-control by Chloropyromorphite	Metallic alloy, complex silicate, Pb/O-, Pb/Ca/O-, Pb/Fe/O-, Pb/Al/O-phases, sorbed to neoformed clay
Zn	Solubility control by zincite	Metallic/alloy	Solubility-control by zincite or $Zn(OH)_2$, or $ZnSiO_3$; sorption control	Zincite, $ZnSO_4$, $ZnCl_2$, elemental Zn, franklinite	Sorption control or solubility-control by zincite	Zn/O-phases (e.g. zincite), metallic alloy, complex silicate, Zn/Ca/O-, Zn/Fe/O-, Zn/Al/O-, Zn/Al/O/S-phases, sorbed to neoformed clay
Cd	Solubility-control by octavite or $Cd(OH)_2$	--	Solubility-control by octavite or sorption to calcite	--	Sorption control	--
Other	--	--	Possible solubility-controlling minerals for Mn, Ba, V; MnO(OH); barite; $Pb_2V_2O_7$	Rutile, barite, graphitic carbon, taenite, (species containing Sb, Sr, Ni, Cr, As, Ag, Rb, Nd, Cr-oxides	--	Ni sorbed to neoformed clay

5.1.1. The distribution of valuable elements after milling, sieving and magnetic separation

As reported by Chimenos et al. **1999**, the distribution of valuable elements as described in **Figure 5.3** is mainly concentrated on particle size 1–3mm and the main elements contained in this fraction are lead, zinc, and copper. The main composition of bottom ash might differ from one incineration plant to another, and from one country to another.

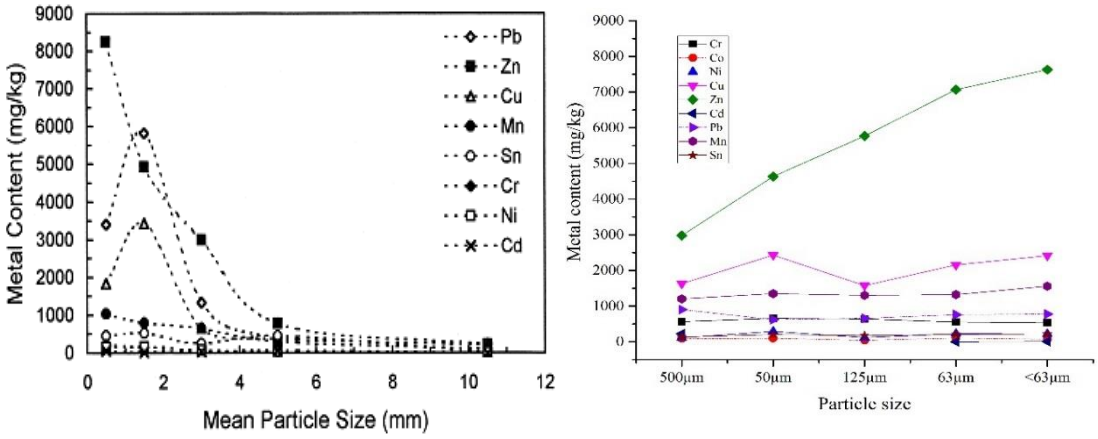

Figure 5.3: The comparison of lead, zinc, copper, manganese, tin, chromium, nickel and cadmium distribution in bottom ash. The result from literature (left) and from this study (right).

The results of this study show that concentrations of lead, zinc, copper, manganese, tin, chromium, nickel, and cadmium are lower than those seen by Chimenos et al. [Chimenos **1999**], whose results, displayed in **Figure 5.3,** show an an increase of zinc with a decrease of the particle size from 5 mm down to below 1 mm. The results of the present study (**Figure 5.3**), however, show that it happens especially in the grain size fraction from 500 µm down to < 63 µm.

The enrichment of zinc (at a boiling point of 907 °C) in the small grain size fraction can most likely be explained by its low evaporation temperature. During the combustion process (around 800–1000 °C), zinc is transformed into a gas, leaves the combustion chamber, and reacts in this way with oxygen. In WtE plants, most of the zinc is concentrated as zinc oxide in the flue gas cleaning system, but it could also be possible that a certain quantity of zinc oxide particles are deposited in the fine particle size fraction of the bottom ash. In this study, the finest particle grain size has the highest amount of zinc, with zinc content in the range of

8000–9000 ppm. Copper is mainly contained in the heavy non-magnetic fraction, but it is also contained in the magnetic fraction because it adheres to the magnetic fractions (**Figure 4.32**).

5.2 The recovery of copper and other valuable materials from fine fraction bottom ash

The enrichment of copper and other elements after density separation with sluice-box and gold-pan experiment is shown in **Figure 5.4.** The sluice-box process conducted in this research shows that valuable metals are mainly collected in the upper zone of the sluice box. **Figure 5.3** shows that the concentration effect of different metals in the sluice-box and subsequent gold-pan process depends on the grain size fraction.

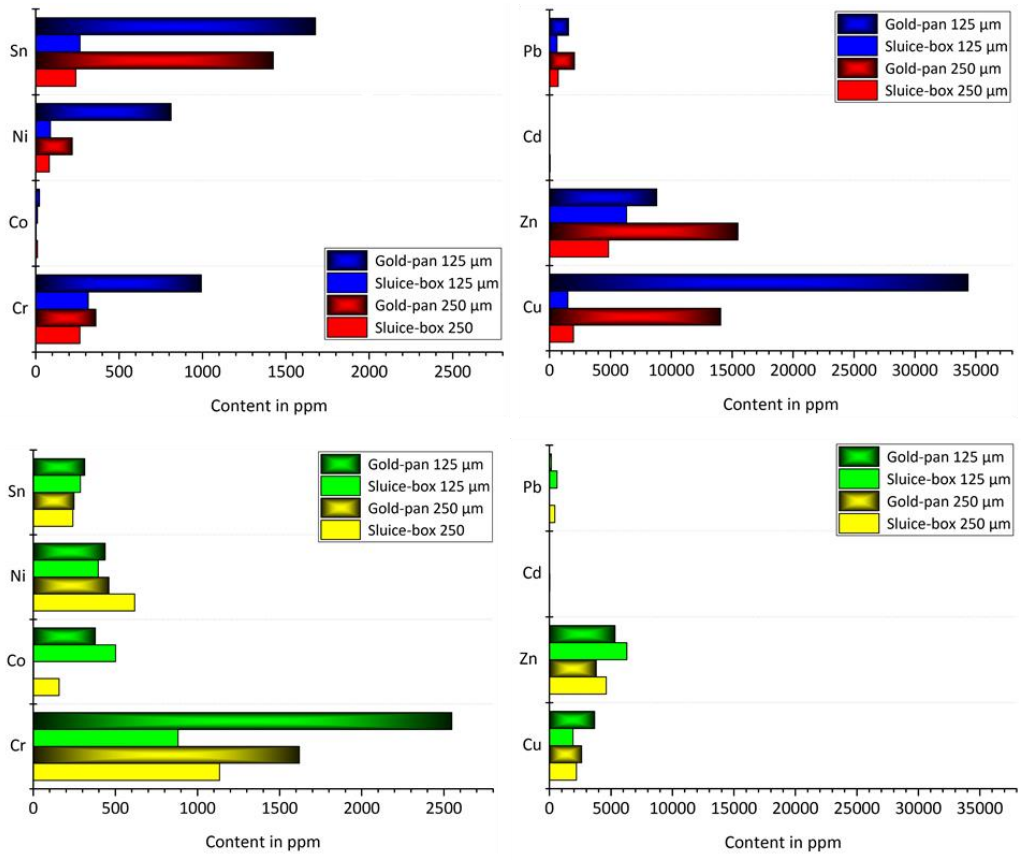

Figure 5.4: The comparison of sieved, sluice-box and gold-pan product, distinguished by particle size and magnetic properties different.

As seen in **Figure 5.4**, the concentrations of Cu and Sn in the non-magnetic fraction were increased after sluice-box and gold-pan process. With the

exception of zinc, it can be seen that the metal concentrations after gold-pan process in the non-magnetic fraction were higher in the grain size fraction 125–250 μm in comparison to 250–500 μm.

Typical of non-magnetic fractions after gold-pan process are shown in **Figures 4.14** and **4.15**. This fraction contains metallic copper in the form of wire mixed with silicon dioxide and calcium-silicon-aluminium compounds. The concentration of copper, which was about 1500–2500 ppm in the original material, could be enriched up to 14,000–34,000 ppm (**Figure 5.4**) after gold-pan process.

5.3 The characteristic of light fraction (mineral fraction) after gold-pan process

In contrast to particles in the heavy non-magnetic fractions, particles in light non-magnetic fractions mainly consist of calcium oxide, silicon dioxide, and aluminium oxide (**Figures 4.24** and **4.28**). The very first separation of these light particles was during separation with sluice-box process. Sluice-box process effectively removed the dirt and the light particles at the same time.

In some samples, zinc oxide particles (**Figure 4.25**) were detected together with silicon dioxide. As reported by Jeannet A. Meima et al. [Meima **1997**], the behavior of zinc depends on the pH value (**Figure 5.5**). At a certain pH value, solid zinc is dissolved in the bottom ash leachate. When the pH value changes, it is possible that zinc precipitates once again, so that the existence of some zinc compounds can be the result of dissolution-precipitation-absorption reactions. Aluminosilicate has the ability to adsorb the zinc from leachate to form corresponding compounds. Other potential sorbent minerals in bottom ash are amorphous or crystalline Fe and Al-(hydro)-oxides, hydrous aluminosilicates, and calcite [Meima **1997**]. So, this mechanism might occur.

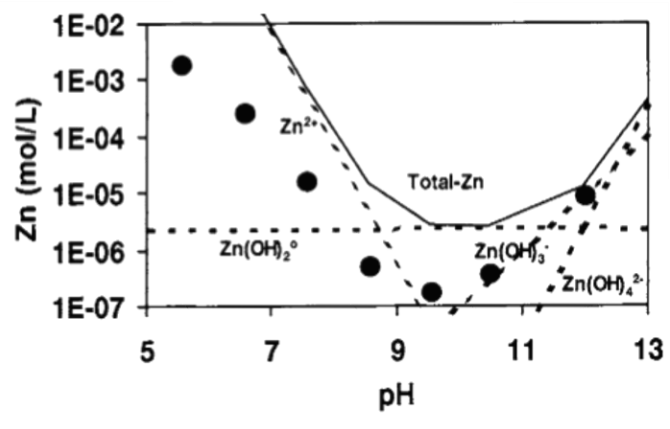

Figure 5.5: The effect of inorganic complexation on the solubility of zinc [Meima **1997**].

The main goal of this study was to examine whether the entire removal of iron and heavy metals from bottom ash is possible with crushing, milling, sieving, and wet magnetic separation of bottom ash, in combination with running a sluice-box, gold-pan, and vacuum process. It is possible that a high amount of fine-milled minerals will be produced. The metal recovery from bottom ash will be economical [Deike **2015**] only if the residual mineral material can be used as raw material in another process. Therefore, it is necessary to know whether mineral material of such purity can be produced that it can be used in the cement industry as raw material. The initial aluminium, silicon, and calcium content of bottom ash is shown in **Figure 5.6 (left),** before wet magnetic separation and subsequent operations.

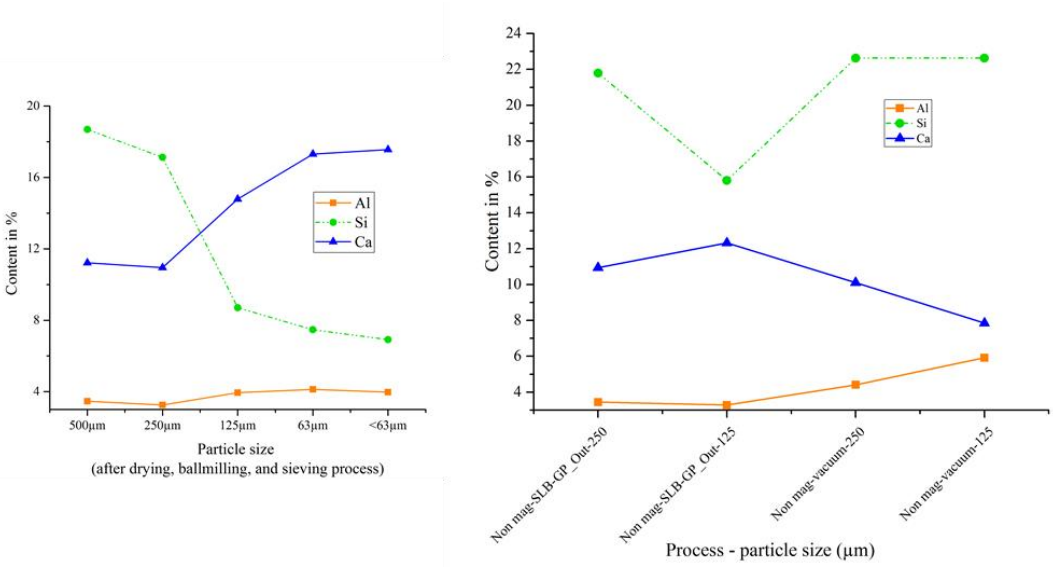

Figure 5.6: The major compound of bottom ash which has similar cement composition. The comparison of Al, Si and Ca concentration before and after separation.

As reported by Yinming et al. [Li **2016**], the reusability of bottom ash in cement production depends mainly on the contents of volatile compounds such as alkali salts, chlorine, and sulfates, which are abundant in bottom ash. These compounds, especially chlorine, contribute to corrosion in the cement kiln.

Initially, after the sieving process, sulphur and chlorine content in smaller grain size fractions is higher than in larger grain size fractions (**Figure 4.20**). In addition, the same effect is seen for calcium (**Figure 4.3)**. The element mapping in **Figures 4.7** to **4.9** shows that sulphur mainly exists together with calcium, which perhaps could explain why the content of both elements in the smaller grain size fractions is higher. Due to washing in sluice-box and gold-pan process, sulphur and chlorine content was reduced drastically, as shown in **Figure 4.20**. This effect is caused mainly by the dissolution of water-soluble salts of chloride or sulfates such as $CaCl_2$ and Na_2SO_4, etc. [Bunge **2015**]. The remaining sulphur and chlorine, which is not easily washed out, can perhaps be attributed to compounds like calcium chloride hydroxide (Ca(OH)Cl), as reported by Sheng Chen [Chen **2012**].

In order to reuse bottom ash in the cement industry, the heavy metal content should be reduced down to concentrations [Li **2016**] given in **Table 5.2**.

Table 5.2: The limiting of maximum dosage of heavy metals in the raw material for cement production [Li **2016**].

Heavy metal	unit	Max dosage of heavy metal
Hg		0.23
Tl+Cd+Pb+15×As	mg/kg-cli	230
Be+Cr+10×Sn+50×Sb+Cu+Mn+Ni+V		1150

As shown in **Figure 4.21**, the existing heavy metal content in the light non-magnetic fractions is too high and, therefore, additional work is needed to improve this situation.

5.4 The improvement to recover metallic fraction

Metallic copper was found mostly in the particle size fraction ≥500 µm. As mentioned in chapter 4.7, a greater quantity of metals can be collected in the

particle size ≥500 µm with an optimized milling process. The results of this study show that a longer milling time flattens the metallic particles, which can easily be separated by a sieving process. The appropriate improvement is re-milling for 2 minutes and afterwards sieving (0.7 mm). All particles larger than 0.7 mm are metallic particles such as copper, brass, and aluminium and very often alloys of these elements (**Figure 5.7**). As seen in **Figures 5.8** and **5.9**, with smaller mesh sizes the quantity of metallic particles is reduced and the quantity of mineral particles is increased.

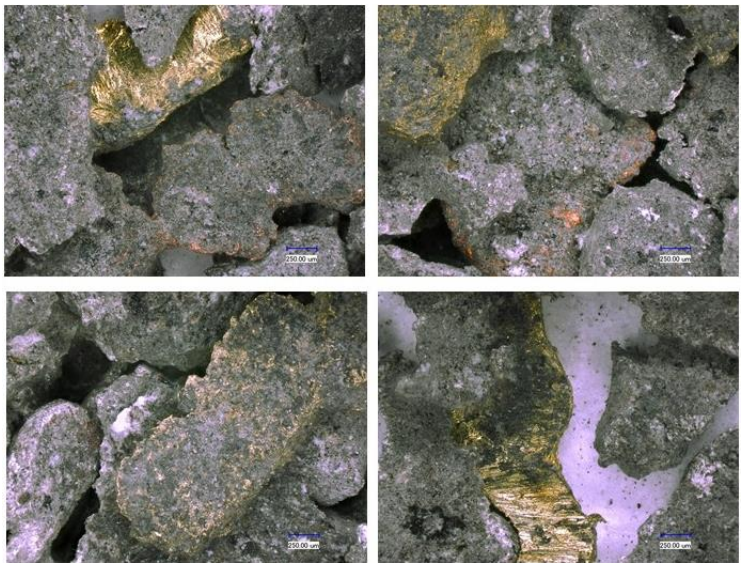

Figure 5.7: Collected particles in the particle size ≥ 0.7 mm, mostly consisted of flattened metallic particles copper, brass and aluminium.

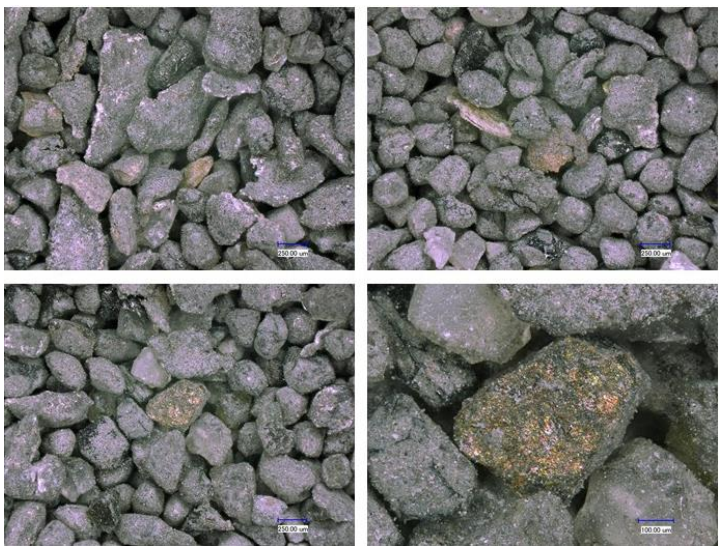

Figure 5.8: Collected particles in the particle size 0.25 – 0.5 mm. It consists of fewer metallic particles than the larger particle size, it has a lot of glass particles.

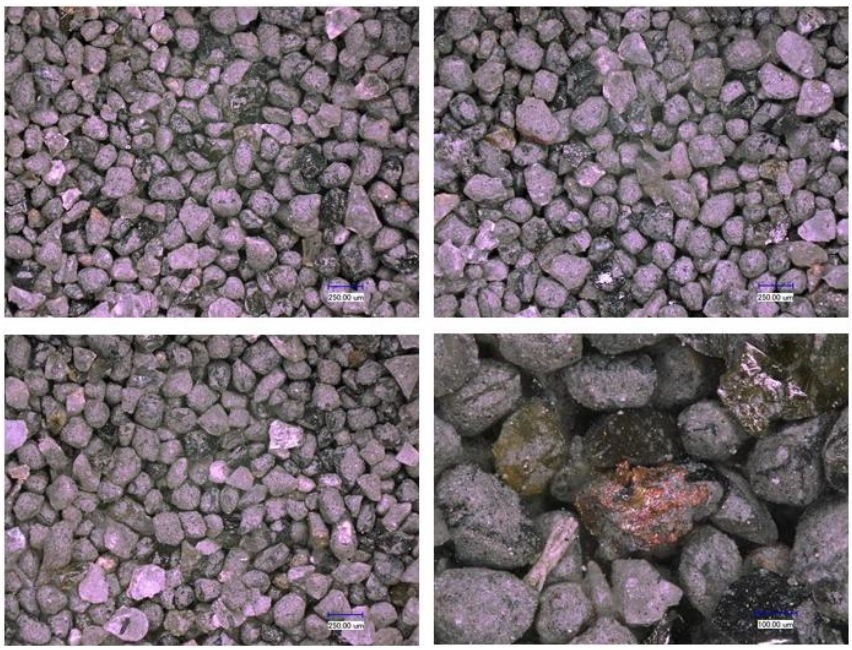

Figure 5.9: Collected particles in the particle size 0.125 – 0.25 mm. It was dominated by glass particles, the smaller particle size has the less metallic fractions.

Because of the heterogeneity of bottom ash, even when milled down to ≤ 0.25-mm size, the production of clean mineral fractions is relatively hard to achieve, because it must be expected that some small metal particles still adhere to larger particles, as shown in **Figure 5.10**.

Figure 5.10: The appearance of bottom ash particle which is constructed by heterogenous constituent.

But it has to be considered, the longer the milling time, the higher the risk of fine metallic particles in the finest particle grain size fraction. Milling times of more than 2 minutes will produce more metallic fractions in the finer particle grain size, because the particles usually show a tendency to crack at the particle edges (**Figure 5.11**) and fractured very small particles are collected in the finer particle size fraction.

Figure 5.11: The flattened metallic particles with fractured at the edge showed in the yellow circle.

As long as the milling parameters are optimal, the content of metallic fraction in the finest particle size can be reduced. However, there is still the possibility that a few metallic particles have been broken down and are collected in the smaller particle grain size. That is why density separation is also needed to separate the rest of the metallic particles.

5.5 Modified approach to recover copper and other heavy metals

A modified approach to recovering metallic fractions from bottom ash (**Figure 5.12**) has been developed, to make the process easier and more efficient.

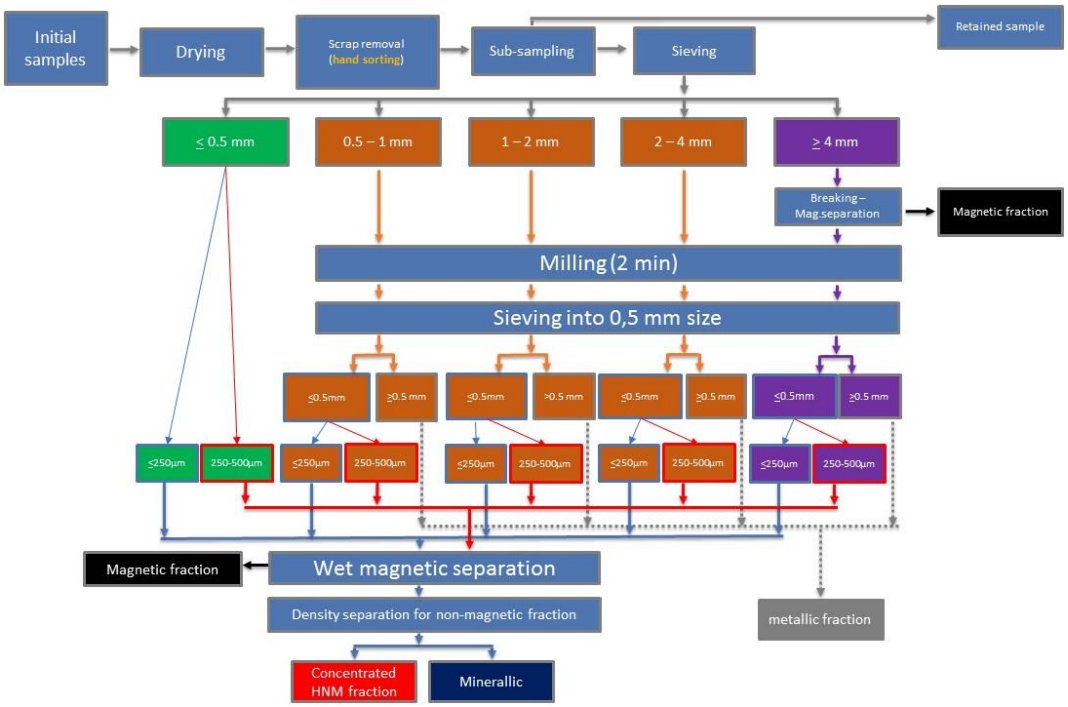

Figure 5.12: Flowchart diagram to recover metallic fraction contained in bottom ash.

The basis of the new approach is a rough screening after scrap removal and sub-sampling with the mesh sizes shown in the second row of **Figure 5.12.** The distribution of the grain size fractions is shown in **Figure 5.13**.

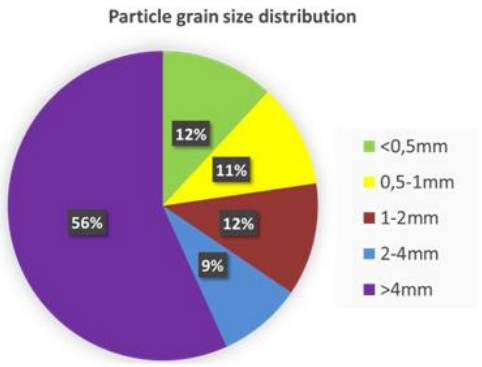

Figure 5.13: The particle grain size distribution of bottom ash of plant B.

After sieving, each grain size fraction is separately milled 2 min and subsequently sieved with a mesh size of 0.5 mm. Particles in the grain size fraction > 0.5 mm are mainly flattened metals, which are collected and named a metallic fraction. Particles of the grain size fraction < 0.5 mm are treated in the modified sluice-box process, where wet magnetic separation takes place. The product of this step is named a magnetic fraction. After sluice-box process, the gold-pan and

vacuum processes are the final density separation processes. The products are named at the end HNM (heavy non-magnetic) fraction and mineral fraction.

The metal fraction can be separated from the mineral fraction by using a proper milling process (approx. 2 min, *Retsch* disc mill), which results in flattened metallic particles that can easily be collected by sieving process. If the milling time is too long, the risk of very fine metal particles in the fine grain size fractions increases; and if the milling time is too short, more glass particles are collected together with the metallic particles. In **Figure 5.14**, particles from the metal fraction are shown.

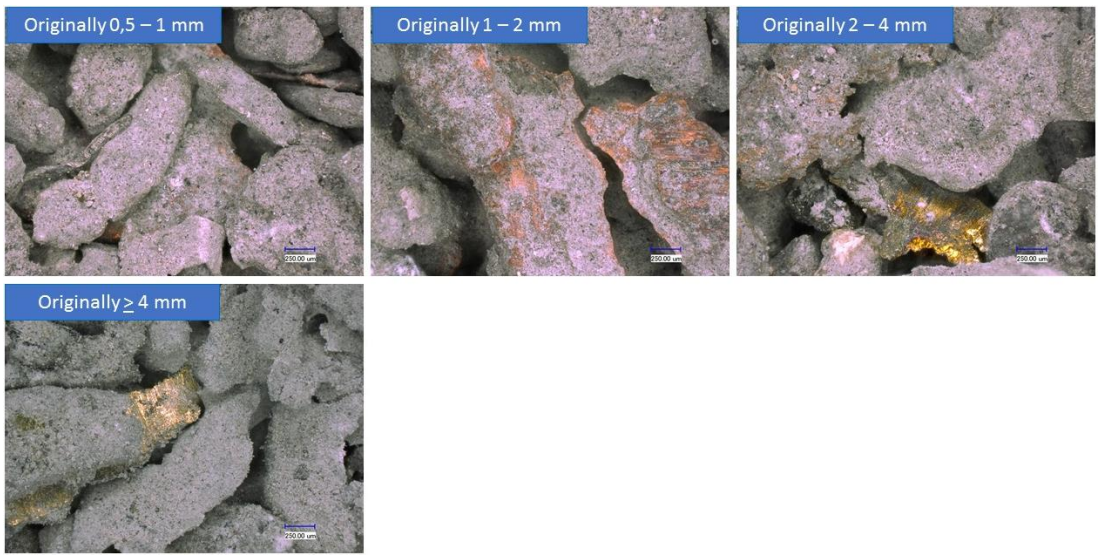

Figure 5.14: The metallic fraction contained in bottom ash of plant B.

In **Figure 5.15**, it is shown that, in the heavy non-magnetic fraction, the metal content is lower in the smaller grain size fraction (< 0.25 mm (a)) and higher in the larger grain size fraction (0.25–0.5 mm (b)).

Figure 5.16 shows that the smaller grain size fraction (< 0.25 mm (a)) of the light non-magnetic fraction (mineral fraction) might contain some very small metallic particles that are adhering to the fine mineral particles. The mineral particles in the larger grain size fraction (0.25–0.5 mm (b)) look very clean, however, because the particles are not so strongly agglomerated as in the smaller grain size fraction.

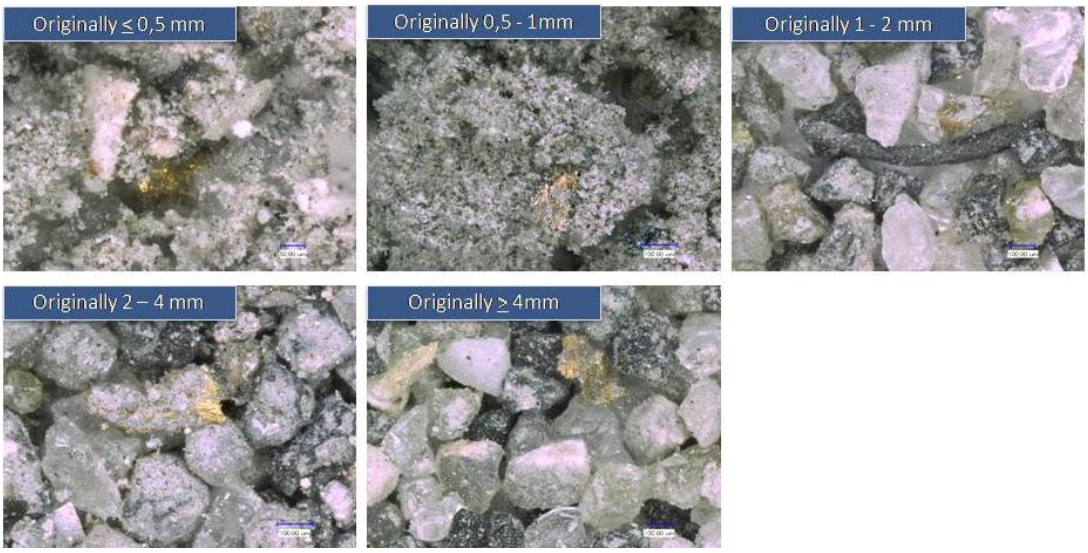

(a). Particle grain size ≤ 0.25 mm.

(b). Particle grain size 0.25 – 0.5 mm.

Figure 5.15: Heavy non-magnetic products contained in bottom ash of plant B. After density separation, the fracture of metallic particle and other form of metallic particle (such as wire) are concentrated in HNM product.

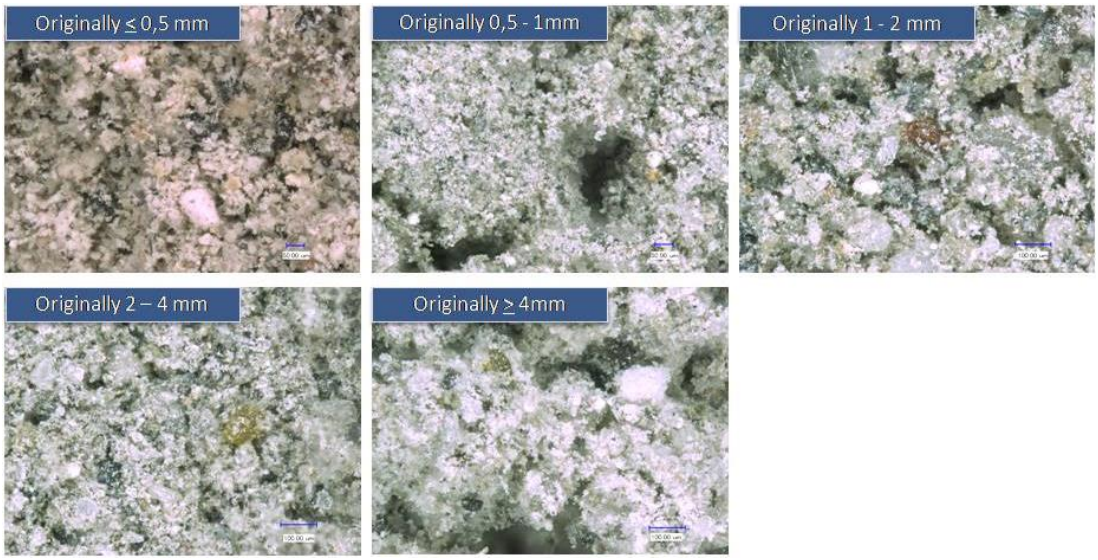

(a). Particle grain size ≤ 0.25 mm

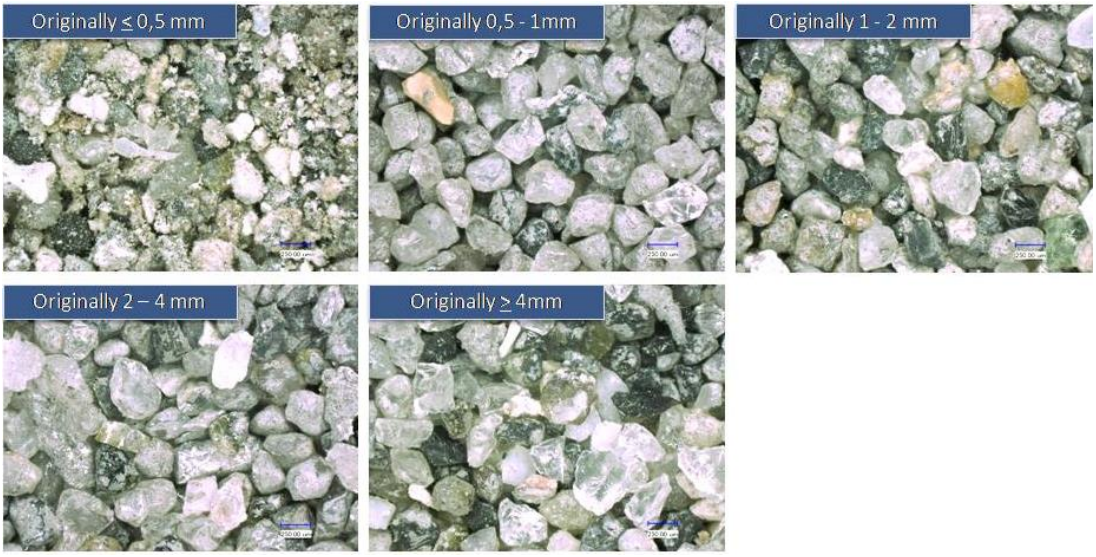

(b). Particle grain size 0.25 – 0.5 mm

Figure 5.16: The light non-magnetic fraction (mineral fraction) contained in bottom ash of plant B. After density separation, collected minerallic particles have contained many glassy particles and some aluminium particles, while other particles are stone or sand-like particles.

These results show that an optimized milling to flatten the metallic particles could be a really interesting way to increase the efficiency of metal recovery form bottom ash. In addition, it could be interesting because flat non-ferrous metals may be easier to separate with an eddy-current separator. However, the optimum milling parameter and the suitable sieving number to produce this flattened metallic particle could differ from one bottom ash source to another.

6 Conclusion

Solid residues called bottom ash, produced from Waste-to-Energy (WtE) plants, have increased every year. In Germany, it reaches over than 5 million tonnes per year nowadays. The use of bottom ash in public road construction depending on different laws in different Germany federal states can be difficult. Heavy metals can leach out over the time and endanger the environment and pollute the water ground.

The contribution of this study is the treatment of fine grain size bottom ash (< 2 mm) to entirely recover the metals from bottom ash and produce a clean mineral fraction that can be used in the cement industry as raw material.

Because the metal particles are glued together with the slag, in this approach, principles of ore processing are used. The bottom ash is milled and classified by sieving technology. Because knowledge about the structure of metal particles in bottom ash is limited, initially the particles are characterized by optical microscope, then by scanning electron microscope and energy dispersive spectroscopy.

In the further course of this study, a semi-continuous wet magnetic separation technology was developed on the basis of a modified sluice-box process. With this technology, a proper separation of magnetic particles is possible. From the particle characterization, it is known that no pure iron particles exist in fine bottom ash fractions. The strong magnetic effect is accounted for by the iron oxide magnetite. This study has shown that elements such as chromium, nickel, and cobalt can be separated from bottom ash with magnetic separation of magnetite, because magnetite acts as a collector for these elements.

In this study, a process was developed to flatten non-ferrous metal particles with an optimized milling process. Afterwards, it is possible to separate the metal particles easily with a sieving process. After this step, the mixture of heavy non-magnetic and light non-magnetic fractions is separated via density separation.

For this separation step, a gold-pan and vacuum process is used. With washing of bottom ash by sluice-box and gold-pan processes, it was possible to drastically reduce the sulphur and chlorine content in the residual mineral fraction of the bottom ash.

The combination of wet magnetic separation in the sluice-box process and an additional gold-pan process together with a vacuum process clearly shows a promising result for waste treatment of bottom ash in the context of recovery of metallic fraction. With these processes, it is possible to separate and concentrate very fine metallic particles, such as copper, lead, and tin, from bottom ash, which are normally too small for eddy-current separators. However, unwanted materials such as silicon dioxide (glass particles) are still collected also, together with the valuable materials in a too-high range, so additional work is needed.

After the liberation of metal particles from bottom ash by the process developed in this study, it is necessary that the residual mineral fraction be so clean that it can be used as raw material in the cement industry. Improvements in the quality of the mineral fraction have been achieved, but the cleaning process needs further optimization. But the results from his study show that the chemical analysis of these very fine and heterogeneous fractions with sometimes large metal particles inside, needs special attention. Very often, normal XRF analyses are unsatisfactory. In this field, much work is needed in the future.

The results of this study show clearly that copper in bottom ash exists mainly as metal. The results of this study show that it is not impossible to get copper out of bottom ash by a cheap and easy process. Further work is needed for optimization, but it makes perfect sense to do this, because the copper content of bottom ash is as high as that in the poor natural copper ores that are mined today. But copper in bottom ash has the advantage, shown in this study, that this copper is already a metal, so that additional metallurgical work to separate copper from oxygen and sulphur as is required in processing of natural ores, is not necessary in processing copper from bottom ash.

7 References

[**Born 1997**] Born, J. G. P.; Veelenturf, R. A. L.: "MSWI residues in the Netherlands: putting policy into practice", waste materials in construction: Putting theory into practice, pp841-850. Elsevier Science BV, 1997.

[**Bartl 2012**] Bartl, A.: Barriers and limits for recycling and moving towards "Zero Waste", 2012.

[**Beck 2005**] Beck, R.; Kröger, W.: Bayerische Landesamt für Umweltschutz, 2005.

[**Bunge 2015**] Bunge, R.: Recovery of metals from waste incinerator bottom ash. Rapperswil: Institut für Umwelt und Verfahrenstechnik UMTEC, 2015.

[**Cimpan 2013**] Cimpan, C.; Wenzel, H.: Energy implications of mechanical and mechanical–biological treatment compared to direct waste-to-energy. Waste Management, 2013; 33:1648–58.

[**Wiles 1996**] Willes, C. C.: Municipal solid waste combustion ash: state-of-the-knowledge. J Hazard Mater, 1996; 47: 325–44.

[**CEWEP 2013**] CEWEP (Confederation of European Waste-to-Energy Plants): Data &info: Graph on European waste management 2013. Retrieved from CEWEP (Confederation of European Waste-to-Energy Plants), 2013 Web site: http://cewep.eu/information/data/graphs/m_1415.

[**CEWEP 2016**] http://www.cewep.eu/news/m_1485.

[**Chandler 1997**] Chandler, A.J. et. al.: Municipal Solid Waste Incinerator Residues. The international ash working group. 1997. ISBN: 0-444-82563-0

[**Chimenos 1999**] Chimenos, J.M.; Segarra, M.; Fernández, M.A.; Espiell, F.: Characterization of the bottom ash in municipal solid waste incinerator, 1999, Journal of Hazardous Materials. 64 (1999), pp. 211 – 222.

[**Chen 2012**] Chen, S.; Wei; Chang, F. C.; Shen, Y. H.; Tsai, M. S.; Ko, C. H.: Removal of chloride from MSWI fly ash. Journal of Hazardous Materials 237 – 238 (2012) 116 – 120, 2012.

[**Deike 2012**] https://www.itad.de/information/studien/20130110DEIKEHMVARecyclingpotentialAbschlussbericht.pdf.

[**Deike 2013**] Deike, R.; Ebert, Schubert, D.; Ulum, R.; D. Warnecke, R.; Vogell, M.: Verhalten von Metallen in MV-Schlacken unter Hochtemperatur-bedingungen und die Folgen für ihre Rückgewinnung (Behavior of metals in bottom ash at high temperature conditions and effects on recycling processes) 12. VDI Fachkonferenz: Feuerung und Kessel –Beläge und Korrosion- in Großfeuerungsanlagen, Köln, 12.06.2013.

[**Deike 2013**] Deike, R.; Ebert, Schubert, D.; Ulum, R.; D. Warnecke, R.; Vogell, M.: Metalle in HMV-Schlacke - Darstellung aktueller Abtrenngrade und Potenziale für ein wirtschaftliches und nachhaltiges Urban Mining (metals in bottom ash a potential for an economic and sustainable urban mining) 16. ITAD Mitgliederversammlung Düsseldorf, 20.06.2013 https://www.itad.de/information/studien/16-itad-mitgliederversammlung-1

[**Deike 2013**] Deike, R.; Ebert, Schubert, D.; Ulum, R.; D. Warnecke, R.; Vogell, M.: Recyclingpotenziale von Metallen bei Rückständen aus der Abfallverbrennung (Recycling potentials of metals from bottom ash of waste to energy plants) Berliner Schlackenkonferenz, Berlin , 23.09.2013.

[**Deike 2014**] Deike, R.; Ebert, D.; Schubert, D.; Ulum, R.; Warnecke, R.; M.Vogel: (Characteristics of metals in the fine fraction of bottom ash & how can metal recycling be profitable in volatile global raw materials markets) Int. VDI-Workshop. Recovery of metals and minerals from bottom ash. Amsterdam, 21.05.2014.

[**Deike 2014**] Deike, R.; Ebert, D.; Schubert, D.; Ulum, R.; Warnecke, R.; Vogell, M.: Die Rückgewinnung von Metallen aus Müllverbrennungschlacken (Recovery of metals from bottom ash) WissensNacht Ruhr, Duisburg, 02.10.2014.

[**Deike 2015**] Deike, R.; Ulum, R.; Schubert, D.; Foppe, M.: University Duisburg - Essen, Duisburg Gellermann, C.; Lutz, S.: Fraunhofer Institute for Silicate Research, Würzburg: Mining the Technosphere “Drivers and Barriers, Challenges and Opportunities", 01-02.10.2015, Wien.

[**Deike 2015**] Deike, R.: Die Bedeutung energieintensiver metallurgischer Unternehmen für ein effizientes und nachhaltiges Recycling von Metallen: WFZ ruhr Workshop Hochwertiges Recycling verspricht wertvolle Sekundärrohstoffe: Dortmund, 04.11.2015.

[**Deike 2016**] Deike, R.: Berliner Recycling und Rohstoffkonferenz, Berlin, 07/08.2016.

[**EEA 2013**] https://www.eea.europa.eu/data-and-maps/daviz/trend-in-the-amount-of#tab-chart_1

[**Esser 1992**] Esser, R.: Thermodynamische Aspekte der Abfallverwertung. Abfallwirtschaftsjournal 4 (3), 227–238 (1992).

[**Ferreira 2002**] Ferreira, C.; Ribeiro, A.B.; Ottosen. L.M.: Study of different assisting agents for the removal of heavy metals from MSW fly ashes. In Waste Management and the Environment; Elsevier: Cadiz, Spain, 2002.

[**Goorhuis 2014**] Goorhuis, M.: Developments in collection of municipal solid waste. Handbook of recycling. 2014, pp. 407 – 417. http://dx.doi.org/10.1016/B978-0-12-396459-5.00026-X

[**Gouman 2007**] Gouman, J.J.J.M.; Senden, G.J.; van der Sloot, H.A.: Waste materials in construction putting theory into practice, 2007. ISBN 0-444-82771-4.

[**Gleis 2016**] Gleis, M.: European Activities for Treatment and Recovery of MSWI solid residues. VDI Wissensforum 2016. Düsseldorf 11-12 Oct 2016.

[**Lam 2010**] Lam, C. H. K.; Ip, A.W.M.; Barford, J. P.; McKay, G.: Use of incineration MSW ash: A Review. Sustainability 2010, 2, 1943-1968; doi:10.3390/su2071943.

[**Hjelmar 2009**] Hjelmar, O.; Wahlstrom, M.; Andersson, T.: Treatment methods for waste to be landfilled.Nordic Council of Ministers, 2009. Pp. 79-102.

[**Johnson 1991**] Johnson, A.; Lichtensteiger, T.: in EAWAG Jahresbericht, Dübendorf, Schweiz, 1991.

[**Klein 2002**] Klein, R.; Baumann, T.; Niessner, R.: MSWI bottom ash elution. Tübinger Geowissenschaftliche Arbeiten C61, 2002, 176-179.

[**Kleber 1983**] Kleber, W.: Einführung in die Kristallographie. 1983. Berlin, Verlag Technik.

[**Knorr 1999**] Knorr, W.; Hentschel, B.; Marb, C. u.a. : in Rückstände aus der Müllverbrennung, (Hrsg. Deutsche Bundesstiftung Umwelt), Erich Schmidt Verlag GmbH&Co., Berlin, 1999.

[**Larasati 2016**] Larasati, A.: Characterization of non-magnetic fraction fine particle WtE bottom ash and its separation processes, 2016, Master Thesis University of Duisburg-Essen.

[**Li 2016**] Li, Y.; Hao, L.; Chen, X.: Analysis of MSWI bottom ash reused as alternative material for cement production, 2016. Procedia Environmental Sciences 31 (2016) 549 – 553.

[**Lombardi 2015**] Lombardi; L.; Carnevale, E.; Corti, A.: A review of technologies and performances of thermal treatmentsystems for energy recovery from waste. Waste Management 37, 2015, pp 26–44.

[**LP 1996**] LP, D.: Etude de la stabilisation d'un mâchefer aux liantshydrauliques–DEA de Génie Civil, Ecole des Mines de Douai, UST Lille I, 1996.

[**Marchese 2010**] Marchese, F.; Genon, G.: Effect of leaching behavior by quenching of bottom ash from MSW incineration, 2010. Waste management and research 29(10) supplement 39 – 47. DOI: 10.1177/0734242X10387848.

[**Meima 1997**] Meima, J. A.; Comans, R. N. J.: Overview of geochemicals processes controlling leaching characteristics of MSWI bottom ash. Studies in Environmental Science Volume 71, 1997, pp. 447–457. doi:10.1016/S0166-1116(97)80228-2

[**Meima 1997**] Meima, J. A.; Commans , R. N. J.: "Overview of geochemical processes controlling leaching characteristics of MSWI bottom ash", Waste Materials in Construction: Putting Theory into Practice, pp 447-457. Elsevier Science BV, 1997.

[**Muchová 2009**] Muchová, L.; Bakker, E.; Rem, P.: Precious metals in municaipal solid waste incineration bottom ash. Water air soil pollution: Focus (2009) 9:107 – 116. DOI 10.1007/s11267-008-9191-9.

[**Muchová 2010**] Muchová, L.: Wet physical separation of bottom ash. 2010. Dissertation thesis TU Delft. ISBN: 9789064644405

[**Oeters 1989**] Oeters, F.: Metallurgie der Stahlerstellung. Springer Berlin Heidelberg 27.10.1989.

[**Pan 2008**] Pan, J. R.; Huang, C. P.; Kuo, J. J.; Lin, S. H.: Recycling MSWI bottom ash and fly ash as raw materials for Portland cement. Waste Management 28, 2008 1113 – 1118. Taiwan.

[**Pfrang 1999**] Pfrang-Stotz, G.; Reichelt, J.: Müll und Abfall 5, S.262-268, 1999.

[**Pecqueur 2001**] Pecqueur, G; Crignon, C.; Quénée, B.: Behaviour of cement-treated MSWI bottom ash, 2001. Waste Management 21 (2001) 229 – 233.

[**Pratiwi 2016**] Pratiwi, A. A.: Characterization of magnetic fraction fine particle WtE bottom ash and its separation processes, 2016, Master Thesis University of Duisburg-Essen.

[**Prayogi 2016**] Prayogi, A. P.: Optimization of gold-pan process for separation of fine particle sizes from bottom ash of waste to energy plants, 2016, Master Thesis University of Duisburg-Essen.

[**Tang 2014**] Tang, P.; Florea, M.V.A.; Spiesz, P.; Brouwers, H.J.H.: The application of treated bottom ash in mortar as cement replacement. EurAsia Waste Management Symposium. April 2014. YTU 2010 Congr. Center Istambul Turkiye, 2014 pp. 1077 – 1082.

[**Tang 2015**] Tang, P.; Florea, M.V.A.; Spiesz, P.; Brouwers, H.J.H.: Characteristic and application potential of municipal solid waste incineration (MSWI) bottom ash from two waste-to-energy plants, Constr. Build. Mater. 83 (2015) 77 – 94.

[**Sabbas 2003**] Sabbas, T.; Polettini, A.; Pomi, R.; Astrup, T.; Hjelmar, O.; Mostbauer, P.; Cappai, G.; Magel, G.; Salhofer, S.; Speiser, C.; Heuss-Assbichler, S.; Klein, R.; Lechber, P.: Management of municipal solid waste incineration residues. Waste Management 23 (1), 61–88, 2003. Treatment and Use of Air Pollution Control Residues from MSW Incineration.

[**Sakai 2000**] Sakai, S. I.; Hiraoka, M.: Municipal solid waste incinerator residue recycling by thermal process. Waste management 20 (2000) 249-258. 1999.

[**Shen 2003**] Shen, H.; Forrsberg, E: An overview of recovery metals from slags. Waste management 23 (2003) 933 – 949. 2002.

[**Subasinghe 1992**] Subasinghe, G.K.N.S: Optimal design of sluice-box process for fine gold recovery. 1992. Minerals Engineering, Vol. 6, No. 11, pp. 1155-1165.

[**Thomé-Kozmiensky 2014**] Thomé-Kozmiensky, K. (2014, January 24). Vivis TK Verlag Karl Thomé-Kozmiensky. Retrieved from Vivis TK Verlag Karl Thome-Kozmiensky Web site: http://www.vivis.de/

[**Traina 2007**] Traina, G.; Morselli, L.; Adorno, G. P.: Electrokinetic remediation of bottom ash from municipal solid waste incinerator, 2007. Electrochimica Acta 52, 3380–3385.

[**Trojer 1963**] Trojer, F.: Die oxydischen Kristallphasen der anorganischen Industrieprodukte. E. Schweizerbart, 1963.

[**Umweltbundesamt 2017**] http://www.umweltbundesamt.de/en/topics/waste-resources/waste-disposal/thermal-treatment#textpart-2 (accessed per 18-7-2017).

[**WtERT 2015**] Waste-to-Energy Research and Technology Council (WtERT) GmbH. (2015). Countries: Germany. Retrieved from Waste-to-Energy Research and Technology Council (WtERT) Web site: http://www.wtert.eu

[**Wills 2006**] Wills, B.A; Munn, T. N.: Mineral Processing Technology.Elsevier Science & Technology Books, 2006. 1-354.

[**World Bank 2012**] World Bank, 2012. What a Waste - A Global Review of Solid Waste Management. World Bank, Washington DC.

[**Xiao 2008**] Xiao, Y.; Oorsprong, M.; Yang, Y.; Voncken, J.H.L.: Vitrivication of bottom ash from a municipal solid waste incinerator. 2008. Waste Management 28, 2008. 1020–1026.

[**Xing 2004**] Xing, W.: Quality improvement of granular secondary raw building materials by separation and cleansing techniques. Thesis Delft University of Technology, Delft, the Netherlands, 2004. ISBN 90-9017932-1.

[**Xia 2017**] Xia, Y.; He, P.; Shao, L.; Zhang, H.: Metal distribution characteristic of MSWI in view of metal recovery. Journal of environmental sciences, pp178-179. 2017.

[**Youcai 2002**] Youcai, Z; Lijie, S.; Goujian, L.: Chemical stabilization of MSW incinerator fly ashes. J. Hazard. Mater, 2002, 95, 47 – 63.